Geological Survey of Sweden

Report within the government assignment Geological Storage of Carbon Dioxide in Sweden

Dynamic Modelling and Risk Assessment of Potential CCS Reservoirs

Modelling & Simulation Study Report

Report commissioned by SGU

www.sgu.se

Konsultrapport 13
Diarie-nr: 3261-670/2026

This report has been produced by GLJ Ltd. on behalf of The Geological Survey of Sweden (SGU). The authors are responsible for the content of the report.

Reference to the report: SGU, 2026: *Report within the government assignment Geological Storage of Carbon Dioxide in Sweden. Dynamic Modelling and Risk Assessment of Potential CCS Reservoirs. Modelling & Simulation Study Report. Project Number: 25146.* Konsultrapport 13. Geological Survey of Sweden.

Head of unit: Lena Yotis (SGU)

June 2026

Geological Survey of Sweden
Box 670, 751 28 Uppsala
phone: 018-17 90 00
e-mail: sgu@sgu.se
www.sgu.se

Förord

Sveriges geologiska undersökning (SGU) har inom regeringsuppdraget ”Geologisk lagring av koldioxid i Sverige” (2023–2025) undersökt potentialen för permanent geologisk lagring av koldioxid (CCS – Carbon Capture and Storage) i två geografiska områden i Östersjön: sydvästra Skåne och sydvästra Östersjön, samt Gotland och sydöstra Östersjön. SGU har samlat in stora mängder nya geologiska och geofysiska data som bidragit till att öka kunskapen omkring den sedimentära berggrundens beskaffenhet, samt stärkt dataunderlaget för bedömning av lagringspotentialen i de båda områdena. Dynamisk reservoarmodellering av utpekade reservoarbergarter i områdena, där injektering av koldioxid och lagringpotential över tid, är en väsentlig del av projektet. SGU har inom ramen för regeringsuppdraget gett GLJ Ltd (Kanada) i uppdrag att utföra dynamisk reservoar-modellering. GLJ Ltd fick också i uppdrag att utföra en teknisk riskutvärdering av osäkerheter rörande lagringskapacitet, injektivitet, och lagringssäkerhet över tid.

Resultat visar att de utpekade reservoarerna i båda områdena uppvisar trovärdig potential för permanent CO_2-lagring. För det sydöstra Östersjöområdet indikeras en teoretisk lagringskapacitet som överstiger 300 Mt CO_2 under flera olika utvärderade scenarier, medan det sydvästra Östersjö-området uppvisar ytterligare betydande potential, med en uppskattad lagringskapacitet som överstiger 100 Mt CO_2. De främsta osäkerheterna som identifierats avser effektiv lagringskapacitet och långsiktig plymmigration. Dessa osäkerheter är typiska för projekt i utvärderingsstadiet och kan hanteras med systematiska arbetsflöden för riskreducering. GLJ rekommenderar fortsatta under-sökningar som riktade seismiska undersökningar, förbättrad petrofysisk karakterisering, verifiering av brunnsintegritet, geomekanisk utvärdering och utökade dynamiska känslighetsanalyser. Sådana undersökningar kommer successivt att minska osäkerhetsintervallen och öka förutsägbarheten i de dynamiska reservoarmodellerna.

Preface

The Geological Survey of Sweden (SGU) has within the government assignment ”Geological Storage of Carbon Dioxide in Sweden” (2023–2025), investigated the potential for permanent geological storage of carbon dioxide (CCS – Carbon Capture and Storage) in two geographic areas in the Baltic Sea: southwestern Skåne and southwestern Baltic Sea, as well as Gotland and the southeastern Baltic Sea. SGU has collected large amounts of new geological and geophysical data, which has significantly increased our knowledge about the properties of the sedimentary bedrock, as well as further strengthened the data documentation for assessing storage potential in the two areas. Dynamic reservoir modeling of identified reservoir rocks in the areas, where carbon dioxide injection and storage potential over time are considered, is an essential part of the project. For this purpose, SGU commissioned GLJ Ltd (Canada) to carry out dynamic reservoir modeling on primary reservoir rocks in both areas. GLJ Ltd was also commissioned to carry out a technical risk assessment of uncertainties regarding storage capacity, injectivity, and storage security over time.

Results show that the identified reservoirs in both areas exhibit credible potential for permanent CO_2 storage. For the southeastern Baltic Sea area, a theoretical storage capacity exceeding 300 Mt CO_2 is indicated under several different evaluated scenarios, while the southwestern Baltic Sea area shows further significant potential, with an estimated storage capacity exceeding 100 Mt CO_2. The primary uncertainties identified concerns effective storage capacity and long-term plume migration. According to GLJ, these uncertainties are typical for projects in the evaluation stage and can be mitigated through systematic risk-reduction workflows. GLJ recommends continued investigations such as targeted seismic surveys, improved petrophysical characterization, verification of well integrity, geomechanical evaluation, and extended dynamic sensitivity analyses, which will gradually reduce uncertainty ranges and increase the predictability of the dynamic reservoir models.

Dynamic Modelling and Risk Assessment of Potential CCS Reservoirs

Modelling & Simulation Study Report

Report Presented by GLJ Ltd. to Geological Survey of Sweden (SGU)

Effective February 28th, 2026

Project Number: 25146

GLJ Ltd.
1920, 401 - 9 Avenue SW
Calgary Alberta T2P 3C5

Geological Survey of Sweden

Table of Contents

List of Figures

List of Tables

February 28th, 2026
Project # 25146

Sofie Lindström
Project Manager, CCS Projects
Geological Survey of Sweden
Kungsängstull 4, 753 19
Uppsala, Sweden

RE: Dynamic Modelling and Risk Assessment of Potential CCS Reservoirs – Final Report

Dear Sofie:

Per your request, GLJ Ltd. (GLJ) has completed the modelling and simulation study of CO_2 injection and long-term storage scenarios in the Faludden sandstone and Arnager Greensand candidate reservoirs. The final report is enclosed.

This report documents the details of the workflow, methodology, findings and recommendations for this study. As part of the deliverables, GLJ permits SGU the use and publication of this full report. In case figures, statements and modelling results or partial report is quoted, please reference the full report.

It is trusted that this report meets your current requirements. Should you have any questions regarding this report, please contact the undersigned.

Yours truly,
GLJ LTD.

Greg Owen, P.Eng.
Senior Vice President, New Ventures

JGO/HS

Use of Product and Deliverables

The Company recognizes and agrees that all forward-looking projections and recommendations or findings associated with current uncertainties within the project and associated deliverables prepared by GLJ will be estimates only, and the Company agrees that such evaluations shall be so represented to third parties. GLJ understands that the Company may wish to use evaluations, reports, and opinions of GLJ in connection with transactions or reporting requirements that are subject to federal or provincial laws, rules, or regulations applicable to securities ("securities transactions"). The Company agrees not to use the evaluations, studies, or opinions of GLJ in public disclosure for a purpose other than that which the content was prepared for as described in the above Proposal without the prior written consent of GLJ, which GLJ shall not unreasonably withhold.

In providing its project deliverables, GLJ understands that the complete content may be provided by the Company to third parties on a confidential basis to facilitate business dealings. GLJ and the Company recognize that opinions expressed by GLJ are provided in the context of the aggregate of the entities studied. Consequently, extraction of portions of GLJ reports, for example for individual property divestiture purposes, is not permitted without clarification of the context of the extracted portion within the overall scope of the engagement, and without the consent of GLJ.

Consent to the use of GLJ's reports does not extend to the direct publication of the full report or any portion of the report, including posting on SEDAR or company websites. Such use of GLJ's reports is strictly prohibited without the specific written consent of GLJ which will normally not be granted.

The Company agrees that GLJ's fee covers only preparation and delivery of evaluations, opinions, and work products. The Company agrees that GLJ's fee shall not cover any testimony solicited and/or subpoenaed from any of GLJ's personnel before any Court or in any administrative proceeding or other similar hearing in which the Company is named as a defendant or respondent, all of which shall be billed to the Company at GLJ's customary fees for such services, unless it shall be determined by such Court or in any such administrative proceeding or other similar hearing or by another Court, that GLJ was negligent or committed willful misconduct in the preparation of the GLJ Report.

Certification of Qualifications

This report has been prepared and reviewed thoroughly by the authors to the best of their knowledge. Data and interpretations presented in this report are of the opinion of the authors and are believed accurate in nature as a function of the quality and quantity of the available data. Estimates and interpretations presented herein are considered reasonable and should be accepted with the understanding that revisions may be justified if additional data is acquired.

PERMIT TO PRACTICE
GLJ LTD.

RM Signature:

RM APEGA ID#:

Date: February 28, 2026
PERMIT NUMBER: P 2066
The Association of Professional Engineers and Geoscientists of Alberta (APEGA)

Aurelie Lagisquet, P.Eng. Manager, Engineering February 28, 2026	Suzy Chen, P.Eng. VP, Integrated Studies February 28, 2026	Shaw Liu, P.Geo. Geomodeller February 28, 2026
Vicky Wang, P.Eng. Manager, Engineering February 28, 2026		Brandon Xue Engineer in Training February 28, 2026

1. Executive Summary

This appraisal study evaluates the suitability of the Arnager Greensand and the Faludden sandstone offshore Sweden as geological storage complexes for long-term CO_2 sequestration. All available geological, petrophysical, and structural data provided by SGU have been integrated into a consistent, simulation-ready geomodel developed in Petrel.

The geomodelling work has been successfully completed and provides a robust, internally consistent framework suitable for dynamic CO_2 injection simulations. Where data coverage was limited, sound geological interpretations and defensible assumptions were applied to ensure alignment with project objectives. Grid architecture and cell size were systematically tested and optimized to balance geological fidelity with computational efficiency, resulting in fit-for-purpose models capable of supporting injectivity, pressure evolution, and plume migration analyses. These models establish a strong technical foundation for evaluating storage performance and can be further refined as new data become available.

In parallel, GLJ conducted an independent qualitative technical risk assessment to evaluate key uncertainties associated with storage performance, injectivity, and long-term containment integrity. The assessment draws on reservoir sensitivity analyses, technical discussions with SGU, and GLJ's subsurface and operational expertise. Its purpose is to clarify the principal technical risks and define practical steps required to further mature and de-risk the projects prior to development.

Strong Technical Foundation and Material Capacity
The results confirm that both formations demonstrate credible and material potential for long-term CO_2 storage.

The southeastern Baltic Sea Area of Interest (AOI) indicates a theoretical storage capacity exceeding 300 Mt of CO_2 under evaluated scenarios. Reservoir permeability is a primary control on injectivity and storage efficiency, offering clear opportunities for optimization through well design and operational strategy. While higher permeability may extend plume migration distances over long timeframes, these behaviors are captured within the modelling framework and can be managed through informed site design and monitoring.

The southwestern Baltic Sea and Skåne AOI demonstrates additional significant potential, with estimated storage capacity exceeding 100 Mt of CO_2. Reservoir permeability and porosity are well-defined performance drivers, providing clear parameters for continued refinement. Simulation results indicate predictable plume development within the structural framework, and sensitivity analyses allow potential migration pathways to be incorporated into monitoring and risk management planning.

Injection Performance and Storage Security
While the evaluation focused on the injection of CO_2 with vertical wells, horizontal wells provide enhanced injectivity and operational flexibility, strengthening development optionality. Residual trapping through capillary forces represents an important long-term containment mechanism in both formations. Further laboratory calibration of hysteresis parameters will refine estimates of trapped CO_2 and further increase confidence in storage permanence.

Risk Profile and Maturation Pathway
The primary uncertainties identified relate to effective storage capacity and long-term plume migration. These are typical for projects at the appraisal stage and are well suited to systematic risk-reduction workflows. Targeted seismic refinement, enhanced petrophysical characterization, well integrity verification, geomechanical evaluation, and expanded dynamic sensitivity analyses will progressively narrow uncertainty ranges and increase predictability.

Importantly, no fundamental geological or technical barriers have been identified that would preclude further advancement. The findings support progression toward advanced dynamic simulations, development of a comprehensive Monitoring, Measurement, and Verification (MMV) framework, and alignment with regulatory requirements.

Strategic Outlook
With phased appraisal and continued technical advancement, the Arnager Greensand and Faludden sandstone are well positioned to become key components of Sweden's long-term carbon management strategy. Continued governmental support will enable the transition from advanced modelling to integrated development planning, unlocking substantial offshore storage capacity and reinforcing Sweden's pathway toward climate neutrality.

2. Introduction and Scope

2.1 Project Description

SGU has been given a government assignment to investigate the potential for geological CO2 storage and associated risks in Sweden.

Two areas (reservoirs) were targeted and SGU has built the static 3D models using Leapfrog Modelling Software (Sequent) based on extensive pre-existing subsurface data (borehole data and analytical results collected primarily between 1960-1990, and some new data as well).

The "Base Scope" of the project is to build 2 dynamic models based on the static models provided to investigate a range of different injection scenarios:

- # of wells, well locations and effect of injection well placement
- Maximum injection rate
- Requirement for water production wells
- CO_2 plume size, concentration and migration speed

Key technical risks are to be identified and reported upon based on scenario modelling work.

2.2 Scope of Work

The scope of work was broken down into the following three stages:

1. Project Kickoff, Data Gathering, and Processing
2. Modelling of Injection Scenarios and Technical Risk Assessment (Base Case)
3. Final Report, Presentations, and Recommendations

GLJ has successfully completed all stages.

Data Gathering, and Processing
The SGU static models were built by SGU personnel using Leapfrog Modelling. GLJ conducted a full data and static model review for validation. Static 3D model conversion from Leapfrog to Petrel was carried out by GLJ.

Modelling of Injection Scenarios and Technical Risk Assessment (Base Case)

- CCS Dynamic Model Input Data
- Dynamic Modelling Workflow including Sensitivity Analysis and Risk Assessment
- Dynamic Modelling Assumptions and Numerical Software

The following assumptions and considerations were made:

- No salt precipitation was considered in this model. This is often observed as reduction in injectivity.
- Constant injection rate is simulated, which can be optimistic, especially for higher rates.
- Geochemical reactions are not considered in the model.
- Higher injection rate can lead to friction lost at wellbore, hence injectivity loss

The following items were out of scope for the current Base Scope:

- Geomechanical modelling
- Thermal modelling
- Wellbore modelling
- Additional dewatering scenarios (however the pressure risks will be assessed for the needs of dewatering wells as per Base Scope)
- Oil & Gas modelling (just initialization with provided properties, no oil and gas history match/forecasting)
- Advanced modelling can be done if required but is not included in current cost estimate
- Additional reservoir zones beyond the two provided by SGU (Optional Scope)
- Simulation of leakage along faults or old boreholes (Optional Scope)

3. Geology & Geomodelling

3.1 SGU Leapfrog Models

SGU has developed two Leapfrog geological models for the evaluation of offshore CO_2 storage: one covering the southwestern Baltic Sea and Skåne (area identified with **A** in Figure 1), and another covering the southeastern Baltic Sea (area identified with **B** in Figure 1). To support these models, SGU has acquired new subsurface data including the drilling of four boreholes in the two areas and more than 3,000 km of 2D seismic reflection data in area A. In addition, SGU has organized, digitized, and reprocessed extensive pre-existing subsurface datasets, primarily collected between 1960 and 1990 during oil exploration activities in area B. Borehole data and associated analytical results from both legacy wells and the newly drilled project boreholes have been compiled and integrated.

SGU has developed an eight-layer geological model for the southeastern Baltic Sea and a six-layer geological model for southwestern Baltic Sea and Skåne (Figure 2), incorporating stratigraphic interpretations. The primary target zone for CO_2 storage in the southeastern Baltic Sea modelling area is the Faludden sandstone, while in the southwestern Baltic Sea and Skåne modelling area, it is the Arnager Greensand. For the purposes of volume comparison and dynamic simulation, GLJ constructed a 3D stochastic model using the same datasets and estimated the bulk rock volume, net rock volume, and pore volume for each area. The results obtained by GLJ and by SGU show good agreement.

The 3D static geological models constructed by SGU for both areas incorporate stratigraphic and structural interpretations, including information on reservoir geometry, thickness, and depth. No reservoir properties (e.g., effective porosity, facies, net-to-gross) are included in these models. The 3D static geological models for both areas of interest were developed using Leapfrog modelling software (Seequent), which allows data export in multiple formats. For this study, the Leapfrog models were exported and subsequently imported into Petrel software.

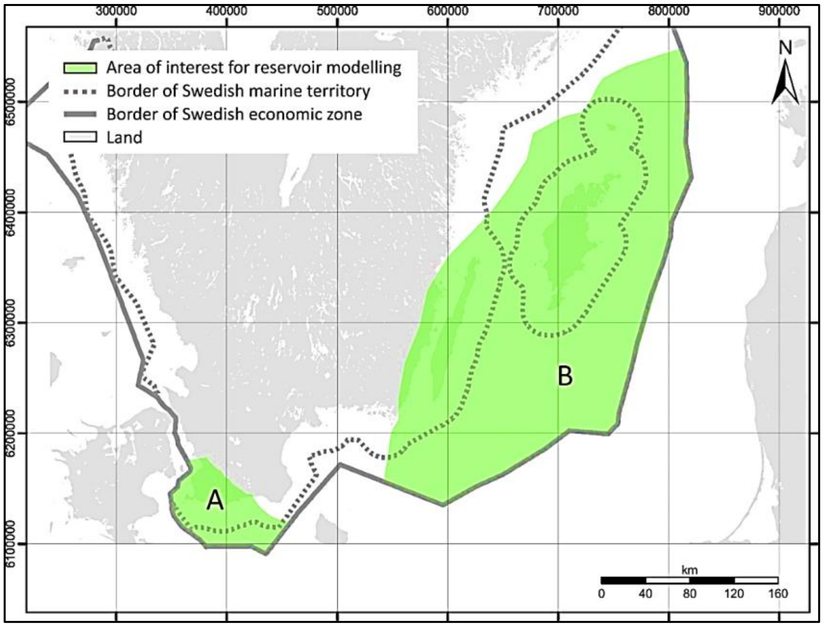

Figure 1: Location of areas of interest (AOI) in green (SGU)

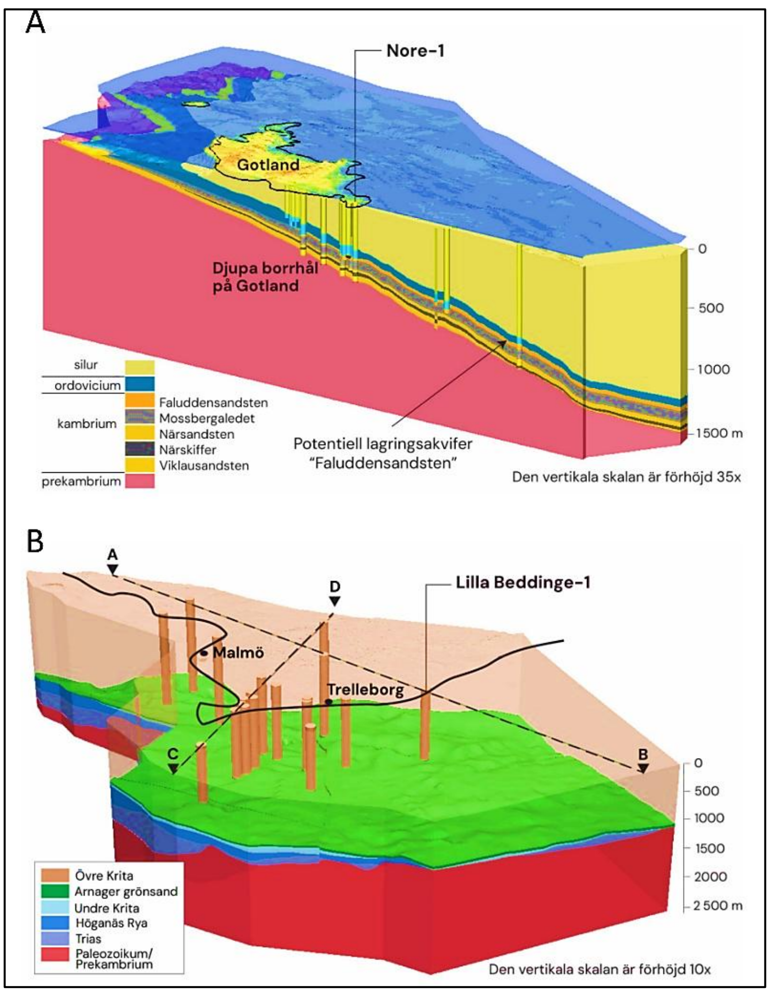

Figure 2: A regional-scale image of the 3D static geological models for A. the southeastern Baltic Sea and B. southwestern Baltic Sea and Skåne (SGU)

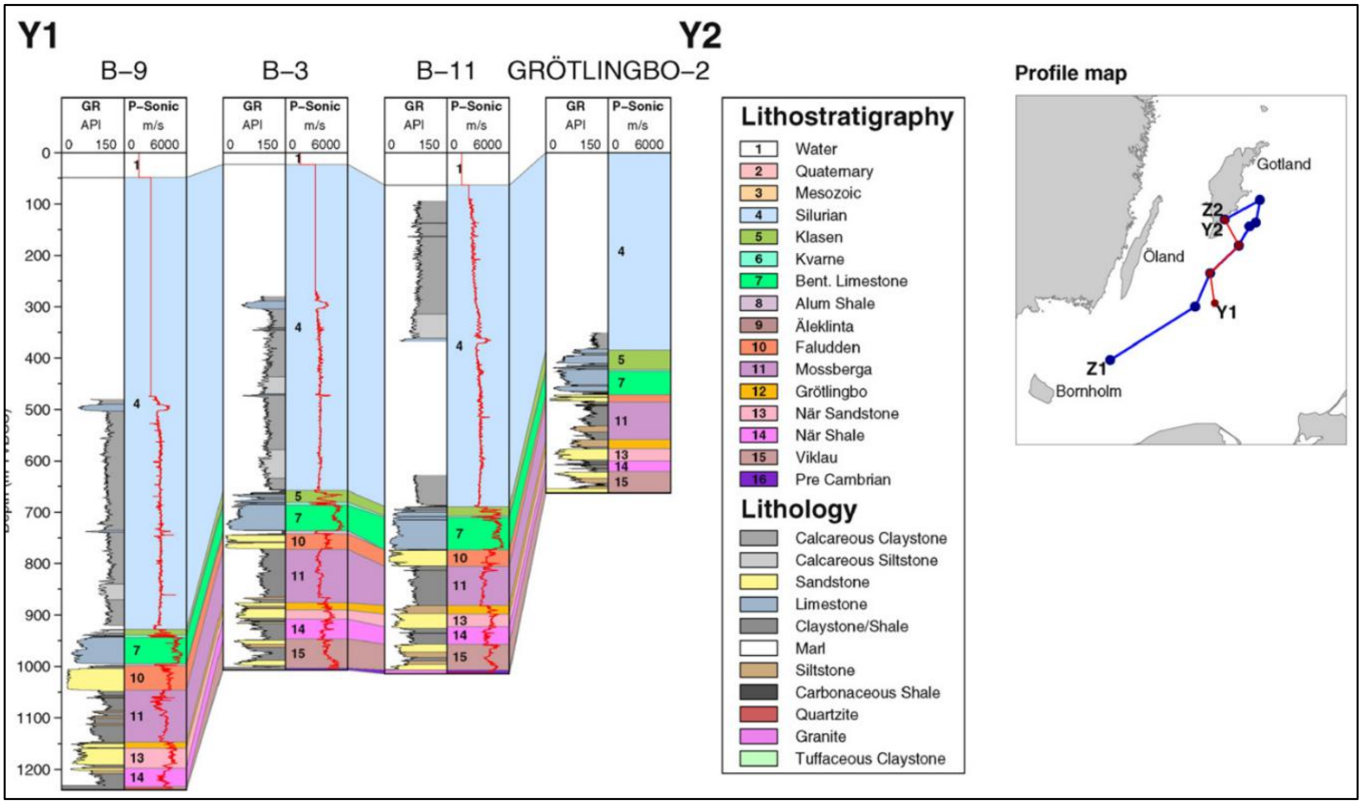

Figure 3: A well correlation panel from the southeastern Baltic Sea (SGU)

The porosity and permeability values provided by SGU (Table 1) are in good agreement with the statistical data presented by Shogenova et al. (2009) (Table 2) for the Faludden sandstone of the Baltic Basin.

Table 1: Summary of various properties for the Faludden sandstone (SGU)

Parameter	Average	Onshore south Gotland			Offshore, outer Swedish sector of the Baltic Sea to the SSE below 800 m depth		
		Low	Mean	High	Low	Mean	High
Gross thickness, m	41[2)]	0[3)]	15[3)]	30[3)]	30[1)]	40[3)]	55[3)]
Net/gross ratio, cut off phie=10% or 100 mD	0.8[1)]	0.7[2,3)]	0.8[2,3)]	1[2,3)]	0.6[1)]	0.7[1)]	0.8[1)]
Total porosity, %	15.3[2)]	10[2)]	15[2)]	20[2)]	10	12	18
Gas perm. mD	788[2)]	100[1)]	350[1)]	2000[1)]	100[1)]	200[1)]	500[1)]
Kh/Kv	0.97[2)]	-	-	-	-	-	-
Temp., °C	>31° C at 800 m	24	26	28	32	37	45
Therm. Cond. W/mK	4.0	3.5	4.1	4.6	3.2	4.5	4.5
Salinity, g/l		Faludden-1, 653 m, 60 g/l					
TDS, mg/l		Nore-1, 560 m, 54 g/l [6] Nore-2, 560 m, 60 g/l [6]					
Formation pressure		56.4 bar at 556 m in Nore-1					
Comments		Almost all empirical core data comes from cores in the southernmost part of Gotland. The Faludden sandstone is here in a shallower position (c. 550 m depth) in comparison to the potential injection area to the SSE where it is located at depths down to c 1100 m. There is likely a trend of decreasing porosity and permeability associated to the increasing depth to the SSW. This has e.g. been noted in a paper by Shogenova et al (2009) and further addressed in a publication by Sopher et al (2014). However, the wire-line logging data does not show any evident changes in e.g. the B7 and Bp wells in comparison to the wells representing shallower depths on south Gotland. The decreasing factor is uncertain and may be in the range 0.8-0.9 and mainly affect the high values.					

Table 2: Values of physical and chemical parameters of the Baltic Cambrian rocks, Shogenova et al. (2009)

Parameter	Depth, m											
	80–800				800–1800				1800–2300			
	Min	Max	Mean	*N*	Min	Max	Mean	*N*	Min	Max	Mean	*N*
Wet density, kg/m^3	2070	2680	2260	60	2130	2810	2300	111	2400	2640	2530	98
Porosity, %	1.5	39.8	18.6	60	8.0	22.5	14.2	111	0.4	12.4	5.5	95
Permeability, mD	0.001	1292	311	38	0.02	1106	251	83	0.003	957	12	273
SiO_2, %	62.0	88.6	83.3	60	57.0	99.4	89.3	115	61.1	99.8	89.7	98
Al_2O_3, %	0.4	17.7	5.3	60	0.05	16.6	3.6	115	0.05	14.6	4.3	98
CaO, %	0.03	16.5	2.2	60	0.03	11.1	0.6	115	0.03	6.4	0.7	98

Min, minimum; max, maximum; mean, average; *N*, number of measured samples.

Regionally, porosity decreases with increasing reservoir depth (Figure 4). Figure 4 indicates a porosity reduction of approximately 8–9%. However, above 1000m depth, there is no significant porosity decreasing trend observed in wells (B7 and B9).

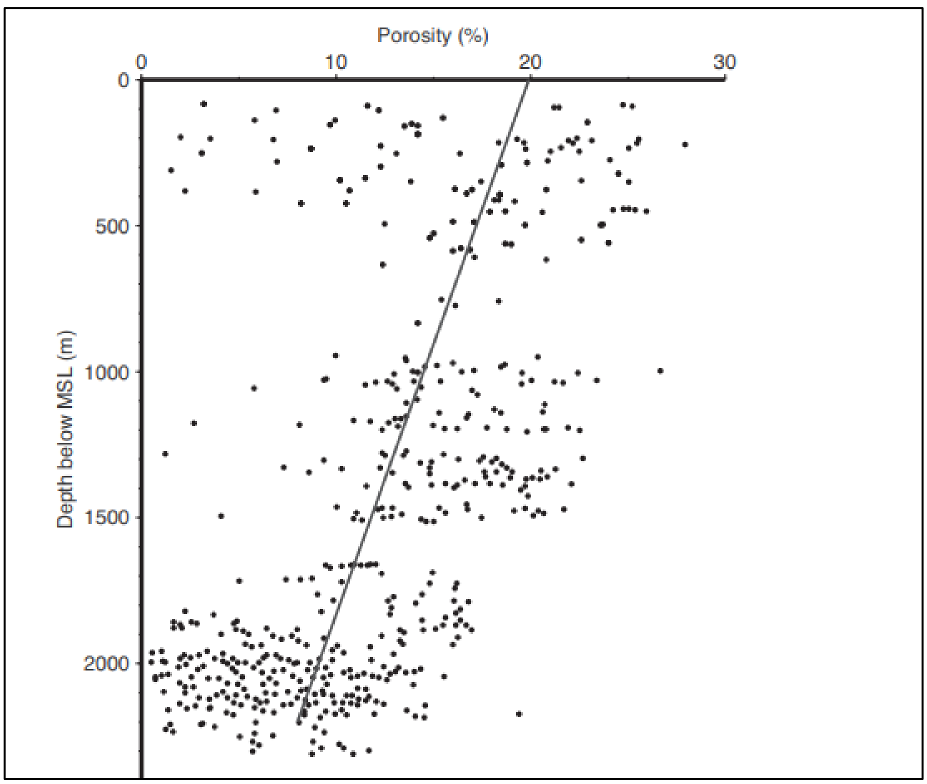

Figure 4: Porosity data and least squares linear porosity depth trend. Sopher et al. (2014)

Southeastern Baltic Sea

In the southeastern Baltic Sea, south of the island of Gotland, geology is characterized by a Paleozoic sedimentary succession. At the base of this succession lies a Cambrian section that contains reservoirs of interest, including the Faludden sandstone, for CO_2 storage. These reservoirs occur at depths between approximately 500 m and 1,600 m below sea level across the area of interest, with depths increasing gradually from northwest to southeast. Figure 3 illustrates the typical sedimentary sequence in the southeastern Baltic Sea area.

For reservoir modelling in the southeastern Baltic Sea, SGU requested dynamic reservoir modelling exclusively for CO_2 injection into the Middle Cambrian Faludden sandstone. A shallow-marine sandstone is shown in Figure 3 at depths between approximately 500 m and 1,250 m. The reservoir is generally considered to be laterally homogeneous, with typical porosities of about 10–16% and assessed reservoir permeabilities of 200 440 mD below depths of 800m. Higher permeabilities are observed in shallower boreholes on south Gotland. A gradual decreasing permeability trend with greater depth is thus considered. The Faludden sandstone reaches a maximum thickness of around 50 m in the southeast and gradually thins toward the northwest, where it pinches out stratigraphically prior to surface outcrop.

The Faludden sandstone is composed predominantly of fine- to medium-grained, well-sorted quartz arenite. The unit is generally clean with only minor proportions of clay minerals. Thin interbeds of siltstone or shale occur locally but do not significantly affect reservoir continuity. Cementation is dominated by carbonate minerals, primarily calcite with subordinate dolomite, while quartz cement is of minor importance. Diagenetic processes have largely preserved primary porosity; although silica cementation increases with greater depth in the sandstone, there is no evidence of any significant changes in reservoir quality.

The primary seal consists of Ordovician variably argillaceous carbonates with bentonite clays, and Silurian shaly and variably calcareous mudstones.

Southwestern Baltic Sea and Skåne

Within the area of southwestern Baltic Sea and Skåne, the sedimentary sequence primarily consists of Mesozoic strata. The upper 700 – 2,000 m typically comprises Upper Cretaceous limestones and marls, representing the Höllviken Formation. Beneath this, a variable sequence of shales and sandstones occurs, containing the potential reservoirs for CO_2 storage in the area. Consequently, the target layers for this investigation generally lie at depths between 700 m and 2,000 m across the region.

Within this sequence, three reservoir intervals are of interest for CO_2 storage: (1) the Arnager Greensand, together with other Lower Cretaceous sandstone units; (2) sandstone reservoirs within the Höganäs–Rya Formation; and (3) the Bunter and Ljunghusen sandstones. Due to technical difficulties during one of the new drilling operations in Skåne, the drill string became stuck in an unconsolidated sand interval within the Arnager Greensand, making it impossible to continue coring. Consequently, no new data or samples were obtained from the deeper potential reservoirs. Therefore, this study focused on the Arnager Greensand for dynamic simulation.
The Arnager Greensand is a laterally extensive shallow-marine sandstone, with porosities ranging from 20 to 30% and highly variable permeabilities ranging from less than 100 mD to several darcies. The reservoir dips gently towards the northeast and varies in thickness from 17 m to 56 m across the area of interest.

The Arnager Greensand is composed predominantly of fine- to medium-grained glauconitic quartz sandstone. The unit is characterized by abundant glauconite, occurring both as discrete grains and as coatings on quartz grains, imparting a characteristic green coloration to the rock. Accessory minerals include pyrite, micas, zircon, and feldspars, while carbonate content is minor and largely restricted to the northern portions of the unit. Clay occurring as a matrix component is locally variable but does not significantly affect overall lithological continuity.

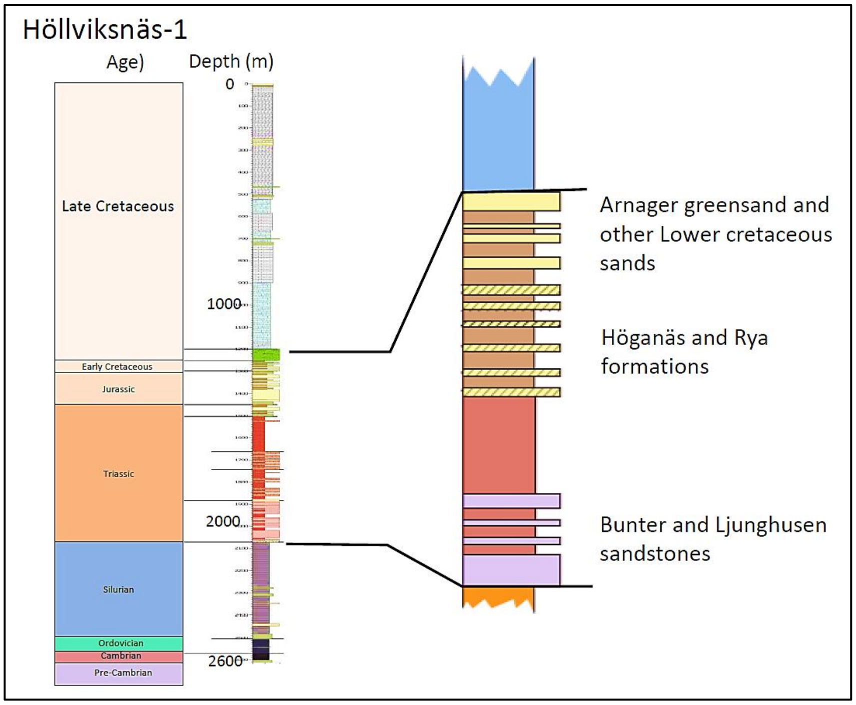

Figure 5: A schematic diagram showing the typical sequence in southern Skåne, as exemplified in the Höllviksnäs-1 well (SGU)

The modelling area of southwestern Baltic Sea and Skåne is subdivided into five structural elements: the Western Skurup Platform (A), Central Skurup Platform (B), Central and Eastern Skurup Platform (C), Höllviken Half-graben (HG), and Falsterbo High (FB), as shown in Figure 6.

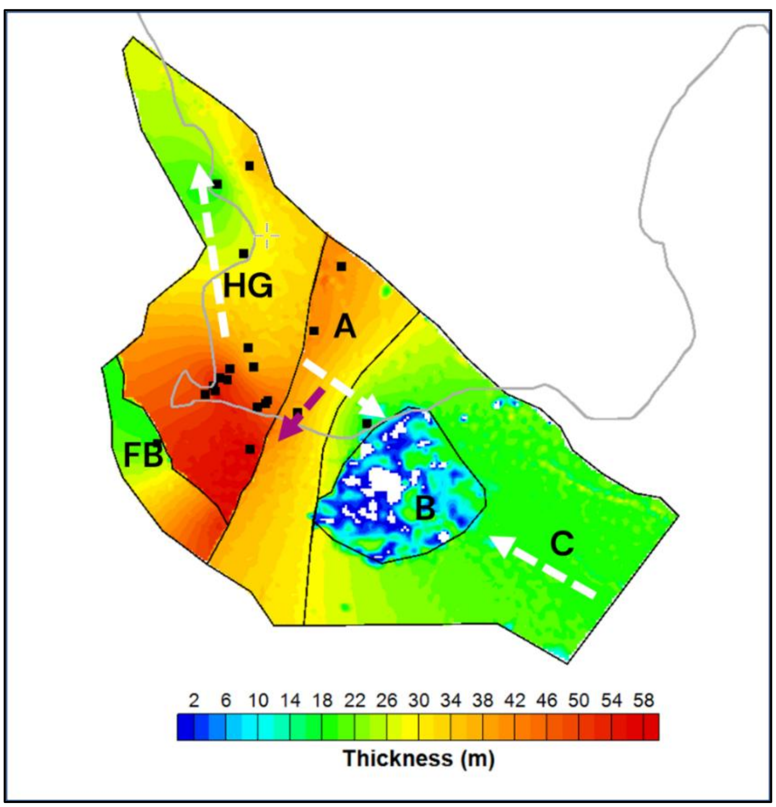

Figure 6: Sub-structure areas in Skåne model (SGU)

SGU observations indicate distinct spatial variations in reservoir properties of the Arnager Greensand. In the Höllviken Half-graben (HG), both net sand thickness and permeability decline toward the north, while higher values occur toward the south and southwest. The reservoir properties on the Central and Eastern Skurup Platform are less known since there is only one well drilled into the Arnager Greensand in this area (Lilla Beddinge-1). A decreasing net sand thickness from southeast to northwest has been suggested, and the Arnager Greensand is interpreted to be thin or absent in the Central Skurup Platform. The property ranges for each sub-area are presented in Table 3.

Table 3: Summary of various properties for the Arnager Greensand (SGU)

Parameter	Average All areas	HG-South (Höllviken Halfgraben) (H-1, H-2, Gr-1, Ma-1öllviken-1, Maglarp-1, Es-1, Ku-1, Hnäs-, Lju-1, Sm-1), Ha-1, Hå-1, Skåre-1)			HG-North (Höllviken Halfgraben) North, area (FCC-1, Ba-1, Nv-1)			Falsterbo High (F-1)			Skurup Platform, Area A (Tr-1, Sv-1, Mo-1)			Skurup Platform Area B			Skurup Platform Area C (L. Beddinge-1)		
		Low	Mean	High	Low	Mean	High	Low	Mean	High	Low	Mean	High	Low	Mean	High	Low	Mean	High
Gross thickness, m	41[2]	30[3]	45[3]	55[3]	15[1]	25[3]	35[3]	15[1]	20[3]	25[1]	15[1]	30[1]	45[3]	0[1]	5[1]	10[1]	10[1]	20[1]	30[1]
Net/gross ratio, cut off phie=10% or 100 mD	0.7[1]	0.7[3]	0.8[3]	0.9[3]	0.2[1]	0.4[1]	0.6[1]	0.7[1]	0.8[1]	0.9[1]	0.3[1]	0.5[1]	0.7[1]	-	0.3[1]	0.5[1]	0.3[1]	0.5[1]	0.7[1]
Total porosity, %	22.5[2]	17[2]	22[2]	32[2]	15	20	23	17	22	32	22[2]	24[2]	31[2]	0[1]	15[1]	20[1]	15[1]	20[1]	25[1]
Gas perm. mD	308[2]	100[1]	350[1]	2000[1]	50[1]	100[1]	200[1]	100[1]	350[1]	2000[1]	50[1]	100[1]	1000[1]	0[1]	50[1]	100[1]	50[1]	100[1]	200[1]
Kh/Kv	0.5?	-	-	-	-	-	-	-	-	-	-	0.5 [5]	-	-	-	-	-	-	-
Temp., °C	40-55°C																		
Therm. Cond. W/mK	1.5	-	-	-	-	-	-	-	-	-	-	-	-	-	-	-	0.8[4]	1.5[4]	2.4[4]
Salinity, g/l		Höllviken-2 Svedala-1 Höllviken-1 Trelleborg-1 Granvik-1	1200 m 1495 m 1247 m 1193 m 1251 m	124 g/l 160 g/l 123 g/l 158 g/l 130 g/l															
TDS, g/l		Skåre-1, 1213 m, 148 g/l FFC-1, 1610 m, 174 g/l															L. Beddinge-1, 1275 m, 141 g/l [6]		
Comments		The Arnager Greensand consists in the south of largely unconsolidated, medium-grained sand with high porosity and permeability. Towards the north and the FFC-1 and Barsebäck-1 wells the sandstone becomes gradually finer grained and less permeable which also coincides with the gradual decrease in gross thickness as well as the gross to net sand ratio. The results from the core analyses represent scattered intervals in few wells and of relatively consolidated parts of the sandstone.						Very little is known about the sandstone properties in this area. The assessments are based on well information from Falsterborev-1 and evaluation of seismic data. No core data exists. Judged to have similar properties as in the south part of the Höllviken Halfgraben			The properties of the Arnager Greensand in the western part of the platform, (Area A) is in the south judged to be like the properties in the Höllviken Halfgraben, as indicated by core data from the upper part of the Arnager Greensand in Trelleborg-1. In comparison, core analyses from Svedala-1, located north of Trelleborg-1 show slightly lower permeability. Although, the porosity is still relatively high. To the east, towards Area B there is a gradual decrease in permeability and net sand. Again, this seems to coincide with a decreasing thickness of the sandstone. The characteristic of the sandstone in Area C is poorly known. Likewise, we anticipate a sandstone that decreases gradually in thickness towards Area B where it likely onlaps this central high area. Similarly, we judge the net sand to decrease in the same direction.								

[1] Judged [2] Based on evaluation of core analyses [3] Based on well logs [4] Lilla Beddinge-1 [5] one data point in Svedala-1 [6] TDS (mg/L) = 1.656 · Cl (mg/L) – 3528 (mg/L) (Schovsbo et al 2025)

3.2 GLJ Petrel Models

SGU provided borehole data, including well location, KB, TD, well tops, and well survey information, along with porosity–permeability data and fault point data. These datasets were imported into Petrel. In addition, two Leapfrog structural models were supplied, which were imported into Petrel by GLJ.

When imported into Petrel, the Leapfrog models could not be exported for dynamic simulation because the well tops were not tied to the structural surfaces, preventing the necessary model integration (Figure 7 and Figure 8).

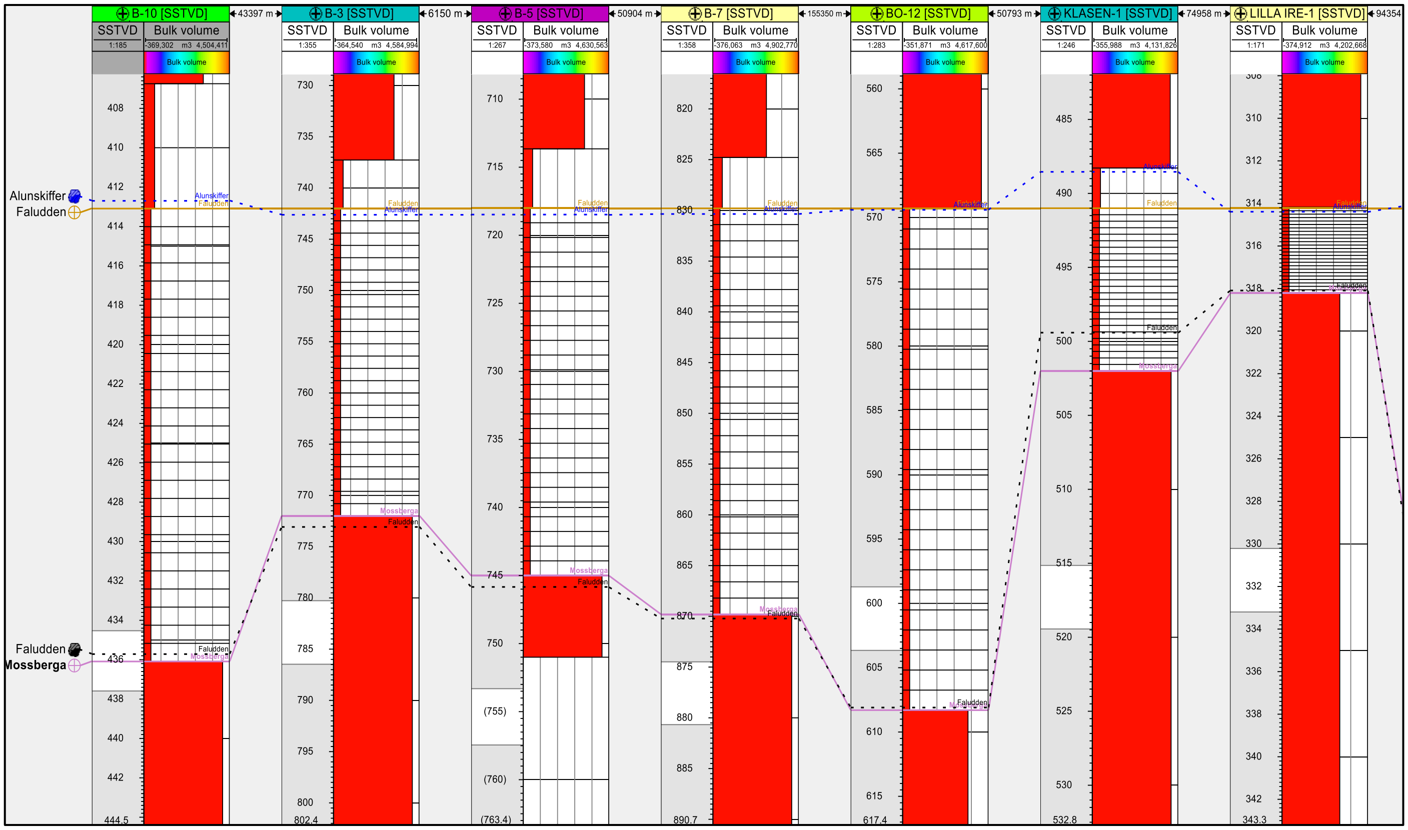

Figure 7: Leapfrog Baltic Sea model well tops vs structure surfaces

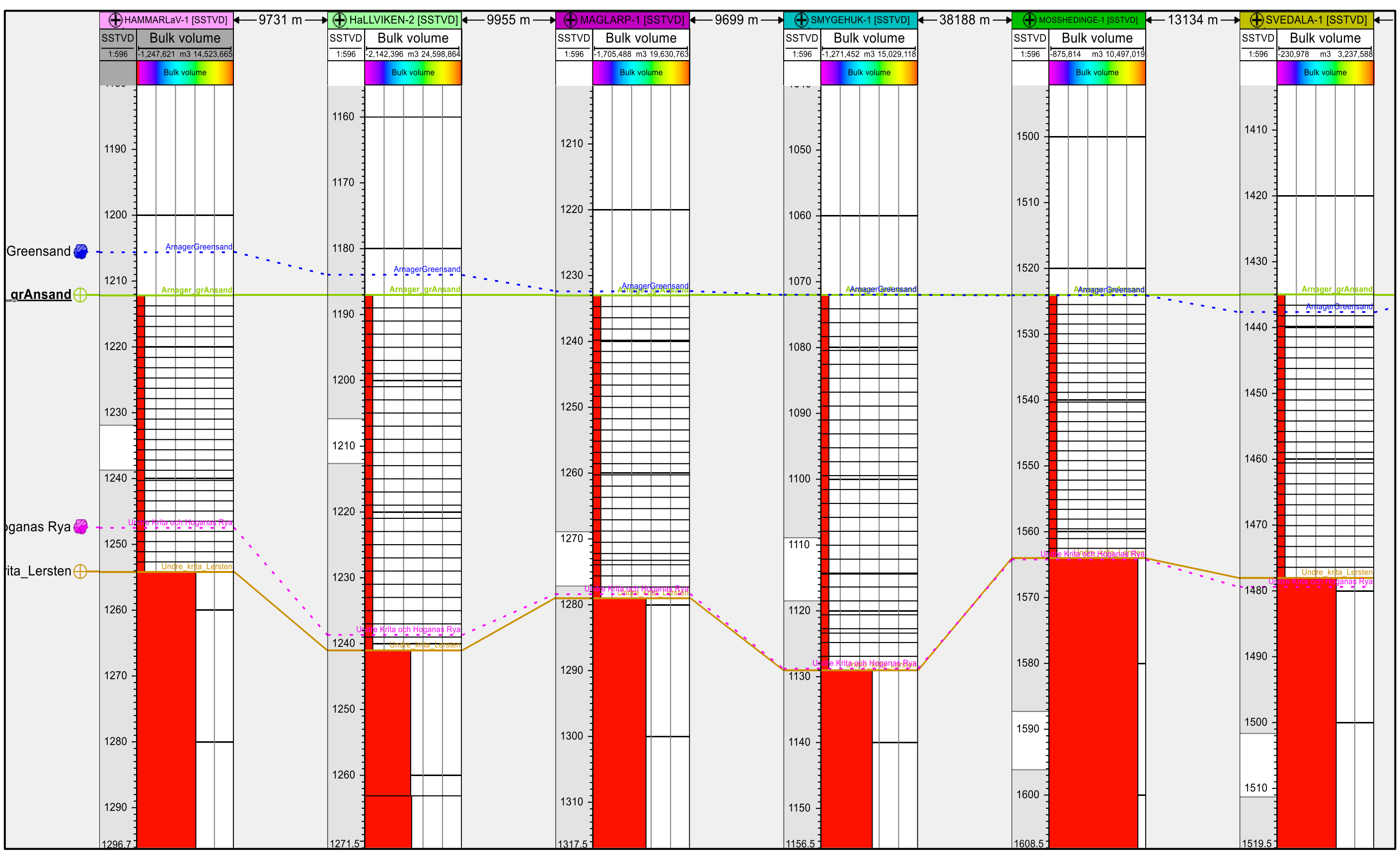

Figure 8: Leapfrog Skåne model well tops vs structure surfaces

Structure Modelling

GLJ reconstructed the geomodel using the same dataset. The boundaries from the Leapfrog models were transferred into the Petrel projects. A regular grid with horizontal cell dimensions of 200 m × 200 m was applied, and the grid orientations are illustrated in Figure 9 and Figure 10.

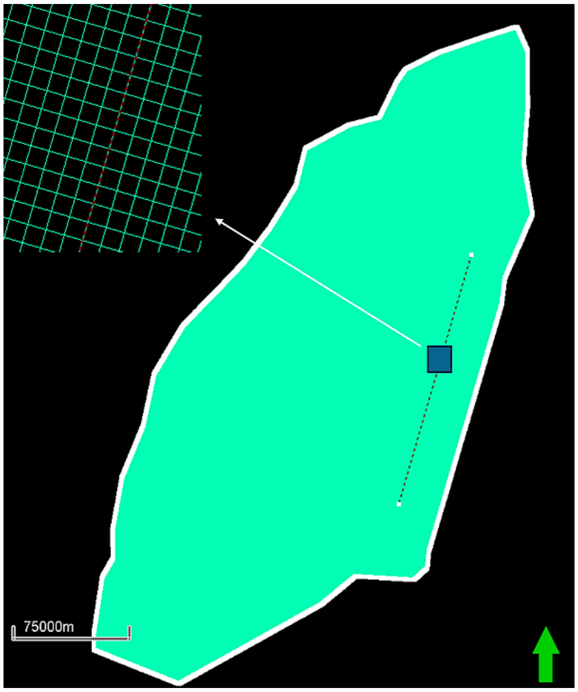

Figure 9: Baltic Sea modelling area

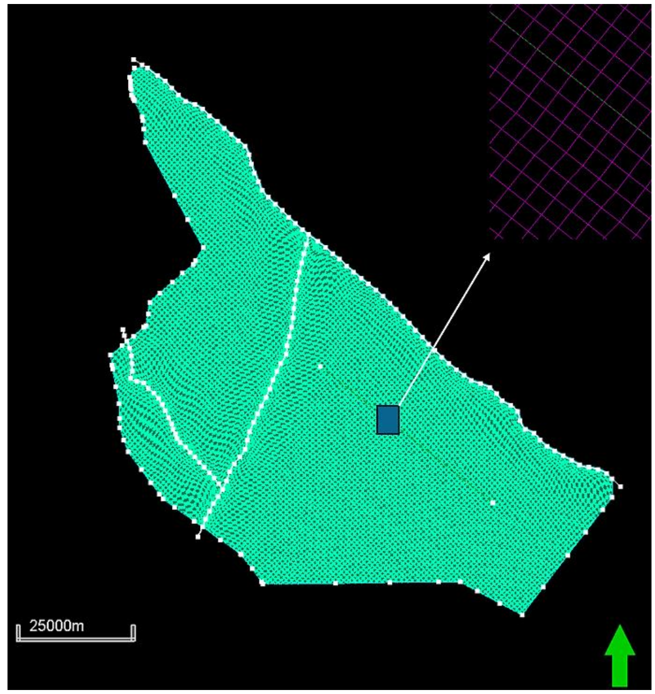

Figure 10: Skåne modelling area

Consistent with the Leapfrog model, three major faults were included in the Skåne Petrel model: Romeleåsen Fault, Svedala Fault, and Öresund Fault. These faults were defined using the fault point dataset (Figure 11).

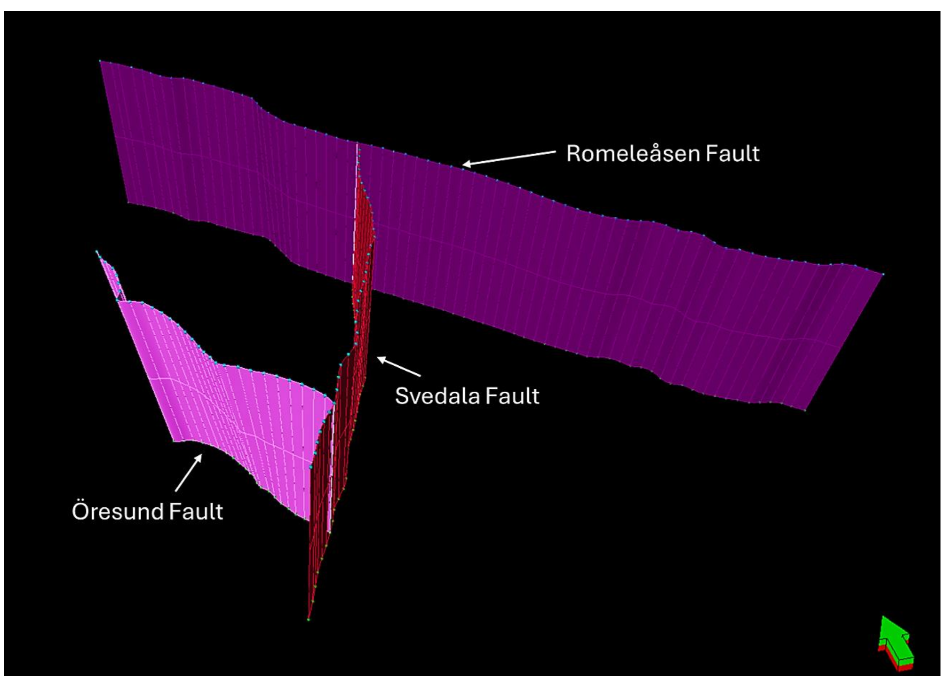

Figure 11: Skåne fault modelling

The Baltic Sea Leapfrog model's eight structural surfaces and well tops, together with four structural surfaces and well tops from the Skåne Leapfrog model, were transferred into the Petrel structural framework (Figure 12 and Figure 13). For the target intervals (Faludden sandstone and Arnager Greensand), a vertical layer thickness of 1 m was used. All other zones were represented by a single layer. The well tops and structural surfaces were successfully tied together, as shown in Figure 14 and Figure 15.

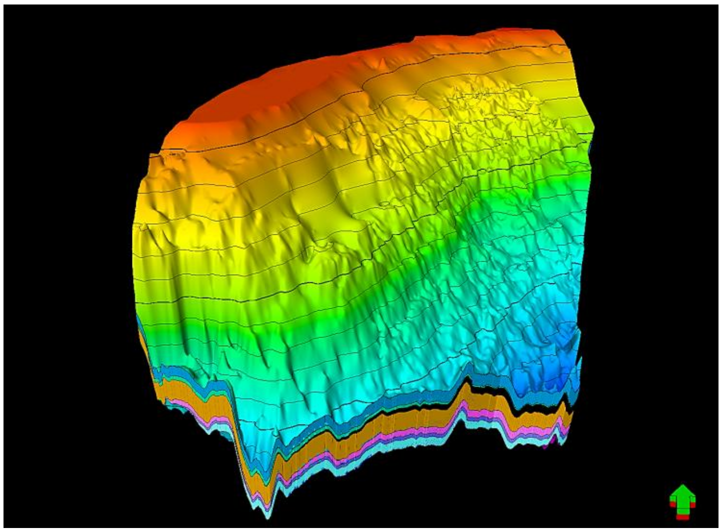

Figure 12: Baltic Sea structure model

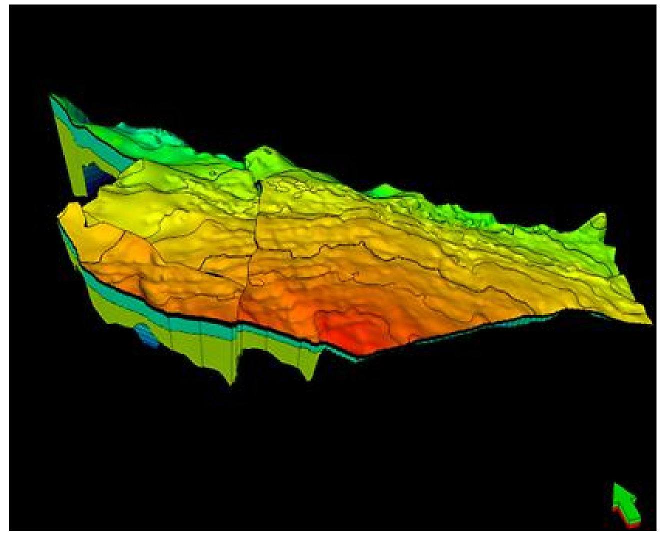

Figure 13: Skåne structure model

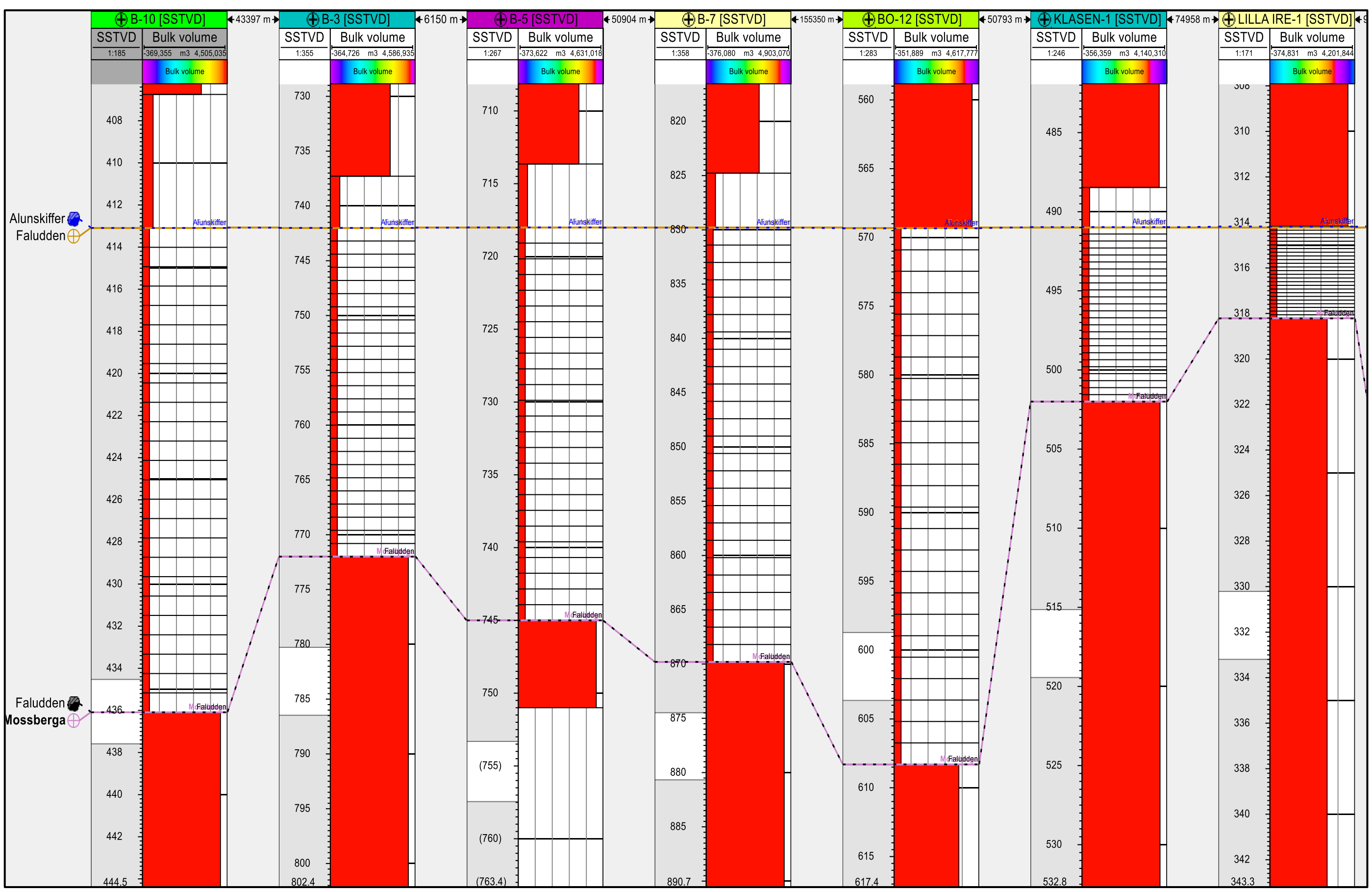

Figure 14: Baltic Sea well tops and structure surfaces tie

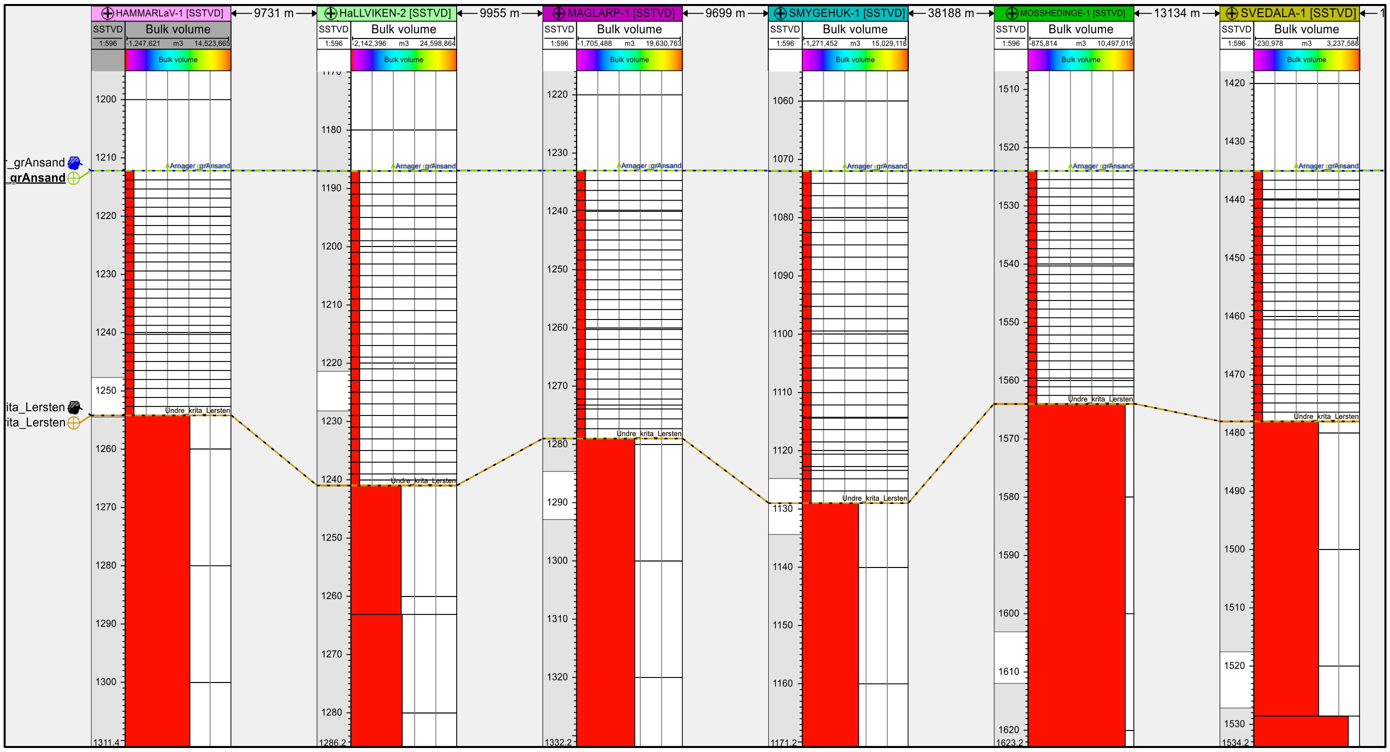

Figure 15: Skåne well tops and structure surfaces tie

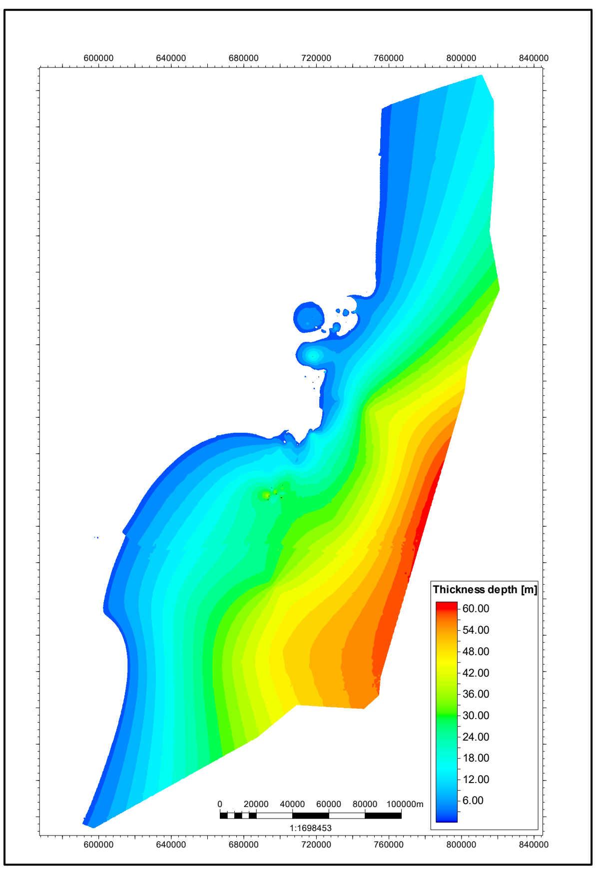

Figure 16: Faludden sandstone thickness map

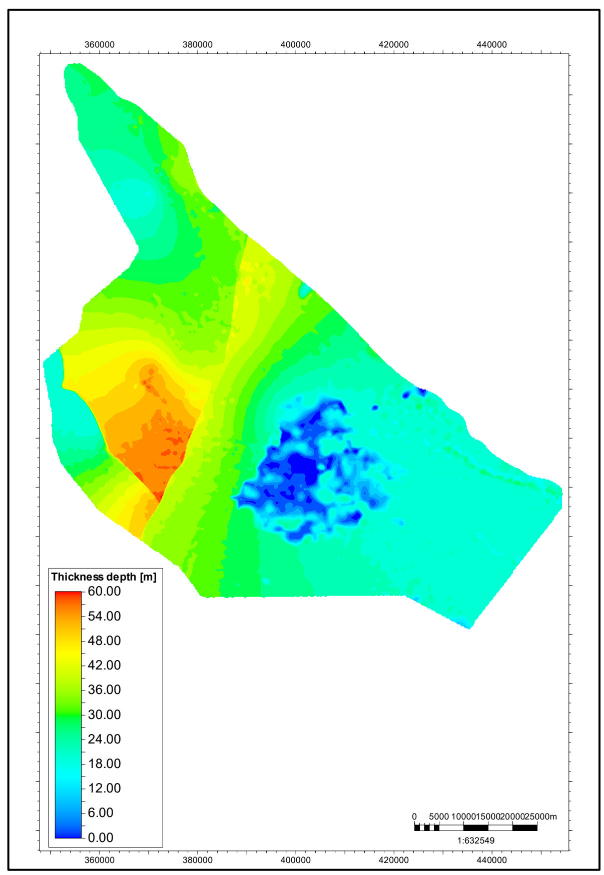

Figure 17: Arnager Greensand thickness map

Thickness maps for the Faludden sandstone and Arnager Greensand were produced using the Petrel models. The Faludden sandstone thickness map (Figure 16) indicates that the reservoir reaches a maximum thickness of about 50 m in the southeast and gradually thins toward the northwest, where it pinches out.

The Arnager Greensand is characterized by a gentle northeast dip and thickness variations ranging from 0 to 60 m. The Arnager Greensand thickness map (Figure 17) shows that in the southern corner of the Höllviken Half-graben (HG), the Arnager Greensand is thicker than in other areas, whereas in the Central Skurup Platform (B) it is thinner than elsewhere.

Property Models

The Faludden sandstone and Arnager Greensand units include 102 and 73 property data points, respectively, but no property logs are available. Given the limited data and the scope of the modelling work, SGU provided average values of porosity, net-to-gross (NTG), and permeability (Table 1 and Table 3) were applied uniformly across both zones. The resulting property distributions are shown in Figure 18 and Figure 19.

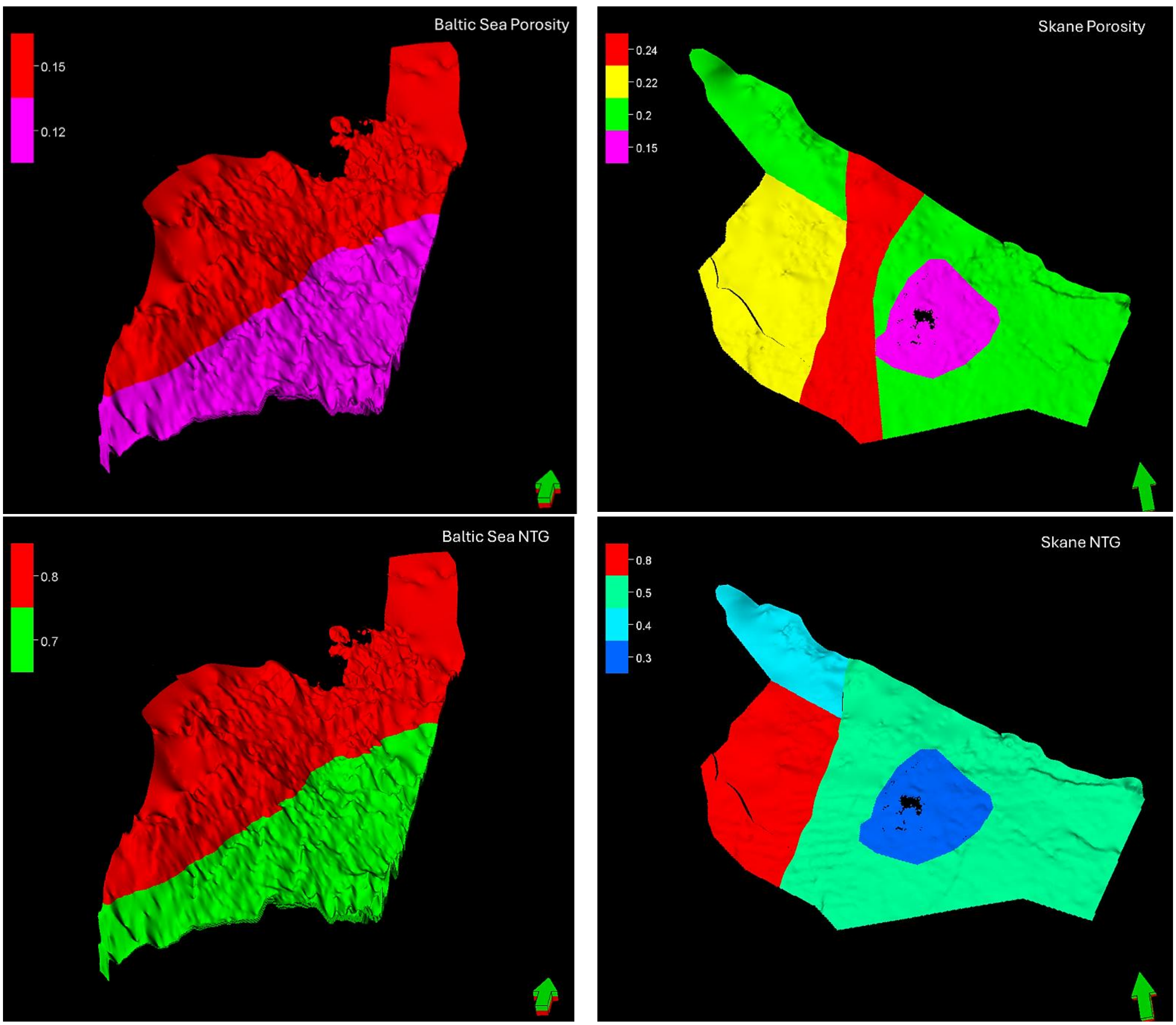

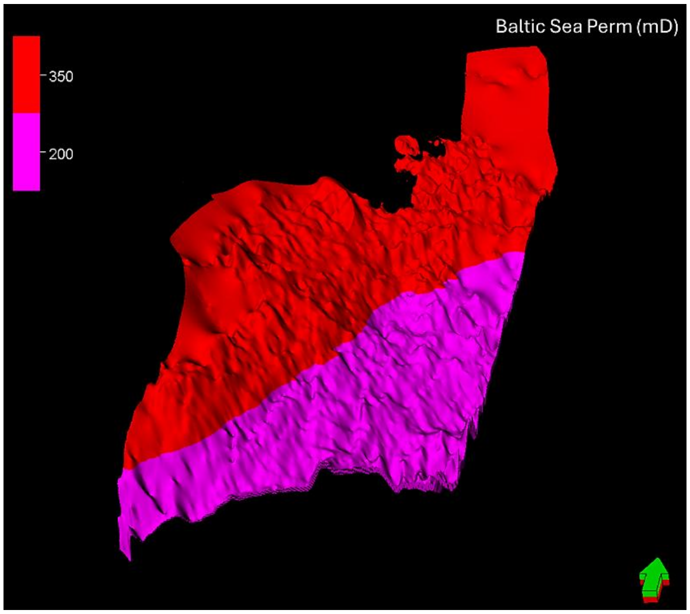

Figure 18: Baltic Sea model property models (top to bottom: porosity, NTG, permeability)

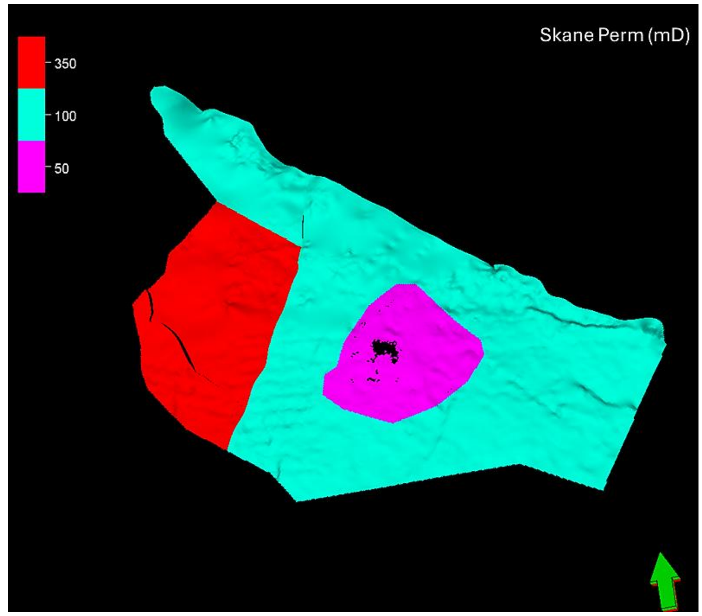

Figure 19: Skåne model property models (top to bottom: porosity, NTG, permeability)

Volumetrics

Original pore volumes were estimated from the porosity and net-to-gross models developed for each reservoir unit. This derived porosity and NTG values were applied as input parameters to compute the original pore volumes. The calculated volumes are presented in Table 4.

Table 4: Faludden sandstone and Arnager Greensand Petrel volumes

Petrel Cases	Bulk volume [x10^6 m^3]	Net volume [x10^6 m^3]	Pore volume [x10^6 m^3]
Faludden sandstone	1,014,413	759,151	102,873
Arnager Greensand	157,391	91,469	19,741

3.3 Upgrading to Simulation Model

The original grid resolution in the Petrel models is 200 m × 200 m × 0.5 m for both the Baltic Sea and Skåne models. Coarser grids with resolutions of 500 m × 500 m × 1 m, 1000 m × 1000 m × 1 m, 500 m × 500 m × 0.5 m, and 1000 m × 1000 m × 0.5 m were subsequently generated, and petrophysical properties were upscaled accordingly for simulation efficiency testing.

3.4 Concerns

Variations in reservoir properties are apparent in both the log plot (Figure 20) and the cross-section (Figure 21). SGU data indicate NTG values for the Arnager Greensand ranging between 0.4 and 0.8, implying substantial heterogeneity. Because the current models use constant properties, they may not adequately represent the distribution of porosity, NTG, and permeability. This limitation could lead to unexpected reservoir behavior, requiring changes to the development strategy. In such cases, CO_2 injection targets may not be met, and project economics may be adversely affected.

3.5 Conclusion

The geomodelling work has been successfully completed, integrating all available data into a consistent and simulation-ready Petrel framework. Appropriate geological interpretations and assumptions were applied where data were limited, ensuring internal consistency while remaining aligned with the project objectives. Grid design and cell size were tested and optimized to balance geological resolution with computational efficiency, resulting in models that are fit for purpose for dynamic CO_2 injection simulations. These models provide a robust basis for evaluating storage performance and for future refinement as additional data becomes available.

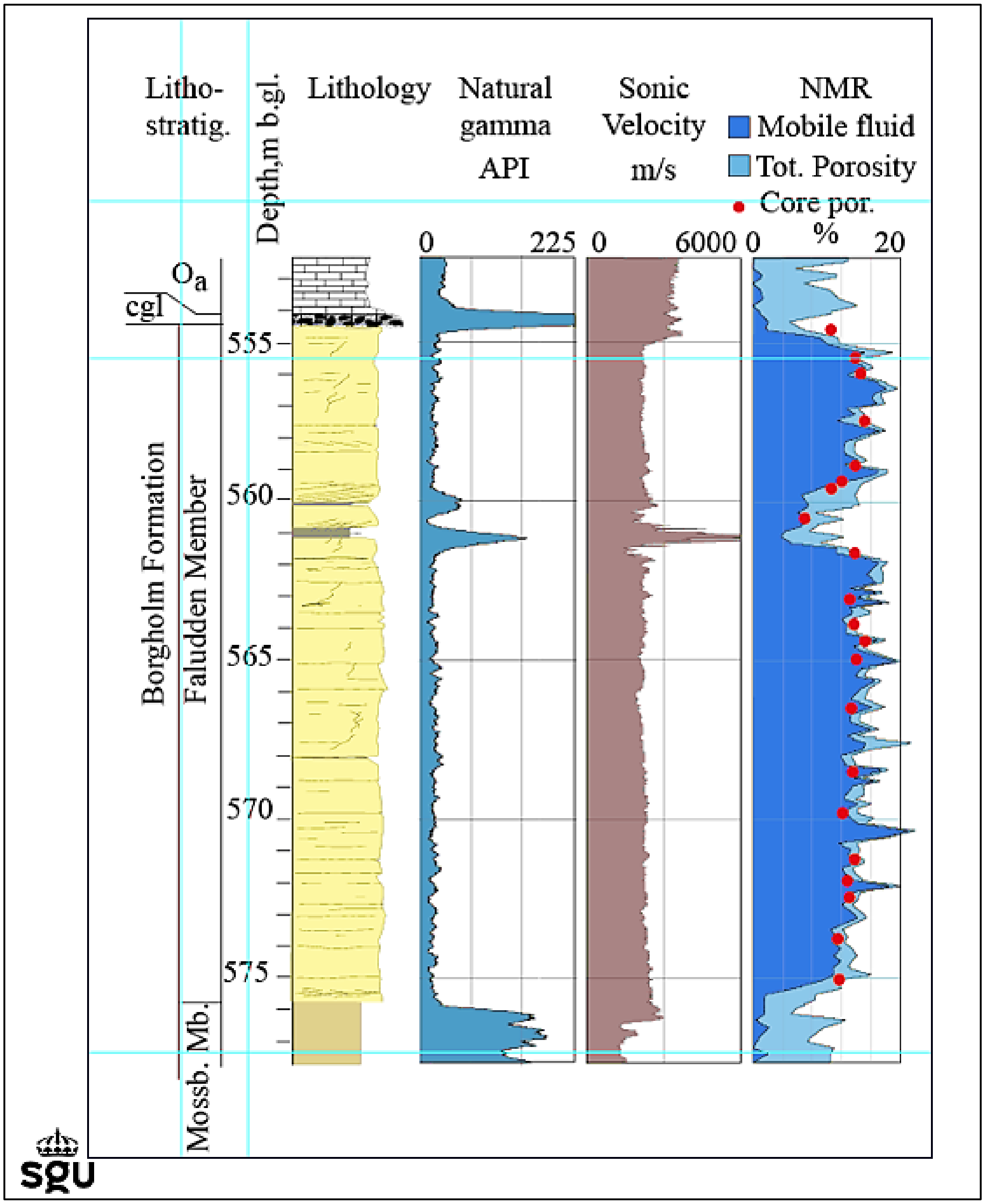

Figure 20: Faludden sandstone in Nore-1 (SGU)

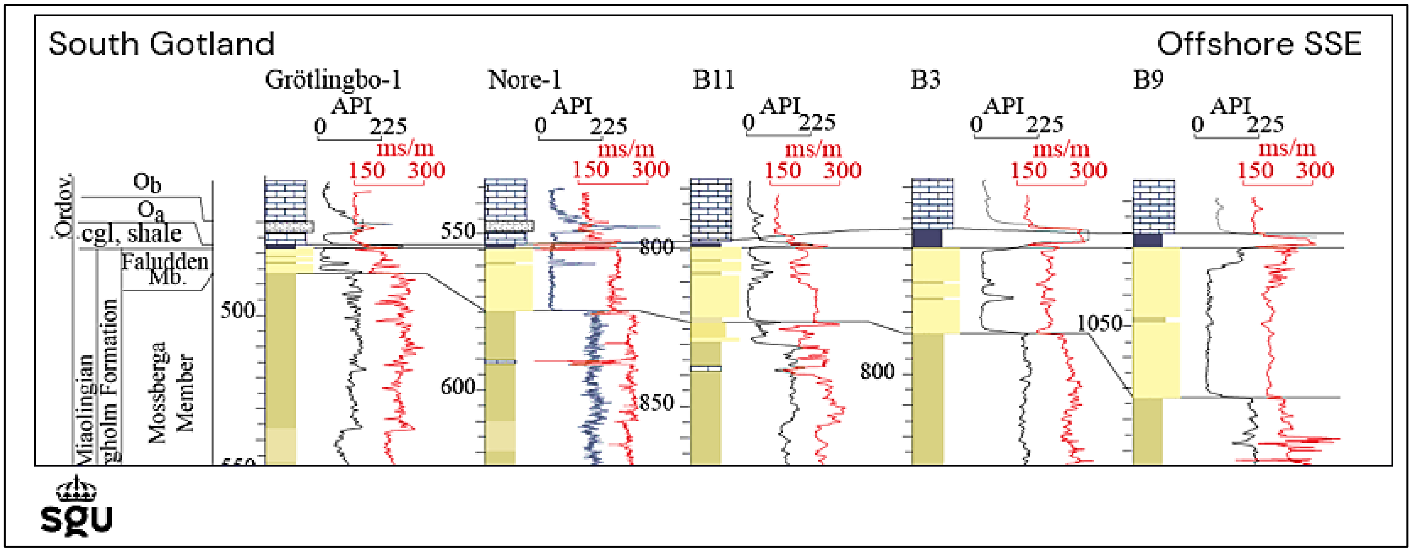

Figure 21: Faludden sandstone – cross section (SGU)

4. Faludden sandstone CO_2 Injection Scenarios

According to the data provided by SGU for the Baltic Sea area, the initial reservoir pressure gradient was set to 97.9 kPa/m; and the reservoir temperature gradient was set as 30.2 °C/km assuming the mean sea level (MSL) temperature is at 10 °C. An average formation-water salinity of 40,000 mg/L was applied.

The gas-water relative permeability curves used for both Baltic Sea and Skåne models are presented in Figure 22 referring to the Generation-4 Integrated Reservoir Modelling Report (Quest CCS Project, 2011). The lowest-hysteresis Krg curve – representing a water-drainage process – indicates a critical gas saturation Sgcrit of 0.05. The mid- and highest-hysteresis Krg curves correspond to water-imbibition processes with Sgcrit of 0.25 and Sgcrit = 0.5, respectively.

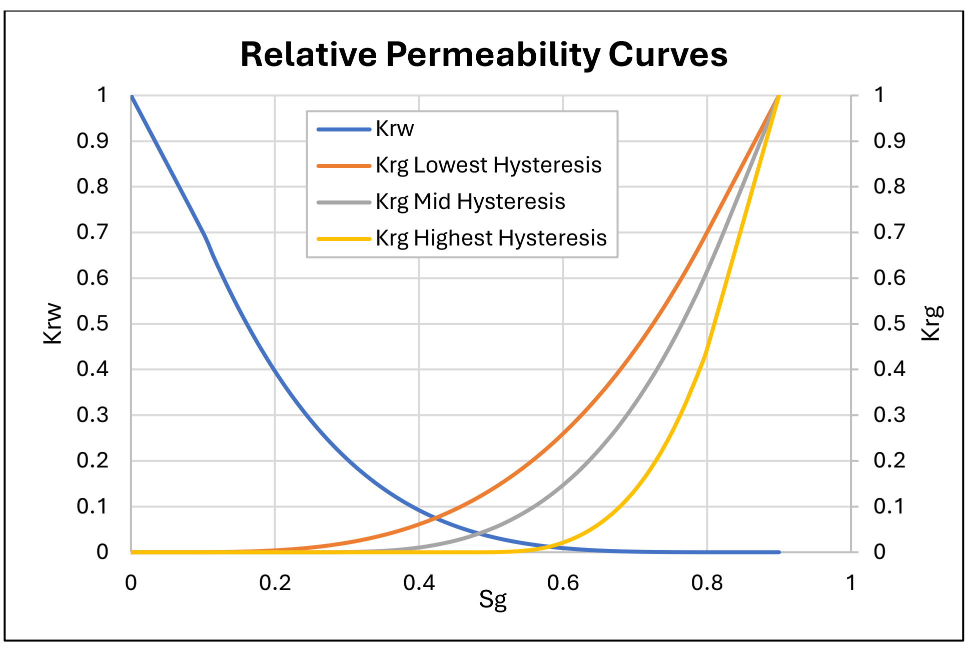

Figure 22: Gas- Water relative permeability curves

Simulation runs were categorized into primary group and secondary group, as summarized in Table 5. The primary group was designed to maximize CO_2 storage capacity while ensuring CO_2 plumes remain below 800 m TVD depth after 30 years of continuous injection followed by 500 years of shut-in. This scenario assumes relatively low CO_2 hysteresis trapping, representing a conservatively safe storage condition where injected CO_2 remains in a high-pressure liquid phase. The secondary group performed sensitivity analysis to assess the influence of key uncertainty parameters on CO_2 storage capacity and plume migration.

For the uncertainty parameters listed in Table 5**,** "Mid perm" refers to mean gas permeability (**Appendix 1.1**), while "High perm" and "Low perm" correspond to the high and low gas permeability categories. A lower vertical-to-horizontal permeability ratio (Kv/Kh = 0.1) was applied in Case 6, whereas the other cases use Kv/Kh = 0.5. A higher well-skin factor (S = +5) was applied in Case 7; all other cases assume a neutral well skin factor of S = 0.

Table 6 provides detailed dynamic model settings. Based on SGU's interpretation, the western side of the area of interest (AOI) was treated as a closed boundary, while the eastern side connects to an additional aquifer. The attached aquifer was assigned an equivalent pore volume to that of the AOI. Each injector was constrained by a maximum injection rate and a maximum bottomhole pressure (BHP). Except for INJ12, all injectors were limited at 1Mt/yr/well. INJ12 was restricted at a lower rate of 0.5 Mt/yr/well. The BHP limit for each injector was calculated using a pressure gradient of 15.7 kPa/m and its local TVD (Quest CCS Project, 2011). Pressure management using water producer wells was considered and explicitly evaluated within the base case scenario development; however, this option was deselected for the current evaluation study.

Table 5: Case definitions for injection in the Faludden sandstone in the Swedish sector of the SE Baltic Sea

Category	No.	Run Period		Uncertainty Parameters	Well number	CO_2 mass injection cumulative [Mt]
		Injection	Shut-in			
Primary Group	1	30 years	500 years	Lowest hysteresis + Mid perm	8	236.4
	2	30 years	500 years	Lowest hysteresis + Mid perm	8 + 4 (Pattern 1)	315.3
	3	30 years	500 years	Lowest hysteresis + Mid perm	8 + 4 (Pattern 2)	323.4
Secondary Group	4	30 years	100 years	Lowest hysteresis + Lowest perm	8 + 4 (Pattern 2)	222.3
	5		**500 years**	**Lowest hysteresis + Highest perm**	**8 + 4 (Pattern 2)**	**344.0**
	6		100 years	Lowest hysteresis + Lowest perm + Lower Kv/Kh	8 + 4 (Pattern 2)	187.7
	7		100 years	Lowest hysteresis + Mid perm + Higher Well Skin	8 + 4 (Pattern 2)	183.5
	8		100 years	Highest hysteresis + Mid perm	8 + 4 (Pattern 2)	323.0
	9		100 years	Mid hysteresis + Mid perm	8 + 4 (Pattern 2)	323.1

Note: Continuous injection was simulated from January 1st, 2026, till January 1st, 2056. Shut-in was initiated thereafter.

Table 6: Reservoir description and well constraints for injection in the Faludden sandstone in the Swedish sector of the SE Baltic Sea AOI

<table>
<tr><th>Reservoir Description</th><th colspan="2">Parameters</th><th>Values</th><th>Comments</th></tr>
<tr><td rowspan="15">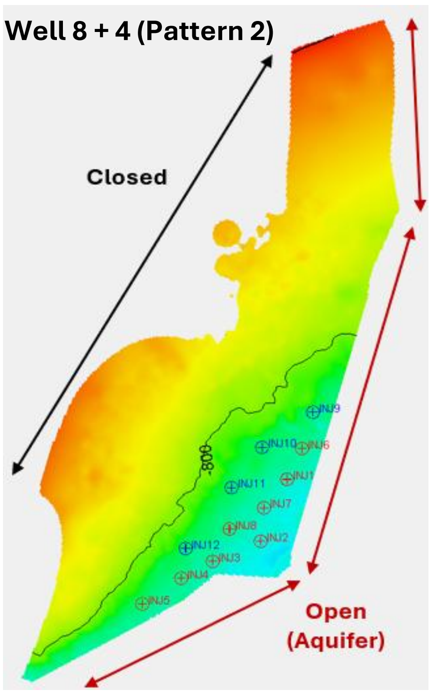
</td><td colspan="2">Pore Volume [m^3]</td><td>2.03 x 10^{11}</td><td>1.02x10^{11} m^3 pore volume + 1.02x10^{11} m^3 aquifer volume</td></tr>
<tr><td rowspan="2">Injection rate [Mt/year]</td><td>INJ1 ~ INJ11</td><td>1.0</td><td rowspan="2">Referring to the settings in the previous report</td></tr>
<tr><td>INJ12</td><td>0.5</td></tr>
<tr><td rowspan="12">Injector BHP [MPa]</td><td>INJ1</td><td>19.0</td><td rowspan="12">15.7 kPa/m x local TVD* (Shell Quest Generation 4 Report)</td></tr>
<tr><td>INJ2</td><td>20.4</td></tr>
<tr><td>INJ3</td><td>18.4</td></tr>
<tr><td>INJ4</td><td>17.1</td></tr>
<tr><td>INJ5</td><td>16.1</td></tr>
<tr><td>INJ6</td><td>17.3</td></tr>
<tr><td>INJ7</td><td>19.1</td></tr>
<tr><td>INJ8</td><td>17.6</td></tr>
<tr><td>INJ9</td><td>15.8</td></tr>
<tr><td>INJ10</td><td>15.1</td></tr>
<tr><td>INJ11</td><td>15.4</td></tr>
<tr><td>INJ12</td><td>15.3</td></tr>
</table>

4.1 Primary Case Scenarios

GLJ first evaluated a four-well injection pattern, which achieved 113.1 Mt of CO_2 injected over the 30-year injection period. The number of injectors was then increased to eight, as suggested by SGU, with the objective of maximizing storage capacity. These two well-layout patterns are shown in **Appendix 1.1**. The eight-well pattern (Case 1) resulted in a cumulative mass of 236.4 Mt over 30 years, as summarized in Table 5**.**

To further assess the storage potential of the model, GLJ expanded the number of injectors to 12 for Case 2 and 3. Four additional injectors were placed northwest of initial eight injectors, but in different spatial arrangements (Figure 23 **(a)** and **(b)**), which are illustrated as Pattern 1 and Pattern 2, respectively. Following 500 years of shut-in, CO_2 plumes from INJ11 and INJ12 in Case 2 migrated beyond the 800 m TVD contour. As a result, the four additional injectors in Case 3 were scattered and repositioned farther north to improve containment. Plumes in Case 3 remained full within the 800 m contour after 500 years of shut-in. Over the 30-year injection period, 315.3 Mt and 323.4 Mt of CO_2 were injected in Case 2 and Case 3, respectively. Based on its superior containment performance and slightly higher storage volume, Case 3 with the Pattern 2 well layout was chosen for detailed analysis. All subsequent sensitivity simulations in the secondary group were performed using the Case 3 well layout.

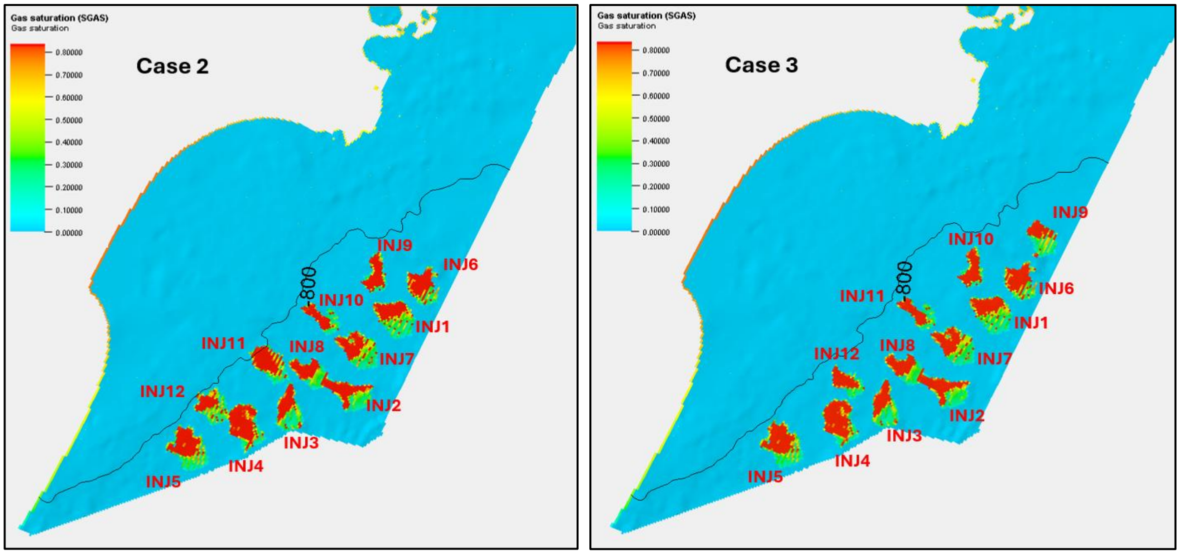

(a) Case 2 (500-yr shut-in) (b) Case 3 (500-yr shut-in)

Figure 23: CO_2 Plumes at the end of 500-yr Shut-in for case 2 and case 3.
(The black line marks the 800m iso-depth for the top of the Faludden sandstone)

The total field CO_2 injection rate and average field pressure for Case 3 are shown in Figure 24 for both the full simulation period and the first 50 years. The field injection initially increased to 11.5 Mt/yr and gradually declined to 9.9 Mt/yr by the end of the 30-year injection period. The average field pressure rose from 3.8 MPa to 6.8 MPa, and then slowly increased to 6.9 MPa as pressure dissipated throughout the AOI and into the attached aquifer. A small influx of water from the eastern aquifer occurred during shut-in due to its slightly higher pressure relative to the average reservoir pressure.

Individual well injection rates and BHPs for all 12 wells in Case 3 are presented in Figure 25 INJ1, INJ2, INJ3, INJ4, INJ6, INJ7, and INJ9 were generally able to maintain the 1 Mt/yr/well target throughout the 30-year injection period. The remaining five injectors exhibited declining flow rates when their respective BHP constraints were reached at various times during the simulation. The per well basis cumulative injected CO_2 amounts for all the studied cases in the Baltic Sea model are summarized in Table 12 of **Appendix 1.2**.

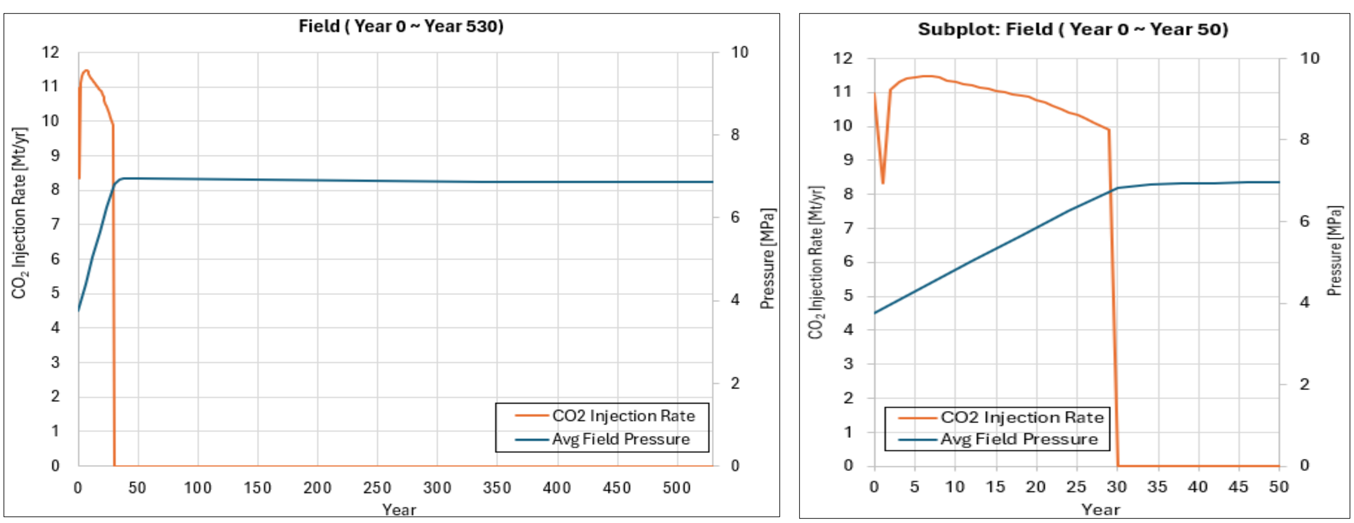

(a) Entire Period: 30-yr Injection + 500-Yr Shut-in (b) Zoomed-in for the first 50 Years

Figure 24: Total field CO_2 injection rate and field average pressure for case 3 in Baltic Sea, plotted for the entire period and zoomed-in first 50 years

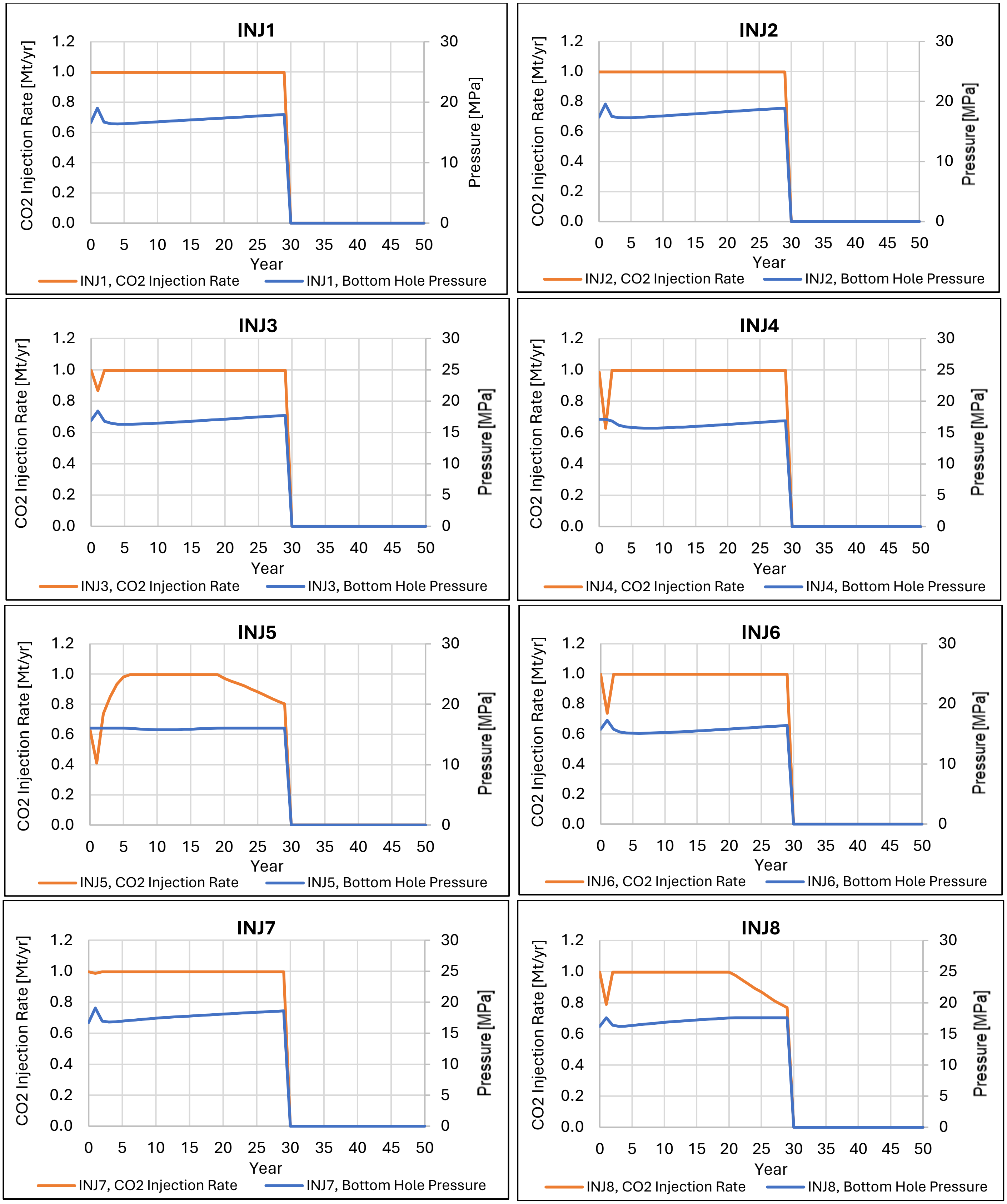
INJ1
CO2 Injection Rate [Mt/yr]
Pressure [MPa]
Year
INJ1, CO2 Injection Rate
INJ1, Bottom Hole Pressure
INJ2
CO2 Injection Rate [Mt/yr]
Pressure [MPa]
Year
INJ2, CO2 Injection Rate
INJ2, Bottom Hole Pressure
INJ3
CO2 Injection Rate [Mt/yr]
Pressure [MPa]
Year
INJ3, CO2 Injection Rate
INJ3, Bottom Hole Pressure
INJ4
CO2 Injection Rate [Mt/yr]
Pressure [MPa]
Year
INJ4, CO2 Injection Rate
INJ4, Bottom Hole Pressure
INJ5
CO2 Injection Rate [Mt/yr]
Pressure [MPa]
Year
INJ5, CO2 Injection Rate
INJ5, Bottom Hole Pressure
INJ6
CO2 Injection Rate [Mt/yr]
Pressure [MPa]
Year
INJ6, CO2 Injection Rate
INJ6, Bottom Hole Pressure
INJ7
CO2 Injection Rate [Mt/yr]
Pressure [MPa]
Year
INJ7, CO2 Injection Rate
INJ7, Bottom Hole Pressure
INJ8
CO2 Injection Rate [Mt/yr]
Pressure [MPa]
Year
INJ8, CO2 Injection Rate
INJ8, Bottom Hole Pressure

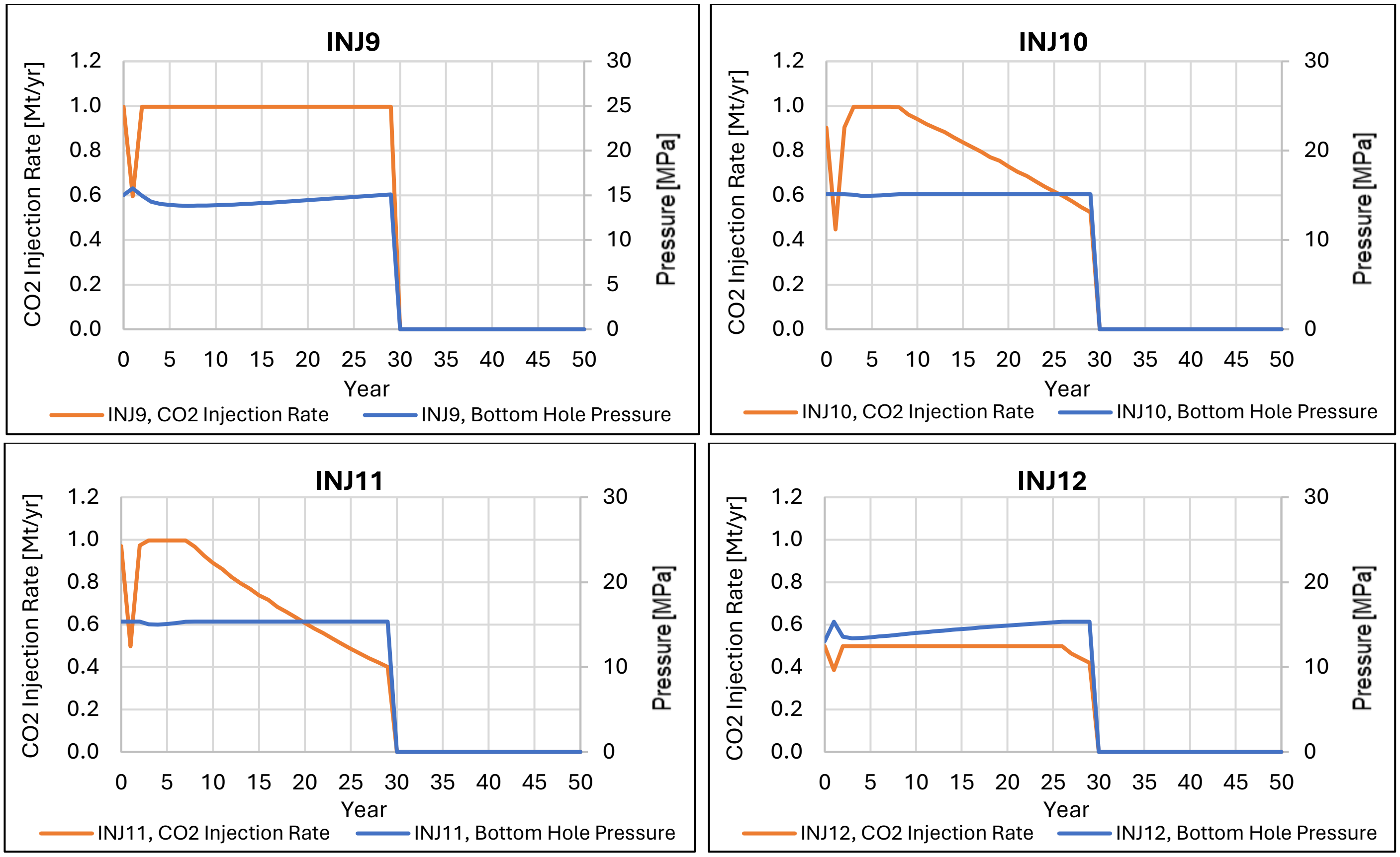

Figure 25: CO_2 injection rate and bottom hole pressure for individual wells in case 3 in Baltic Sea

The plume dimensions are summarized in Table 7**.** In the X-direction, plume extents range from 16,000 m to 27,000 m, while in the Y-direction, they range from 8,000 m to 22,000 m, which is generally smaller than the X direction extent. A top view of the CO_2 plumes around the injectors is shown in Figure 26 **(a)**. As illustrated, the plumes primarily migrate in the up-dip direction of the Faludden sandstone. Figure 26 (b) shows the 3D views of the representative plumes and Figure 26 (c) show the cross-sectional view of the plume from INJ10.

Top-view pressure profiles at the initial time step, at the end of injection, and after the 500-year shut-in period are shown in Figure 27. Around the injector locations, reservoir pressures increase substantially during injection and then gradually dissipate across the AOI and into the attached aquifer over time.

Table 7: Plume dimension of each well for case 3 in Baltic Sea

Well No.	X [m]	Y [m]	Well No.	X [m]	Y [m]
INJ1	23,000	19,000	**INJ7**	25,000	17,000
INJ2	27,000	16,000	**INJ8**	19,000	15,000
INJ3	14,000	22,000	**INJ9**	16,000	18,000
INJ4	21,000	18,000	**INJ10**	21,000	12,000
INJ5	21,000	18,000	**INJ11**	22,000	13,000
INJ6	19,000	19,000	**INJ12**	18,000	8,000

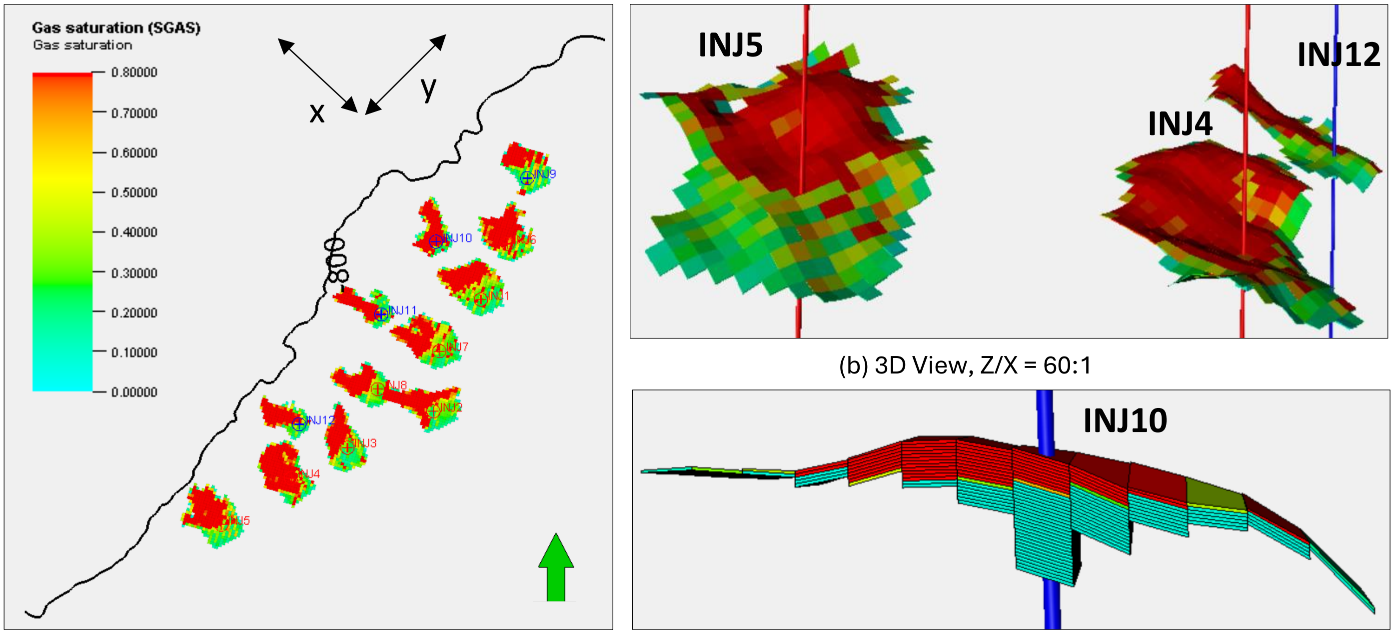

(a) Top View (c) Cross-Section View of A Plume, Z/X = 60:1

Figure 26: Plumes of each well from zoomed-in views at the end of 500-year shut-in for case 3 in Baltic Sea

4.2 Secondary Case Scenarios and Sensitivity Analysis

A sensitivity analysis was conducted in the secondary group simulations using the Case 3 well layout. As shown in Case 4 of Table 5, the lowest-permeability scenario significantly reduced the cumulative injected CO_2 to 222.3 Mt. When combined with a lower Kv/Kh = 0.1, the cumulative injected CO_2 decreased further to 187.7 Mt, as reported in Case 6. A higher well-skin factor (S = +5) also proved to be a key parameter, reducing the cumulative injected CO_2 by more than 40%, as indicated in Case 7. The hysteresis factor has only a minor influence on total storage capacity (Case 8 and 9), but it significantly affects the plume morphology, as shown in **Appendix 1.3**. In general, a higher hysteresis factor leads to smaller plume extents. Field-level and well-level injection rates for the secondary-group cases are summarized in **Appendix 1.2**.

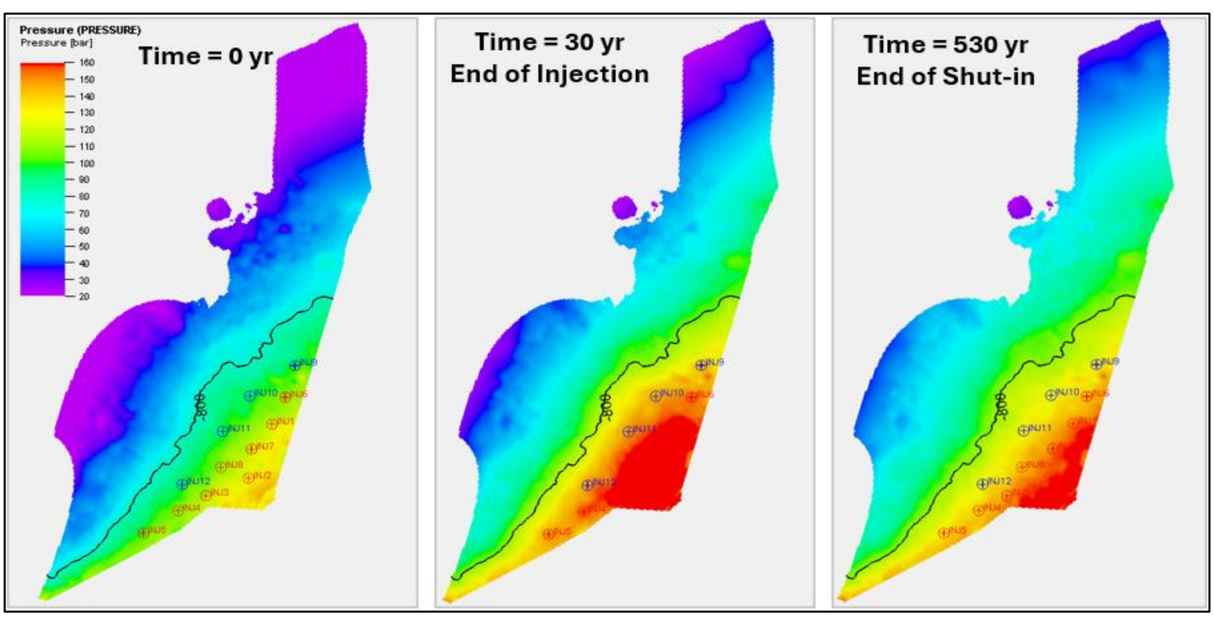

Figure 27: Reservoir pressure at the initial condition, end of injection, and end of shut-in for case 3 in Baltic Sea

Case 5 demonstrates that in the highest-permeability scenario, the CO_2 storage capacity increases to 344.0 Mt, which is more than 20 Mt higher than Case 3. This indicates that system permeability has a relatively strong influence compared to the other parameters tested. However, after 500-year shut in, plumes in Case 5 migrate beyond the 800 m TVD contour, as shown in Figure 28. This suggests that a much higher system permeability accelerates the plume migration, especially when the hysteresis factor is low.

Figure 29 illustrates the trapping mechanisms and corresponding amounts of CO_2 for the three selected three cases representing the lowest, mid, and highest hysteresis factors. A higher hysteresis factor significantly increases CO_2 trapped by capillary forces. When a lower hysteresis factor is applied, the amount of CO_2 trapped through hysteresis becomes relatively small compared to the amount dissolved into the formation brine.

4.3 Summary

The Baltic Sea AOI has the potential to store more than 300 Mt of CO_2. Although higher reservoir permeability can significantly increase storage capacity, it also introduces a greater risk of CO_2 plume migration beyond the 800 m TVD contour after 500 years of shut-in. The well skin factor has a relatively stronger influence in the Baltic Sea model than that in the Skåne model, largely because the injectors operate under higher rate constraints. Furthermore, hysteresis factor can substantially influence the trapped CO_2 by capillary forces, which can be better quantified based on the corresponding lab experiments.

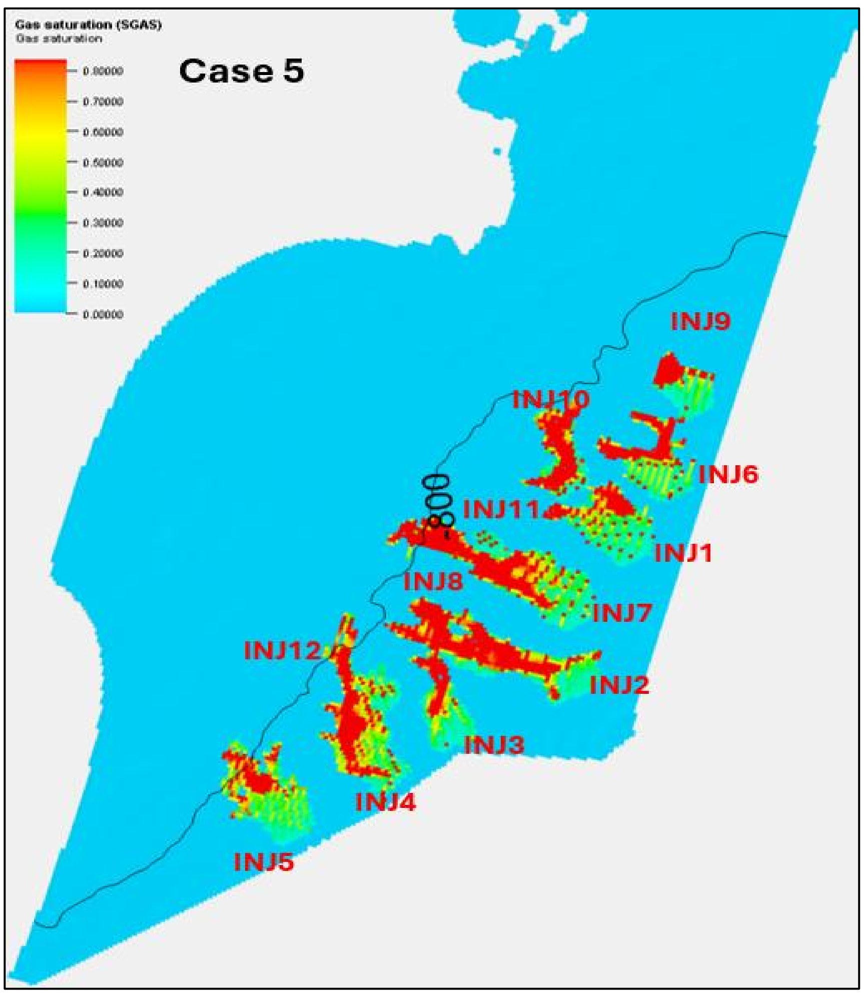

Figure 28: CO_2 Plumes at the end of 500-yr shut-in for case 5

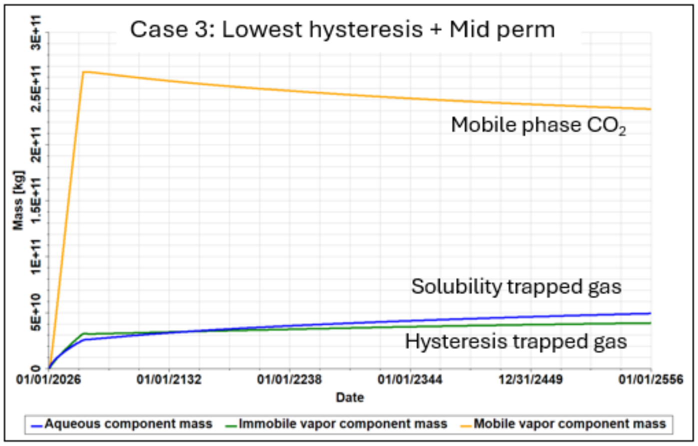

(a) Case 3: Lowest Hysteresis + Mid Perm

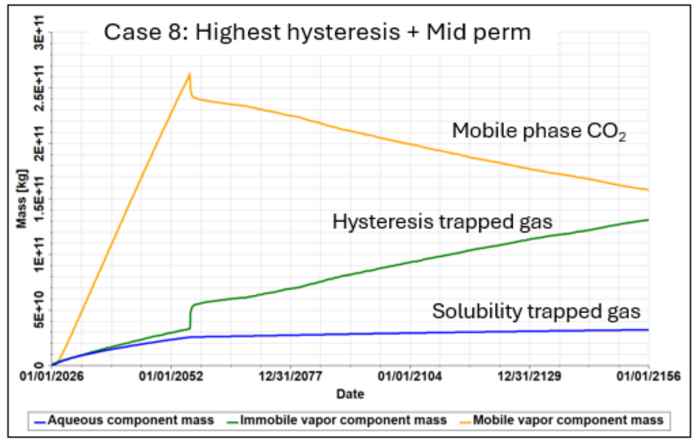

(b) Case 8: Highest Hysteresis + Mid Perm

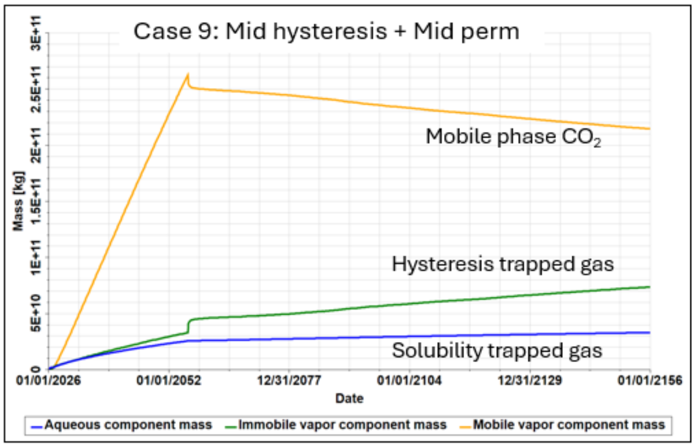

(c) Case 9: Mid Hysteresis + Mid Perm

Case No.	Solubility trapped gas [Mt]	Hysteresis trapped gas [Mt]	Mobile phase CO_2 [Mt]
Case 3**	49.7	41.2	232.1
Case 8*	32.7	131.6	158.5
Case 9*	33.5	74.1	215.0
Note: ** Shut-in for 500 year at Jan 1, 2556; * Shut-in for 100 year at Jan 1, 2156			

(d) Trapping Amounts in the Selected Cases

Figure 29: Trapping mechanisms and breakdown amounts of the selected cases in Baltic Sea

5. Arnager Greensand CO_2 Injection Scenarios

According to the data provided by SGU for the Skåne area, the initial reservoir pressure gradient was set to 97.9 kPa/m; and the reservoir temperature gradient was initialized at 26.1 °C/km, assuming the mean sea level (MSL) temperature is at 10 °C. Formation water Salinity was initialized as a function of TVD depth, ranging from 120,000 to 160,000 mg/L. The gas-water relative permeability curves and hysteresis parameters were the same as those used in the Baltic Sea model.

As with the Baltic Sea analysis, the simulation runs for the Skåne model were categorized into primary and secondary groups, as summarized in Table 8**.** The primary group aimed to achieve a reasonably high CO_2 storage capacity, while ensuring that plumes remained away from the major faults and below the 800 m TVD contour after 30 years of continuous injection followed by 500 years of shut-in, assuming the lowest CO_2 hysteresis trapping. The secondary group performed sensitivity analyses on key reservoir and well parameters. A horizontal well configuration was also evaluated to assess its influence on storage capacity and plume migration.

For the uncertainty parameters in Table 8**,** "Mid perm" refers to mean gas permeability (**Appendix 2.1**), while "High perm" and "Low perm" represent the high and low gas perm categories. A lower vertical to- horizontal permeability ratio (Kv/Kh = 0.1) was applied in Case 5; all other cases used Kv/Kh = 0.5. A well-skin factor of S = +5 was applied in Case 7, while the remaining cases assumed S = 0 (neutral skin).
Table 9 summarizes the detailed dynamic-model settings. Based on SGU's interpretation, the northeast side of the AOI was treated as a closed boundary, while the southwest side connects to an additional aquifer with an

equivalent pore volume. Injection wells were constrained by maximum injection rates and bottom-hole pressure (BHP) limits. INJ1 and INJ3 were constrained at 1 Mt/yr/well due to their location in a high-permeability region, while the other injectors were limited to 0.5 Mt/yr/well. BHP limits were calculated using a pressure gradient of 15.7 kPa/m and local TVD (Quest CCS Project, 2014). Pressure management using water producer wells was considered and explicitly evaluated within the base case scenario development; however, this option was deselected for the current evaluation study.

5.1 Primary Case Scenario

GLJ first evaluated the placement of four injectors in the deeper region as shown in **Appendix 2.1**. The layout is similar to what was indicated in SGU's previous report (Mortensen et al. (2016)). Under this configuration, only 36.1 Mt of CO_2 could be injected over the 30-year injection period. Following SGU's suggestions and additional information provided, five injectors were then placed outside the coastline for Case 1. The corresponding well layout is shown in Figure 63 in **Appendix 2.1**. Table 8 indicates that 86.3 Mt of cumulative CO_2 was injected over 30 years. Figure 30 **(a)** presents the 3D-view plume map, which shows that the plume from INJ4 migrated outside the studied AOI, crossing the Sweden–Denmark international border. The corresponding 2D-view plume map with the coastline is shown in Figure 31 (a). All the injection sites are located offshore and outside the coastline.

To further increase the storage capacity, GLJ added two additional offshore injectors—INJ6 and INJ7—in Case 2, resulting in 101.3 Mt of CO_2 injected over 30 years. The 3D-view plumes for Case 2 are shown in Figure 30 **(b)**. The corresponding 2D-view plume map with coastline is shown in Figure 31(b). After 500 years of shut-in, the plume edges remained 2 to 3 km away from the major faults and significantly distant from the 800 m TVD contour line. Therefore, Case 2 was selected for detailed evaluation. It is worth noting that plumes from both INJ4 and INJ6 encroached beyond the AOI, again crossing the Sweden–Denmark international border. Plumes also encroach across the coastline and get into the onshore areas.

Table 8: Case definitions for injection in the Arnager Greensand

Category	No.	Run Period		Uncertainty Parameters	Well number	CO_2 mass injection cumulative, [Mt]
		Injection	Shut-in			
Primary Group	1	30 years	500 years	Lowest hysteresis + Mid perm	5	86.3
	2	30 years	500 years	Lowest hysteresis + Mid perm	5 + 2	101.3
Secondary Group	3	30 years	100 years	Lowest hysteresis + Lowest perm	5 + 2	60.9
	4		**500 years**	**Lowest hysteresis + Highest perm**	**5 + 2**	**123.6**
	5		100 years	Lowest hysteresis + Lowest perm + Lower Kv/Kh	5 + 2	49.7
	6		100 years	Lowest hysteresis + Mid perm + Higher Well Skin	5 + 2	93.7
	7		100 years	Highest hysteresis + Mid perm	5 + 2	101.1
	8		100 years	Mid hysteresis + Mid perm	5 + 2	101.2
	9		**500 years**	**Lowest hysteresis + Mid perm incl. 4 HZ Wells***	**5 + 2**	**110.8**

Note: Continuous injection was simulated from January 1st, 2026, till January 1st, 2056. Shut-in was initiated thereafter.

Table 9: Reservoir description and well constraints for injection in Arnager Greensand

Reservoir Description	Parameters		Values	Comments
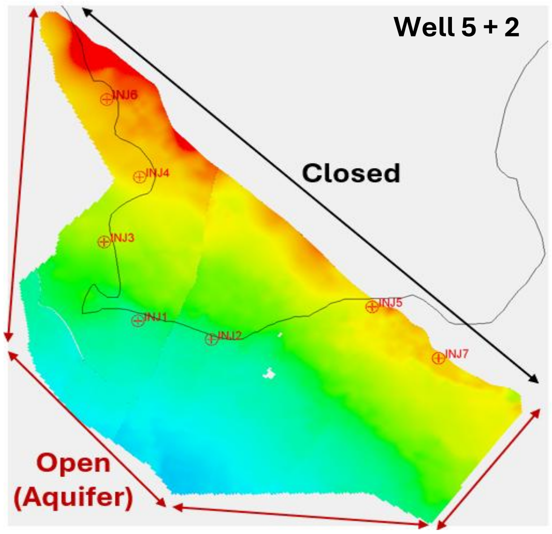	Pore Volume [m^3]		3.94 x 10^{10}	1.97x10^{10} m^3 pore volume + 1.97x10^{10} m^3 aquifer volume
	Injection rate [Mt/year]	*INJ2, INJ4, INJ5, INJ6, INJ7*	0.5	Follow the values in the previous report
		INJ1, INJ3	1.0	
	Injector BHP [MPa]	*INJ1*	17.36	15.7 kPa/m x local TVD* (Shell Quest Generation 4 Report)
		INJ2	17.69	
		INJ3	21.45	
		INJ4	25.87	
		INJ5	25.80	
		INJ6	27.71	
		INJ7	25.94	

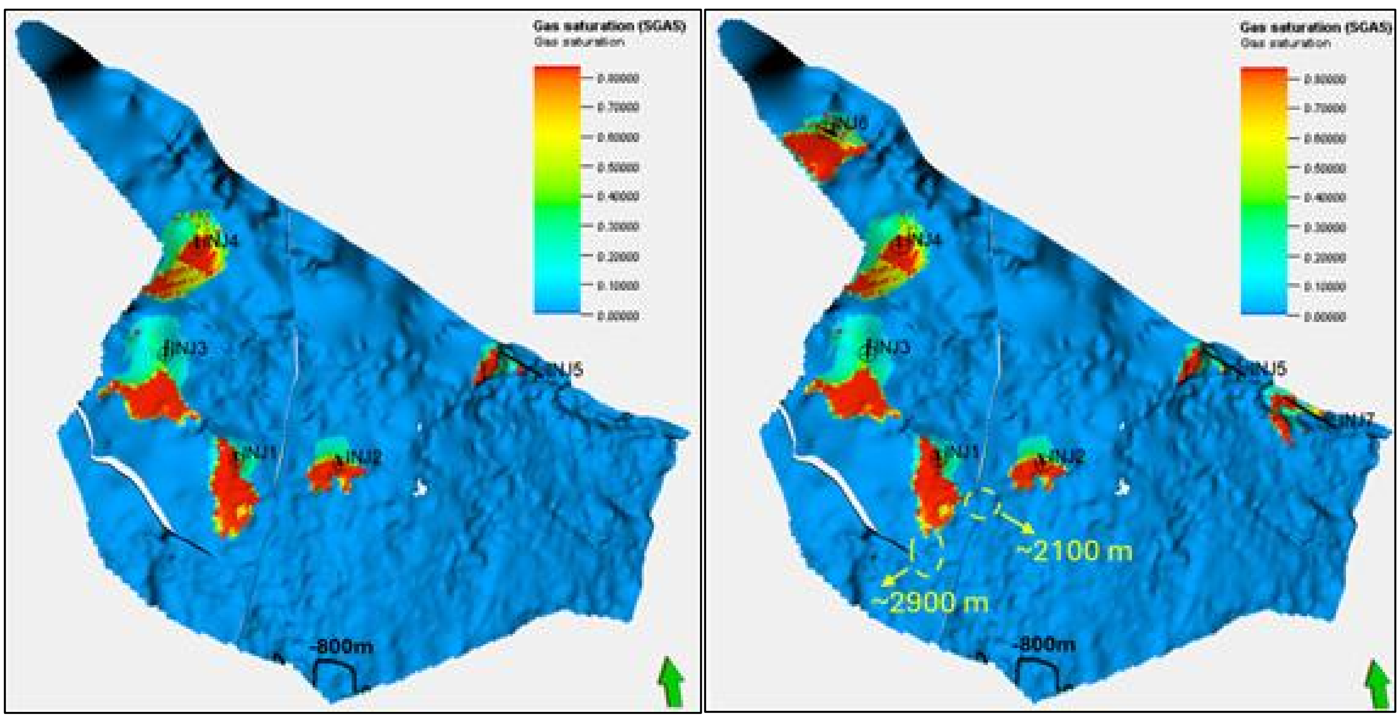

(a) Case 1 (b) Case 2

Figure 30: CO_2 Plumes at the end of 500-yr shut-in for case 1 and case 2 in Skåne

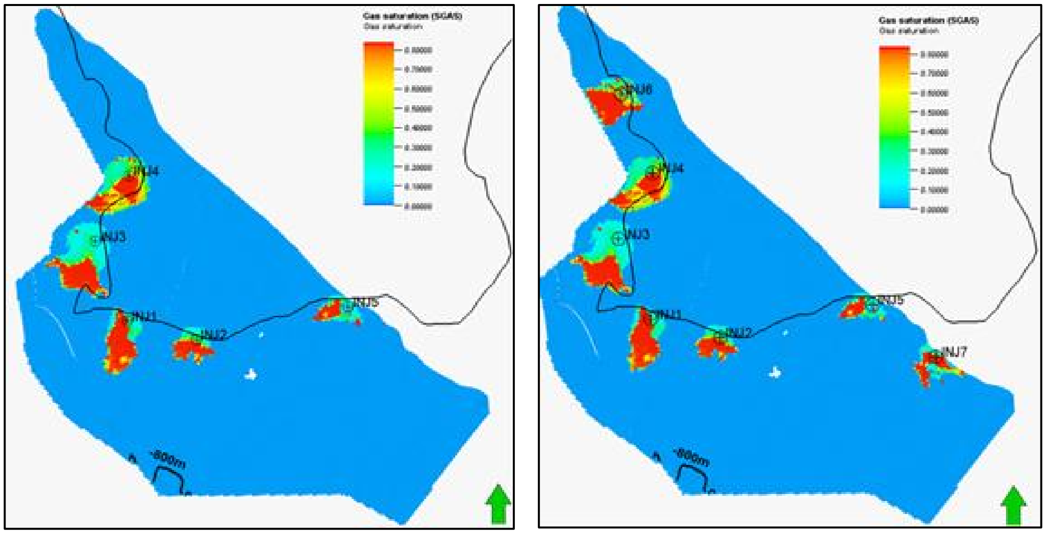

(a) Case 1 (b) Case 2

Figure 31: CO_2 Plumes at the end of 500-yr shut-in for case 1 and case 2 with coastline in Skane, 2D view (The black line marks the coastline)

The total field CO_2 injection rate and average field pressure in Case 2 are shown in Figure 32 for both the entire simulation period and the first 50 years. The field injection initially increased to 3.6 Mt/yr and gradually declined to 3.1 Mt/yr by the end of the 30-year injection period. The average field pressure rose from 5.9 MPa, increased to 10.9 MPa, and then slightly decreased at 10.8 MPa as pressure dissipated across the AOI and into the attached aquifer.

Individual well injection rates and BHPs for all seven wells in Case 2 are presented in Figure 33**.** INJ1 and INJ3 were generally able to maintain the 1 Mt/yr/well target throughout the injection period. The other five injectors were unable to meet the 0.5 Mt/yr/well rate constraint and exhibited declining flow rates as their respective BHP limits were reached early in the injection period. The per well basis cumulative injected CO_2 amounts for all the studied cases in the Skåne model are summarized in Table 14 of **Appendix 2.2**.

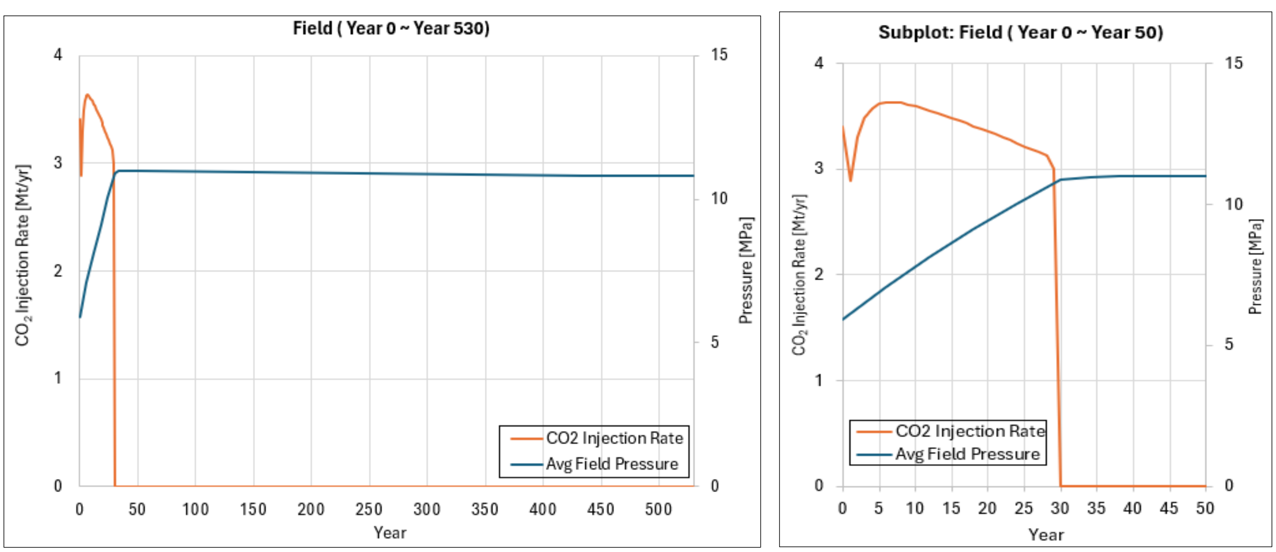

(a) Entire Period: 30-yr Injection + 500-Yr Shut-in (b) Zoomed-in for the first 50 Years

Figure 32: Total field CO_2 injection rate and field average pressure for case 2 in Skåne, plotted for the entire period and zoomed-in first 50 years

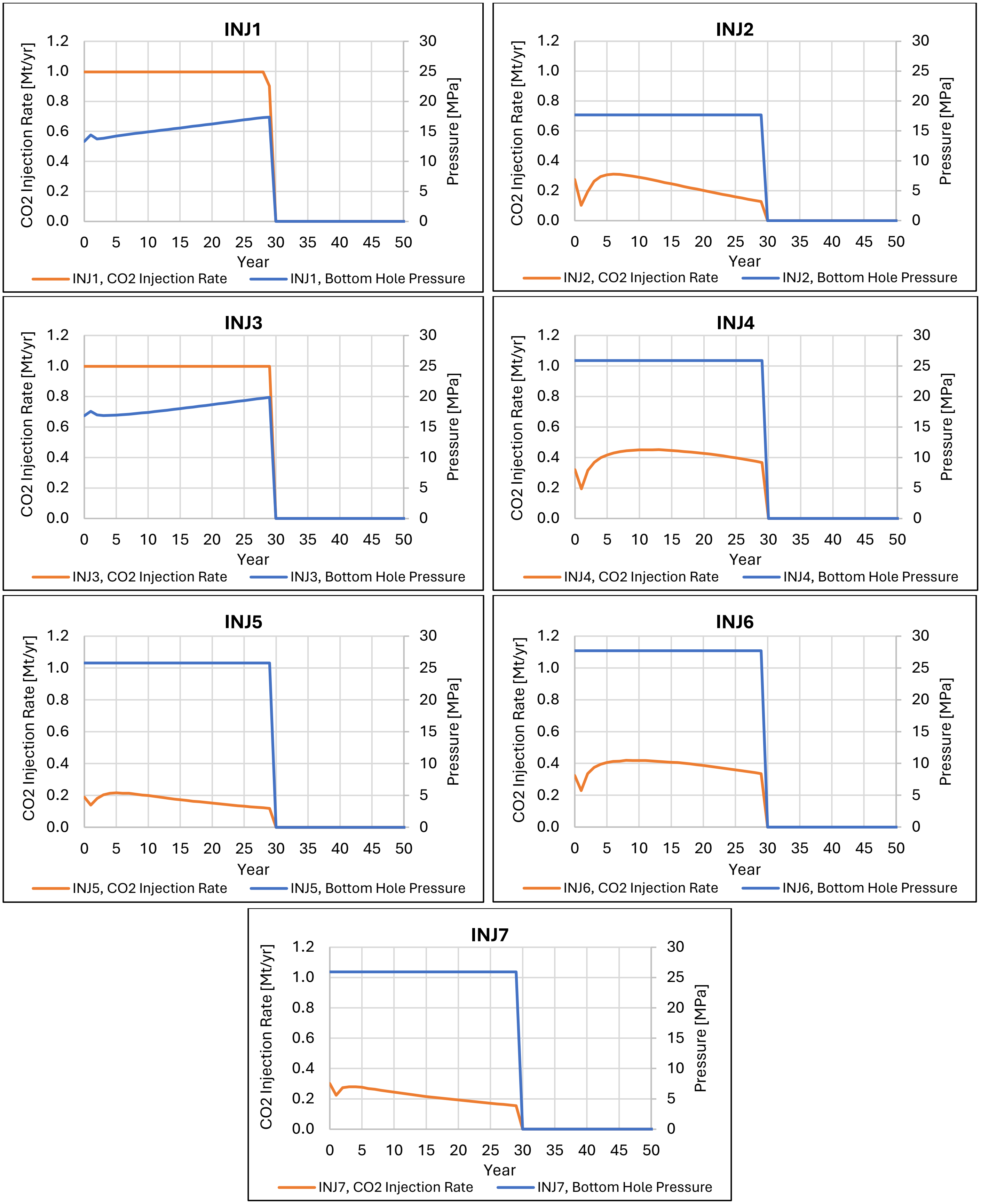

Figure 33: CO_2 injection rate and bottom hole pressure for individual wells in case 2 in Skåne

The plume dimensions are summarized in Table 10. In the X-direction-, plume extents range from 8,000 m to 15,500 m, while in the Y-direction- they range from 9,000 m to 16,500 m, which is generally larger than the X-direction extent. A top-view map of the CO_2 plumes around the injectors is shown in Figure 34 **(a)**. Similar to observations in the Baltic Sea model, plumes in the Skåne model migrate in the up-dip direction of the formation structure and part of the plumes encroaches- into the onshore area. Figure 34 (b) shows the 3D views of the representative plumes and Figure 34 (c) show the cross-sectional view of the plume from INJ10.

Top-view pressure profiles at the initial time step, at the end of injection, and after the 500-year shut-in are shown in Figure 35. Similar to the Baltic Sea case, reservoir pressure in the Skåne case increases substantially near the injector locations and in the deeper formation regions, then gradually dissipates across the AOI and into the attached aquifer over time.

Table 10: Plume geometry of each well for cases in primary group

Well No.	X [m]	Y [m]	Well No.	X [m]	Y [m]
INJ1	8,000	11,500	**INJ5**	9,500	8,500
INJ2	9,000	9,000	**INJ6**	12,000	12,000
INJ3	15,500	16,500	**INJ7**	11,000	10,000
INJ4	11,500	16,500			

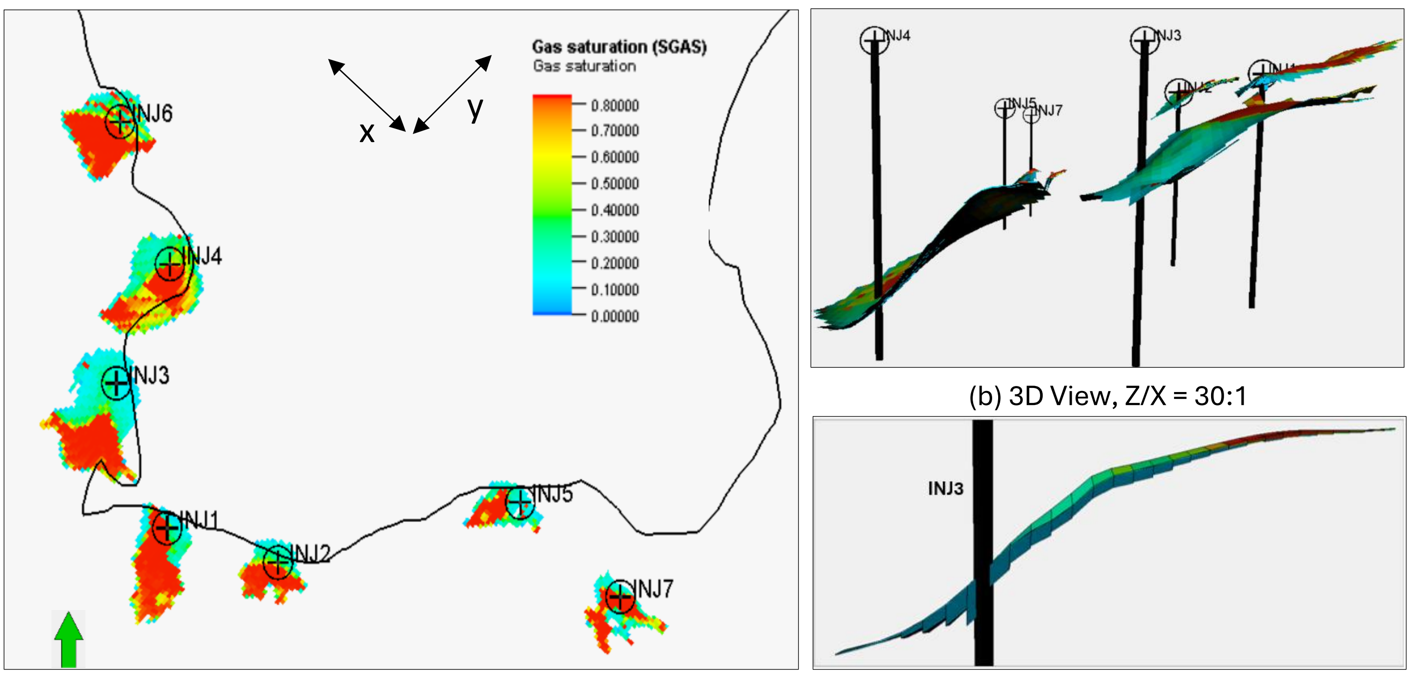

(a) Top View (c) Cross-Section View of A Plume, Z/X = 30:1

Figure 34: Plumes of each well from zoomed-in views at the end of 500-year shut-in for case 2 in Skåne

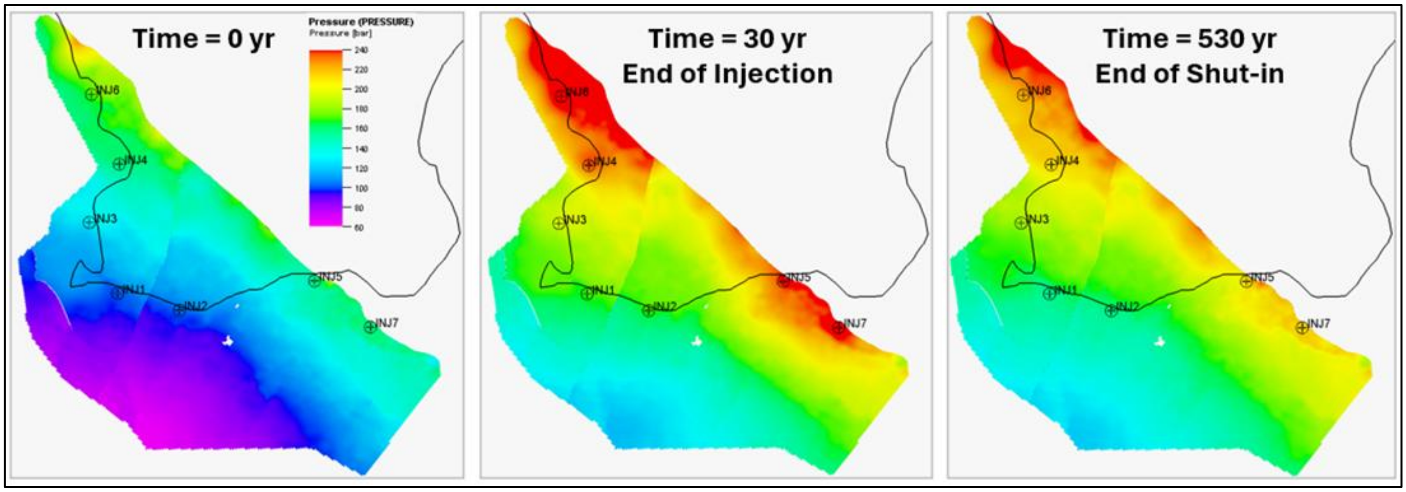

Figure 35: Reservoir pressure at the initial condition, end of injection, and end of shut-in for case 2 in Skåne

5.2 Secondary Case Scenario and Sensitivity Analysis

A sensitivity analysis was conducted in the secondary group simulations using the Case 2 well layout. The lowest-permeability scenario significantly reduced the cumulative injected CO_2 to 60.9 Mt. When combined with a lower Kv/Kh = 0.1, the cumulative injected CO_2 decreased further to 49.7 Mt, as reported in Case 5. A higher well-skin factor (S = +5) reduced the cumulative injected CO_2 by less than 8%, as indicated in Case 6. The hysteresis factor has only a minor influence on total storage capacity (Cases 7 and 8), but it significantly affects plume geometry, as shown in **Appendix 2.3**. In general, a higher hysteresis factor leads to smaller plume extents. Field-level and well-level injection rates for the secondary group cases are summarized in **Appendix 2.2**.

Case 4 demonstrates that in the highest perm scenario, the CO_2 storage capacity increases to 123.6 Mt, more than 20 Mt higher than in Case 2. Thus, system permeability shows a relatively strong influence compared to the other parameters tested. After the 500-year shut in, however, plumes migrate into the major faults and beyond the studied AOI, as shown in Figure 36. The corresponding 2D-view plume map with coastline is shown in Figure 37. This indicates that a much higher system permeability can accelerate plume migration, particularly when the hysteresis factor is low.

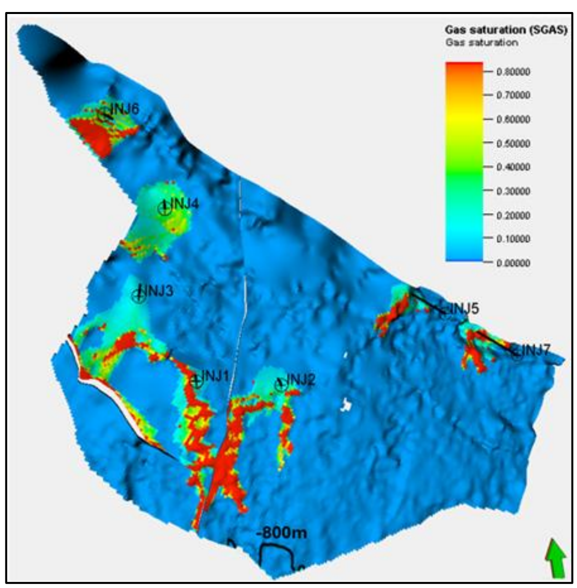

Figure 36: CO_2 plumes at the end of 500-yr shut-in for case 4 in Skåne

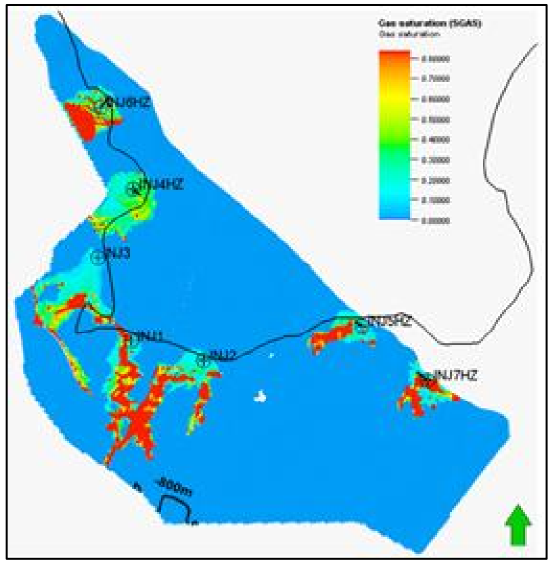

Figure 37: CO_2 plumes at the end of 500-yr shut-in for case 4 with the coastline in Skane, 2D view

Case 9 was created to evaluate the effects of horizontal wells on plume migration and CO_2 storage capacity. As shown in Figure 38, INJ4HZ and INJ5HZ include horizontal laterals approximately 2,000 m in length, while INJ6HZ and INJ7HZ incorporate laterals approximately 3,000 m long. The corresponding 2D-view plume map with the coastline is shown in Figure 37. It is worth noting that the horizontal laterals for INJ4HZ and INJ6HZ were oriented away from the western boundary (the Sweden–Denmark border) to assess whether plume movement could also be redirected. The results indicate that the cumulative CO_2 storage capacity increased by around 10% when four vertical wells were replaced with horizontal wells. However, the CO_2 plumes from INJ4HZ and INJ6HZ still migrated beyond the border after 500-year shut-in. The corresponding 2D-view plume map with the coastline is shown in Figure 39.

Plume migrations for Case 2 and Case 9 are also compared at the time of 100-year shut-in, as shown in Figure 40**.** The corresponding 2D-view plume maps with the coastline are shown in Figure 41. At this time, both INJ4 and INJ4HZ have reached the western border. Horizontal wells generated slightly larger plume extents than vertical wells due to their higher injected CO_2 volumes. The corresponding 2D-view plume maps with the coastline for the rest cases are summarized in Figure 81 of **Appendix 2.3**.

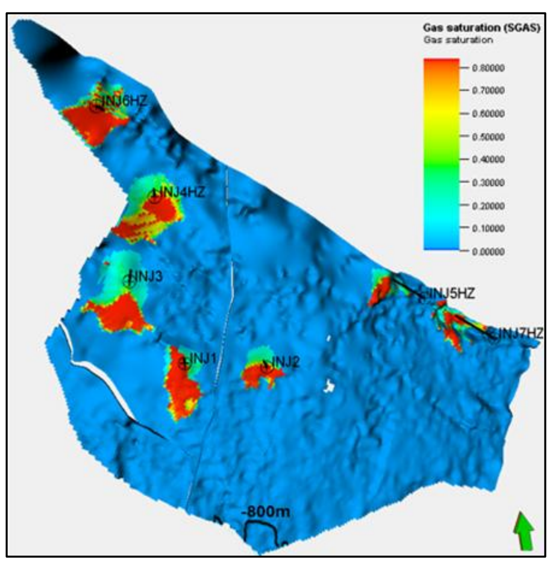

Figure 38: CO_2 plumes at the end of 500-yr shut-in and pressure regions near major fault for case 9 in Skåne

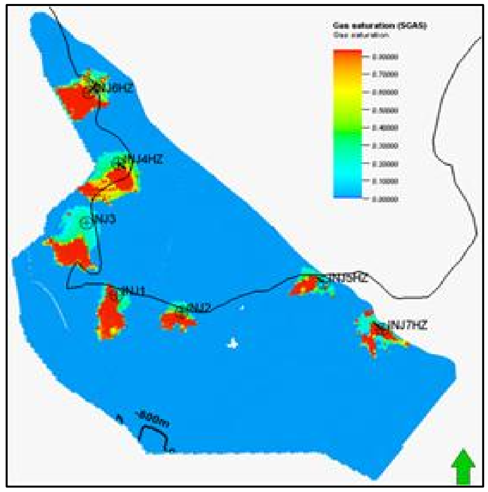

Figure 39: CO_2 plumes at the end of 500-yr shut-in for case 9 with coastline in Skane, 2D view

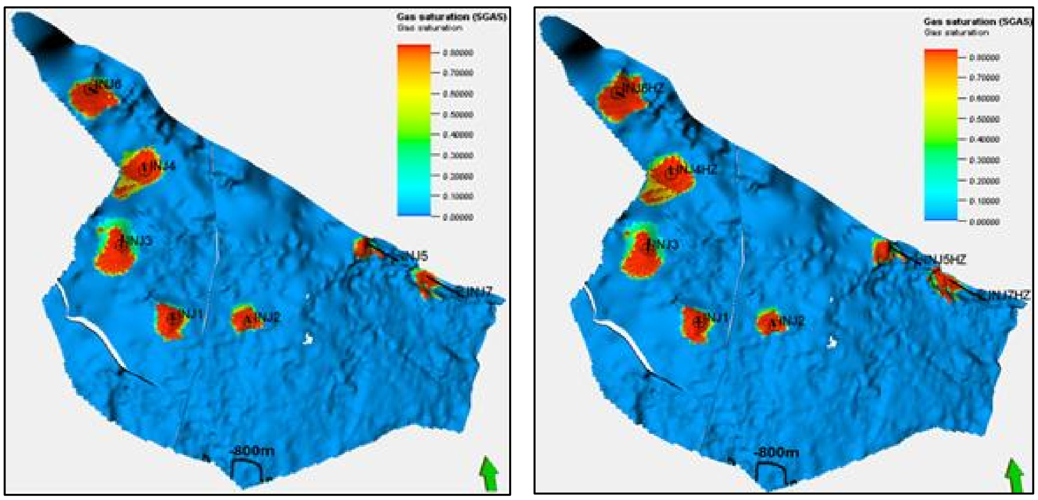

(a) Case 2 (100 shut-in) (b) Case 9 (100 shut-in)

Figure 40: CO_2 plumes at the end of 100-yr shut-in for case 2 and case 9 in Skåne

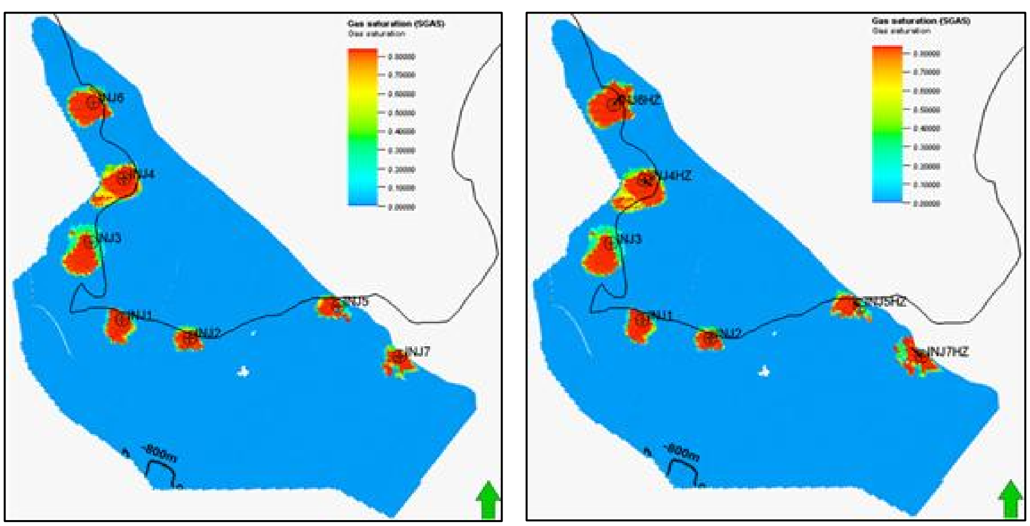

(a) Case 2 (100 shut-in) (b) Case 9 (100 shut-in)

Figure 41: CO_2 plumes at the end of 100-yr shut-in for case 2 and case 9 with coastline in Skane, 2D view

Figure 42 illustrates the trapping mechanisms and corresponding CO_2 amounts for the three selected cases with the lowest, mid, and highest hysteresis factors. Similar to the Baltic Sea cases, the hysteresis factor can significantly influence capillary trapping.

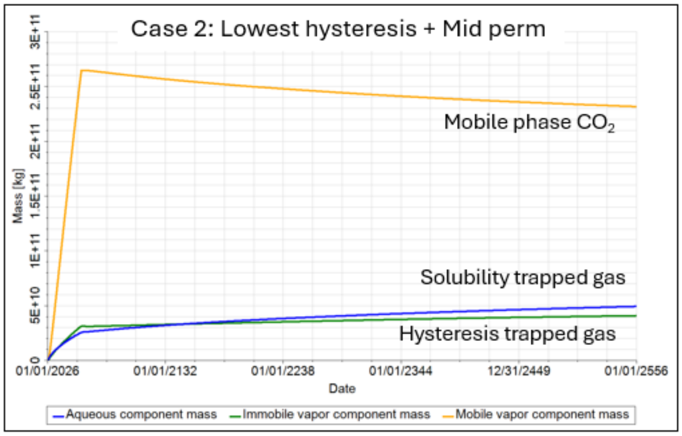

(a) Case 2: Lowest Hysteresis + Mid Perm

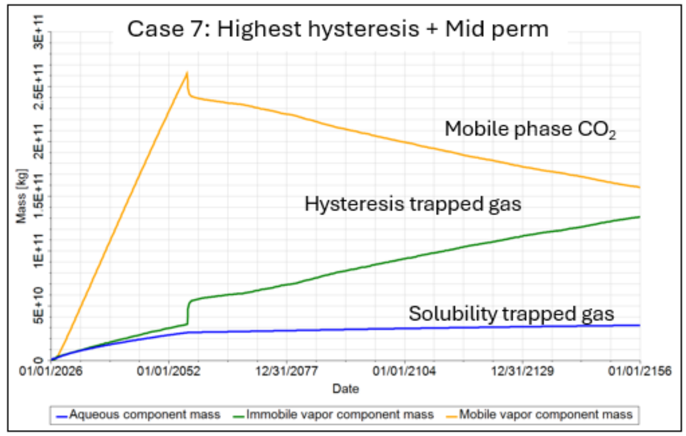

(b) Case 2: Highest Hysteresis + Mid Perm

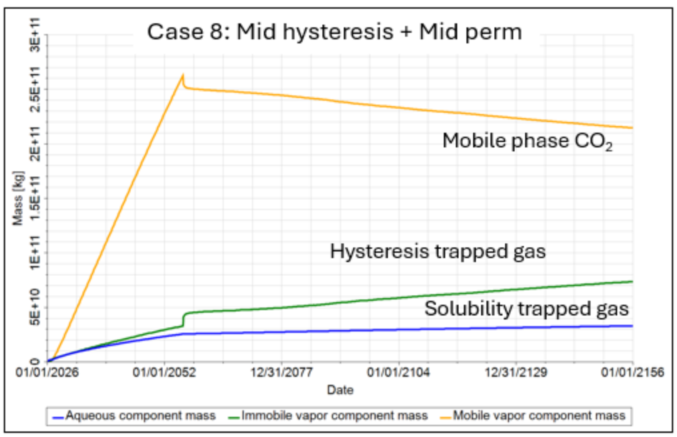

(c) Case 8: Mid Hysteresis + Mid Perm

Case No.	Solubility trapped gas [Mt]	Hysteresis trapped gas [Mt]	Mobile phase CO_2 [Mt]
Case 2**	16.3	13.4	71.6
Case 7*	7.7	44.2	49.2
Case 8*	8.0	24.9	68.3
Note: ** Shut-in for 500 year at Jan 1, 2556; * Shut-in for 100 year at Jan 1, 2156			

(d) Trapping Amounts in the Selected Cases

Figure 42: Trapping mechanisms and breakdown amounts of the selected cases in Skåne

As fault reactivation is one of the major risks in the Skåne AOI, two specific regions (Region 2 and Region 3) near the largest major fault in the model were examined to evaluate their pore-pressure changes during CO_2 injection and the subsequent shut-in period. Region 2 is located between the INJ1 plume and the fault, while Region 3 is situated in the deepest part of the formation, as shown in Figure 43 **(a)**. Figure 43 **(b)** presents the pressure evolution in the two regions, along with the average field pressure over the entire modelling period.

Pressure increases occur throughout the injection phase and stabilize gradually during shut-in. Region 3 exhibits the highest pressure increase, with a ΔP of 6.9 MPa, while Region 2 shows a ΔP of 6.5 MPa at the end of the 30year injection period. The average field pressure demonstrates a ΔP of 5.4 MPa. Regions located closer to the major fault experience a relatively larger pore pressure increase compared with the field average.

Given these observations, it is recommended that detailed geomechanical modelling be conducted to quantify potential fault movement and assess associated risks in the surrounding regions.

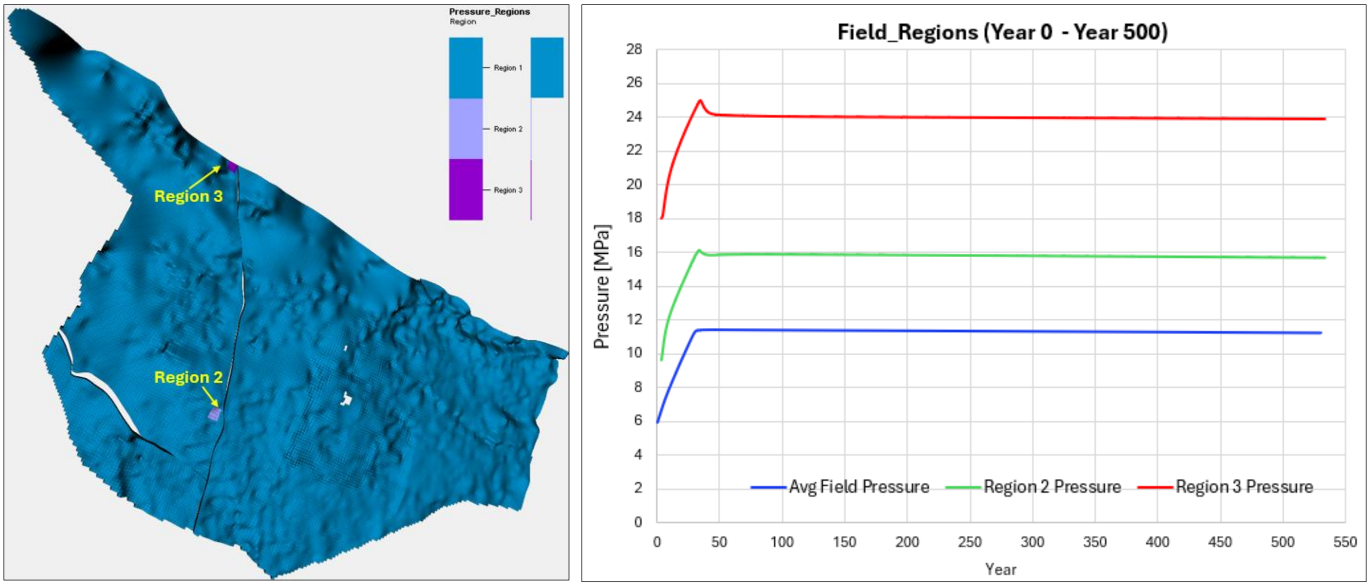

(a) Region Specification (b) Pressure Changes in Regions and Field

Figure 43: Average field and region pressures for case 9 in Skåne

5.3 Summary

The southwestern Baltic Sea and Skåne AOI has the potential to store more than 100 Mt of CO_2. Reservoir permeability and porosity exert significant control on overall storage capacity. While horizontal wells can enhance injection rates, they are not effective in redirecting plume migration. Although the studied injection locations are offshore along the coastline, part of the CO_2 plumes will still migrate into the onshore areas. Furthermore, simulation results indicate a risk of CO_2 plumes encroaching into major fault zones, especially when the reservoir permeability is on the high end.

6. Technical risk assessment

6.1 Overview

GLJ conducted a qualitative assessment of the key technical risks associated with the sequestration and long-term storage of CO_2 in the Arnager Greensand and the Faludden sandstone formations offshore Sweden. This assessment draws on GLJ's interpretation of the sensitivity analyses performed on selected reservoir parameters, technical discussions with the SGU team, and GLJ's internal subsurface and operational expertise. The purpose of this analysis is to provide SGU with an independent, technically grounded evaluation of the key uncertainties affecting storage performance, containment integrity, and injectivity, and to outline recommendations for further data acquisition, appraisal activities, and analytical work required to effectively de-risk the project prior to advancement into subsequent development phases. The technical risk register is available in Appendix 2.4: Technical Risk Register.

6.2 Key insights

From a technical risk perspective, both formations demonstrate promising characteristics for CO_2 storage; however, key uncertainties remain. The most significant risks relate to storage capacity and plume migration, both assessed with high inherent risk due to geological uncertainty and incomplete constraint on migration pathways. There is potential for both underestimation and overestimation of effective storage capacity, with implications for pressure management, long-term containment security, and regulatory compliance.

For the Arnager Greensand interval, injectivity uncertainty is primarily linked to reported Net-to-Gross (NTG) variability (0.4–0.8), suggesting possible reservoir heterogeneity that may not be fully captured in models using constant property values. Additional injectivity considerations for both formations include brine salinity effects and potential salt precipitation during sustained CO_2 injection. Induced seismicity risk was evaluated for Arnager Greensand and is assessed as moderate likelihood with low consequence, contingent on maintaining pressure within safe operational limits.

Containment risks are primarily associated with legacy wellbores and the potential for large plume extents interacting with structural features such as faults. While these risks are currently rated moderate, a pressure management strategy prior to injection is recommended. Monitorability risk is also moderate due to the absence of a site-specific Monitoring, Measurement, and Verification (MMV) plan, which is common at this stage of project development, underscoring the need for early integration of monitoring design into project maturation.

Overall, the identified risks are typical for early-phase CO_2 storage appraisal projects and can be systematically reduced through targeted data acquisition, scenario modelling, and phased development planning.

7. Conclusions

The Arnager and Faludden sandstone offshore Sweden demonstrate credible potential as CO_2 storage complexes, supported by a comprehensive and simulation-ready geomodelling framework. The integration of multidisciplinary datasets into a unified Petrel model represents a key milestone, enabling quantitative evaluation of injectivity, capacity, containment, and pressure evolution under dynamic injection scenarios.

Storage Potential and Key Reservoir Controls

The southeastern Baltic Sea Area of Interest (AOI) demonstrates a theoretical storage potential exceeding 300 Mt of CO_2 under the evaluated scenarios. Higher reservoir permeability enhances injectivity and overall storage efficiency, offering opportunities for optimized development strategies. While increased permeability may extend plume migration distances over long-term shut-in periods, these effects are well captured within the current modelling framework and can be effectively managed through informed site design and operational controls. The analysis further shows that well skin factor plays an important role in injection performance in the southeastern Baltic Sea Area model, reflecting the higher rate constraints applied, an insight that supports targeted well design optimization.

The southwestern Baltic Sea and Skåne AOI exhibits strong potential, with estimated storage capacity exceeding 100 Mt of CO_2. Reservoir permeability and porosity are key performance drivers, providing clear parameters for continued refinement and optimization. Although modeled injection sites are located offshore, simulations indicate that plume behavior remains predictable and manageable within the broader structural framework. Sensitivity analyses demonstrate that even under higher-permeability conditions, plume migration pathways can be identified and incorporated into monitoring and risk management strategies.

Injection Strategy and Trapping Mechanisms

Horizontal wells offer clear advantages in improving injection rates and operational flexibility. While they do not significantly redirect plume migration in the southwestern Baltic Sea and Skåne model, they enhance injectivity and provide valuable development optionality.

The hysteresis factor plays a substantial role in determining the amount of CO_2 trapped by capillary forces in both models. Improved laboratory-derived hysteresis parameters would allow more accurate quantification of residual trapping and long-term storage security.

Path Forward and Risk Reduction
The remaining uncertainties, primarily related to effective storage capacity and long-term plume migration, are typical for projects at this appraisal stage and are well within the scope of systematic risk-reduction workflows. Targeted seismic refinement, enhanced petrophysical characterization, well integrity verification, and expanded dynamic sensitivity studies will progressively increase confidence and narrow uncertainty ranges.

Importantly, no fundamental geological or technical barriers have been identified that would preclude further maturation of these storage candidates. Rather, the results support continued evaluation through advanced dynamic simulation, development of Monitoring, Measurement, Verification (MMV) framework, and alignment with regulatory requirements.

Strategic Outlook
With systematic risk reduction and phased appraisal, the Arnager Greensand and Faludden sandstone have the potential to contribute meaningfully to Sweden's long-term carbon management strategy. Continued governmental support at this stage would facilitate the transition from static modelling to fully integrated dynamic assessment and field development planning, positioning these offshore formations as viable components of a national CO_2 storage portfolio.

8. Recommendation for Future Work

To further enhance technical confidence and support continued project maturation, the following engineering steps are recommended:

Faludden sandstone: Model Refinement and Data Enhancement
- Acquire additional high-quality geological and reservoir data to further constrain key subsurface parameters.
- Periodically update the static geological model as new seismic and well data become available.
- Continuously refine the dynamic reservoir model to improve forecasts of injectivity, pressure evolution, and plume migration.

These steps will progressively reduce uncertainty and strengthen the predictive robustness of the storage assessment.

Arnager Greensand: Geomechanical Strengthening and Model Updates
- Update static and dynamic reservoir models as new data are acquired, ensuring alignment with the evolving subsurface understanding.
- Conduct a comprehensive geomechanical assessment focused on injector locations and fault-proximal regions.
- Evaluate stress evolution during injection to proactively manage subsurface stability and mitigate induced seismicity risks.

This work represents a natural next phase of technical maturation and will further reinforce operational resilience and storage security.

Geochemical Integration: Long-Term Storage Confidence
- Incorporate CO_2–brine and CO_2–rock interaction mechanisms into dynamic reservoir models once laboratory-derived rock-fluid experimental data become available.
- Quantify potential impacts on porosity, permeability, and long-term trapping mechanisms.

While geochemical reactions are not expected to significantly alter storage performance in sandstone systems, integrating these processes will provide an additional layer of technical rigor and long-term assurance.

Collectively, these focused technical advancements will continue to de-risk both storage candidates and support their progression toward safe, efficient, and large-scale CO_2 storage deployment.

9. References

Ane Lothe, Benjamin Emmel, Per Bergmo, Gry Möl Mortensen, Peter Frykman (2015). *Updated estimate of storage capacity and evaluation of Seal for Selected Aquifers (D26)*

Mario Winkler (2011). Quest CCS Project, *Generation – 4 Integrated Reservoir Modelling Report*

Mortensen et al. 2016 Geologisk lagring av koldioxid i Sverige - Lägesbeskrivning avseende förutsättningar, lagstiftning och forskning samt olje- och gasverksamhet i Östersjöregionen

Daniel Sopher, Christopher Juhlina, Mikael Erlströmb (2014). *A probabilistic assessment of the effective CO2storage capacity within the Swedish sector of the Baltic Basin*. International Journal of Greenhouse Gas Control.

Alla Shogenova, Saulius Sliaupab, Rein Vahera, Kazbulat Shogenova, Raisa Pomerancevad (2009). *The Baltic Basin: structure, properties of reservoir rocks, and capacity for geological storage of* CO_2. Estonian Journal of Earth Sciences.

Canada. Natural Resources Canada; Office of Energy Research and Development. (2013). *Aquistore Project, a deep saline* CO_2 *storage demonstration project (Cat. No. M159-14/2013E-PDF).* Government of Canada.

Appendices

Appendix 1: Faludden sandstone (Baltic Sea)

Additional plots related to Faludden sandstone reservoir in the Baltic Sea reservoir input parameters and detailed results of the simulation cases are summarized in the following sub-sections.

Appendix 1.1: Baltic Sea Well Layout and Reservoir Property Variations

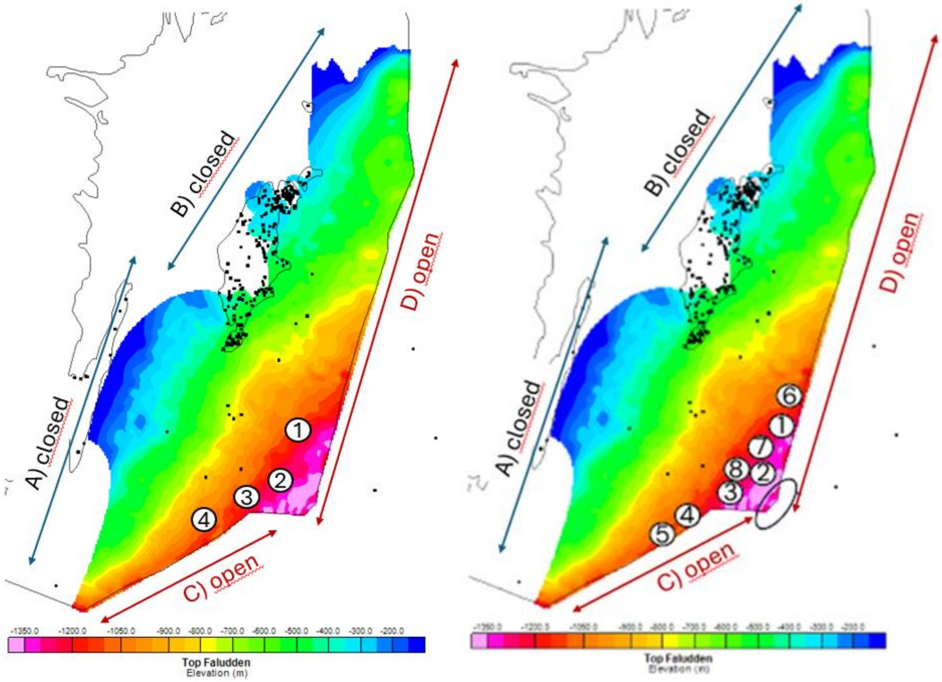

(a) Initial Possible Injection Sites (b) Increased Injection Sites

Figure 44: SGU marked injection sites

Table 11: Summary of various properties for the Faludden sandstone

Parameter	Average	Onshore south Gotland			Offshore, outer Swedish sector of the Baltic Sea to the SSE below 800 m depth		
		Low	Mean	High	Low	Mean	High
Gross thickness, m	41[2)]	0[3)]	15[3)]	30[3)]	30[1)]	40[3)]	55[3)]
Net/gross ratio, cut off phie=10% or 100 mD	0.8[1)]	0.7[2,3)]	0.8[2,3)]	1[2,3)]	0.6[1)]	0.7[1)]	0.8[1)]
Total porosity, %	15.3[2)]	10[2)]	15[2)]	20[2)]	10	12	18
Gas perm. mD	788[2)]	100[1)]	350[1)]	2000[1)]	100[1)]	200[1)]	500[1)]
Kh/Kv	0.97[2)]	-	-	-	-	-	-
Temp., °C	>31° C at 800 m	24	26	28	32	37	45
Therm. Cond. W/mK	4.0	3.5	4.1	4.6	3.2	4.5	4.5
Salinity, g/l		Faludden-1, 653 m, 60 g/l					
TDS, mg/l		Nore-1, 560 m, 54 g/l [6] Nore-2, 560 m, 60 g/l [6]					
Formation pressure		56.4 bar at 556 m in Nore-1					
Comments		Almost all empirical core data comes from cores in the southernmost part of Gotland. The Faludden sandstone is here in a shallower position (c. 550 m depth) in comparison to the potential injection area to the SSE where it is located at depths down to c 1100 m. There is likely a trend of decreasing porosity and permeability associated to the increasing depth to the SSW. This has e.g. been noted in a paper by Shogenova et al (2009) and further addressed in a publication by Sopher et al (2014). However, the wire-line logging data does not show any evident changes in e.g. the B7 and Bp wells in comparison to the wells representing shallower depths on south Gotland. The decreasing factor is uncertain and may be in the range 0.8-0.9 and mainly affect the high values.					

Appendix 1.2: Baltic Sea Injection Rates and Pressures

Table 12: Per well basis cumulative injected CO_2 amount in the Baltic Sea model

Injector No.	Case 1 [Mt]	Case 2 [Mt]	Case 3 [Mt]	Case 4 [Mt]	Case 5 [Mt]	Case 6 [Mt]	Case 7 [Mt]	Case 8 [Mt]	Case 9 [Mt]
INJ1	29.8	29.8	29.8	25.7	29.9	21.2	21.1	29.8	29.8
INJ2	29.8	29.8	29.8	28.5	29.9	23.8	23.8	29.8	29.8
INJ3	29.7	29.7	29.7	22.1	29.9	18.2	17.9	29.7	29.7
INJ4	29.4	29.4	29.4	17.9	29.9	14.9	14.3	29.4	29.4
INJ5	28.6	26.1	27.4	13.2	29.9	11.1	10.4	27.3	27.4
INJ6	29.7	29.7	29.7	23.8	29.9	19.3	19.0	29.7	29.7
INJ7	29.8	29.8	29.8	20.9	29.9	18.0	17.8	29.8	29.8
INJ8	29.7	27.5	28.4	14.9	29.9	13.4	13.0	28.3	28.3
INJ9	-	19.2	29.5	22.4	29.9	18.0	17.6	29.5	29.5
INJ10	-	24.6	23.7	11.3	29.9	10.2	9.7	23.6	23.6
INJ11	-	20.2	21.5	10.9	29.9	10.0	9.6	21.4	21.4
INJ12	-	19.4	14.7	10.7	15.0	9.8	9.3	14.7	14.7

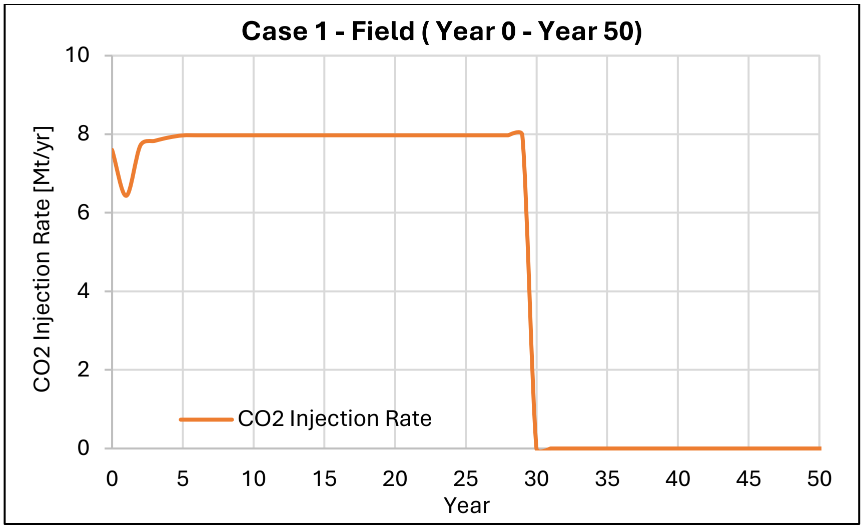

Figure 45: Case 1, Field injection rate

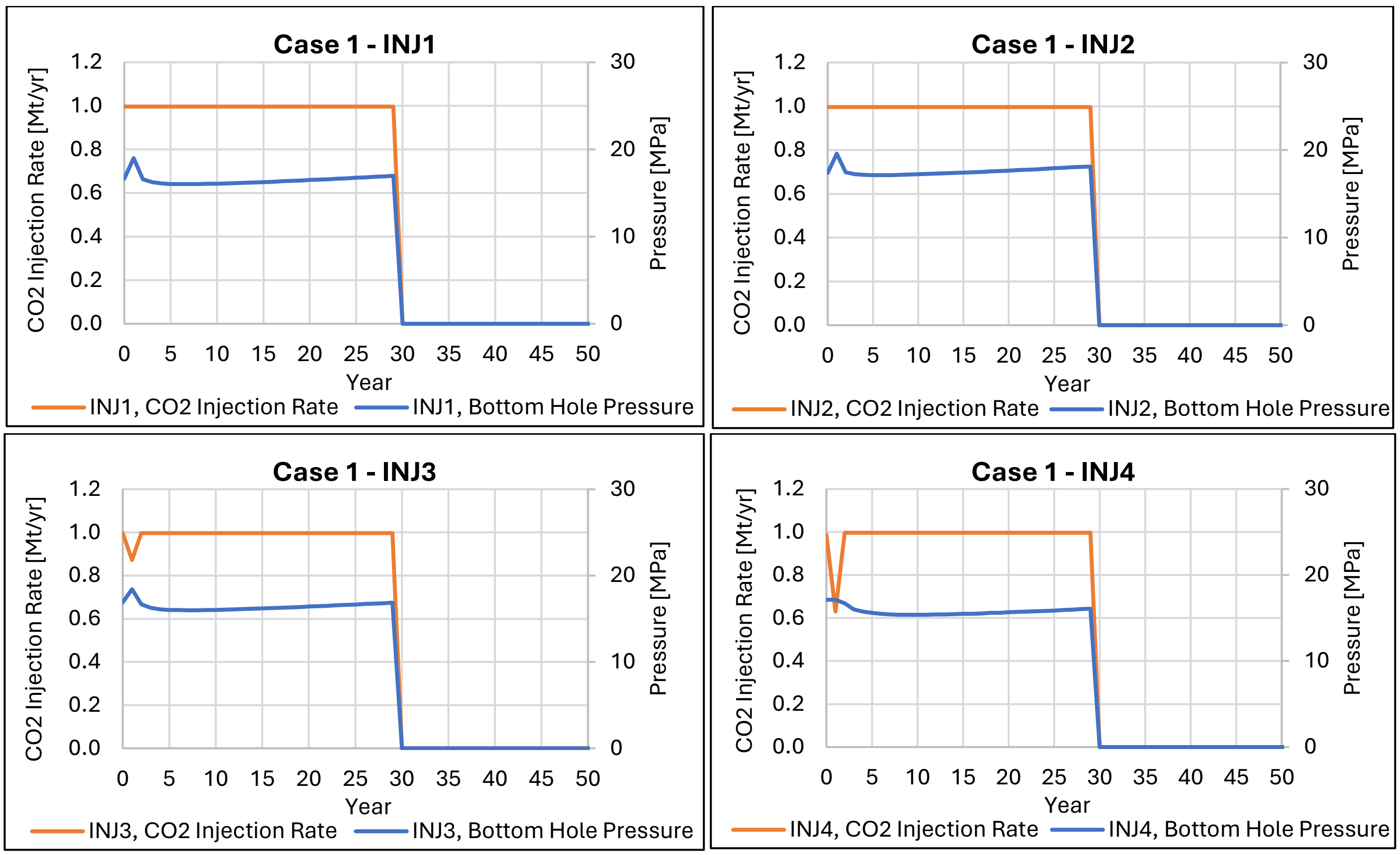

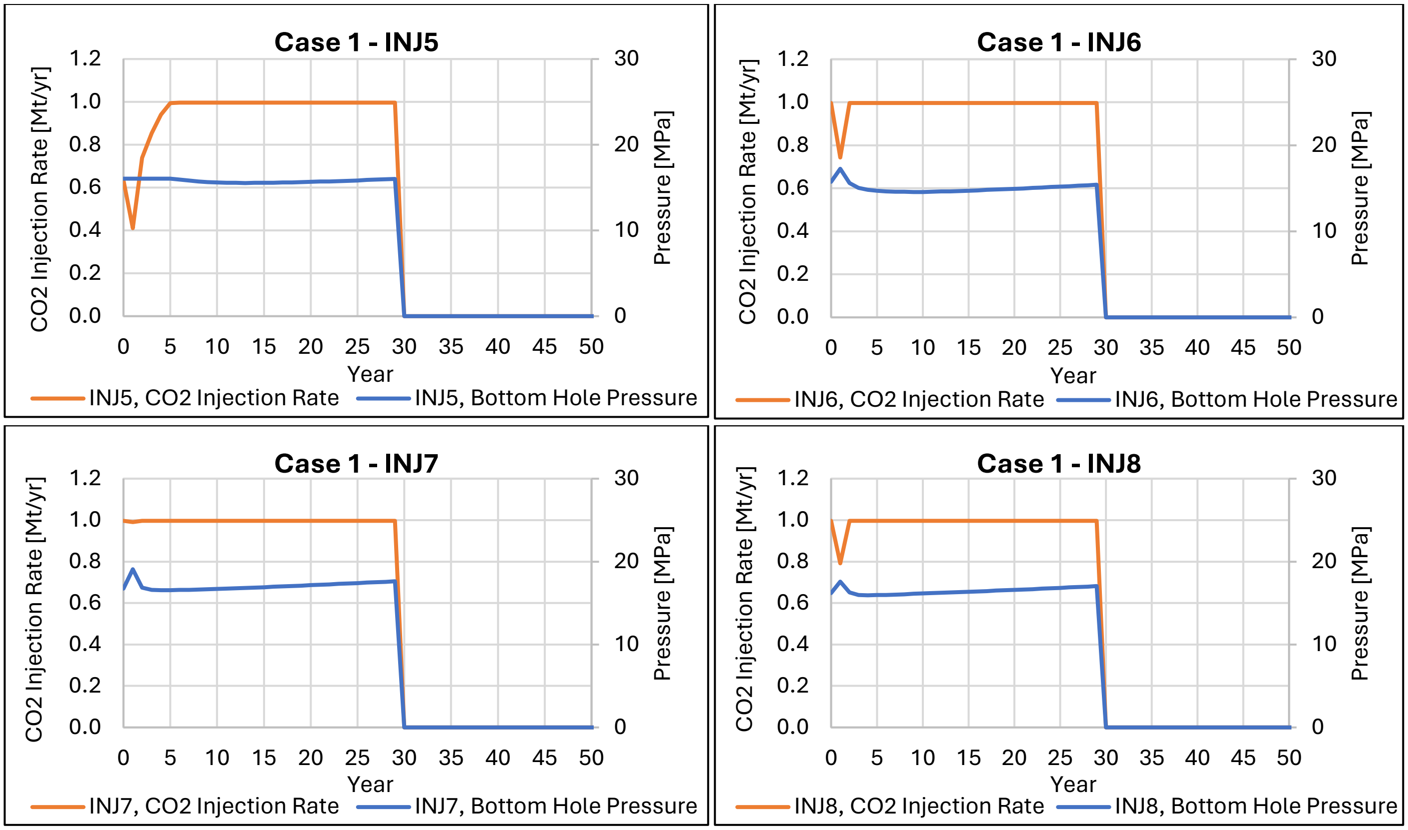

Figure 46: Case 1, Well injection rates and bottomhole pressures

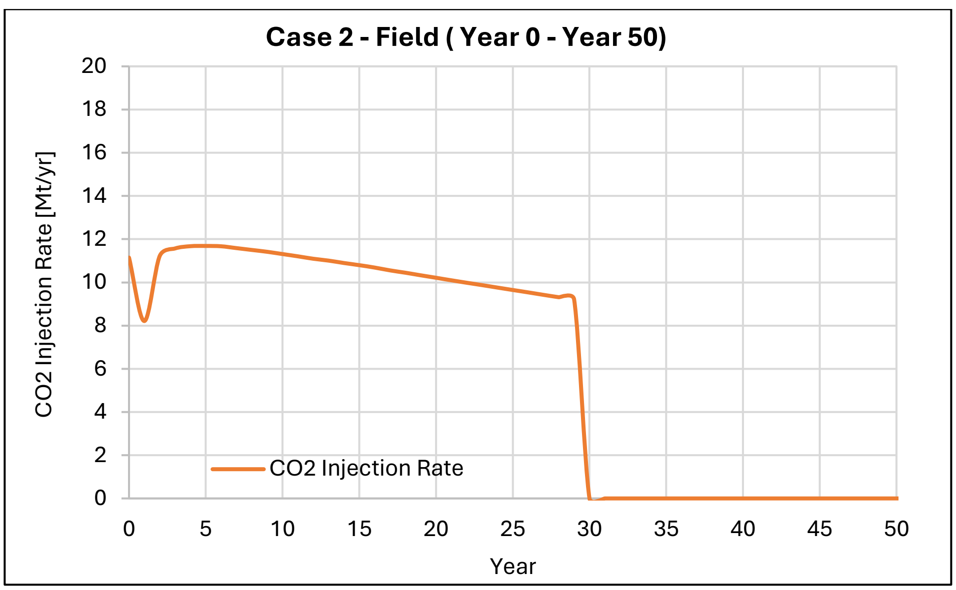

Figure 47: Case 2, Field injection rate

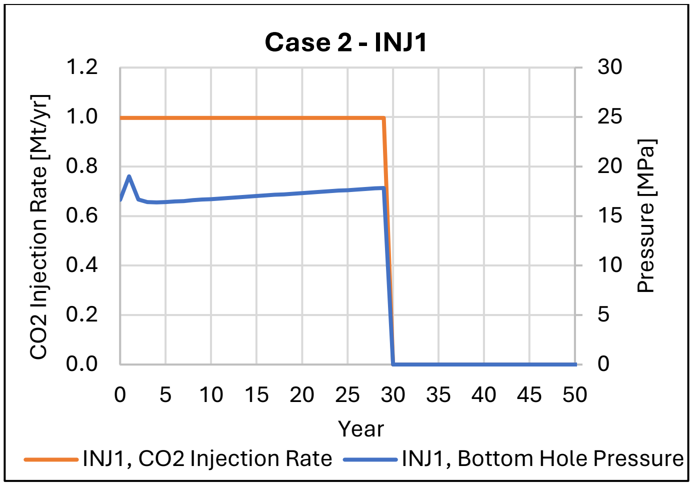
Case 2 - INJ1
CO2 Injection Rate [Mt/yr]
Pressure [MPa]
Year
INJ1, CO2 Injection Rate
INJ1, Bottom Hole Pressure

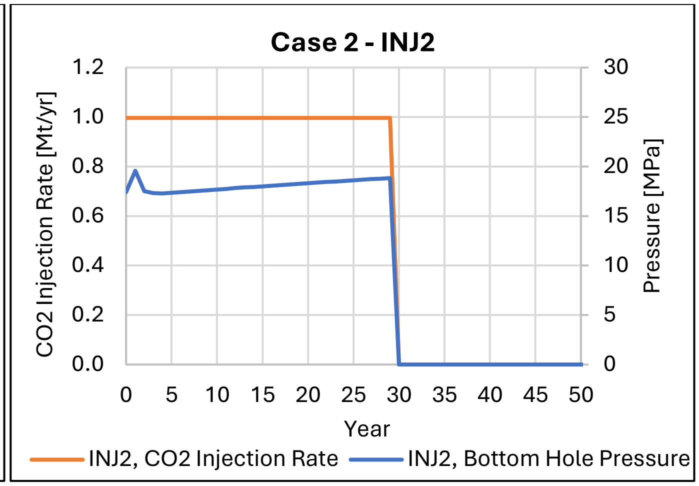
Case 2 - INJ2
CO2 Injection Rate [Mt/yr]
Pressure [MPa]
Year
INJ2, CO2 Injection Rate
INJ2, Bottom Hole Pressure

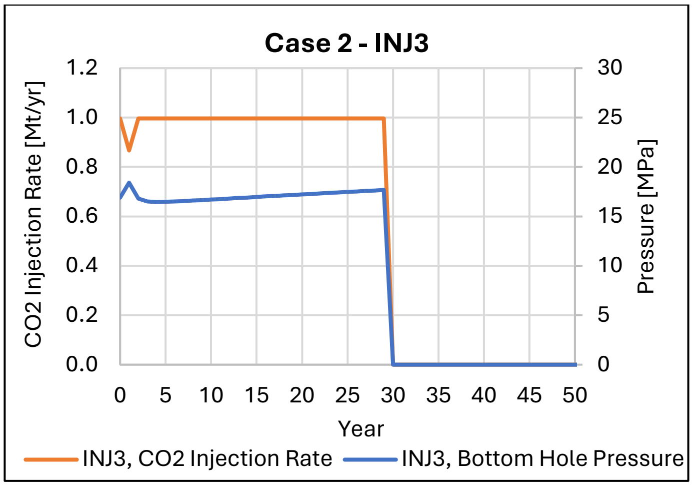
Case 2 - INJ3
CO2 Injection Rate [Mt/yr]
Pressure [MPa]
Year
INJ3, CO2 Injection Rate
INJ3, Bottom Hole Pressure

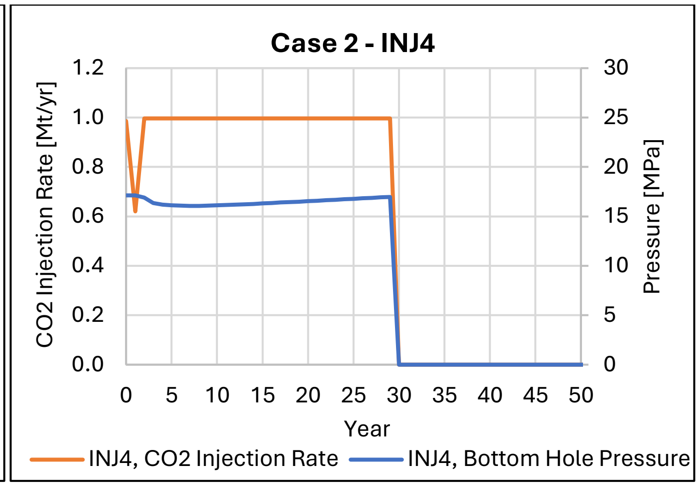
Case 2 - INJ4
CO2 Injection Rate [Mt/yr]
Pressure [MPa]
Year
INJ4, CO2 Injection Rate
INJ4, Bottom Hole Pressure

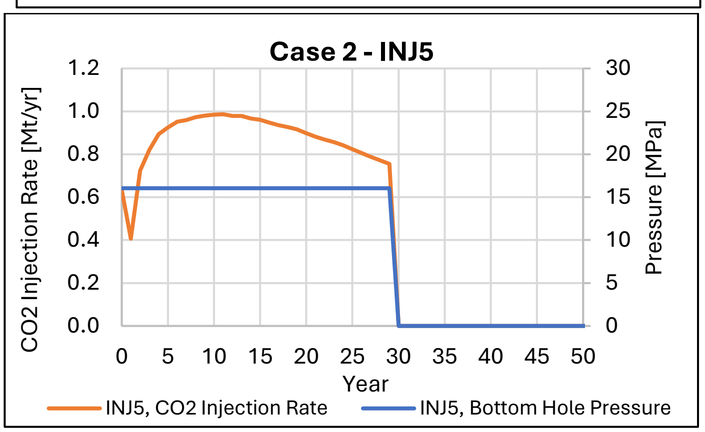
Case 2 - INJ5
CO2 Injection Rate [Mt/yr]
Pressure [MPa]
Year
INJ5, CO2 Injection Rate
INJ5, Bottom Hole Pressure

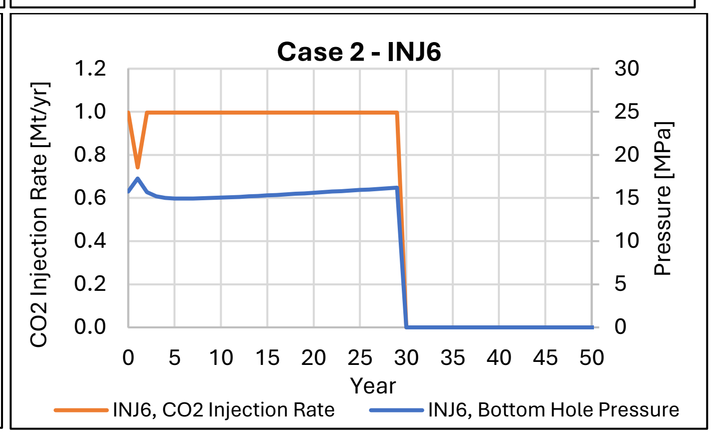
Case 2 - INJ6
CO2 Injection Rate [Mt/yr]
Pressure [MPa]
Year
INJ6, CO2 Injection Rate
INJ6, Bottom Hole Pressure

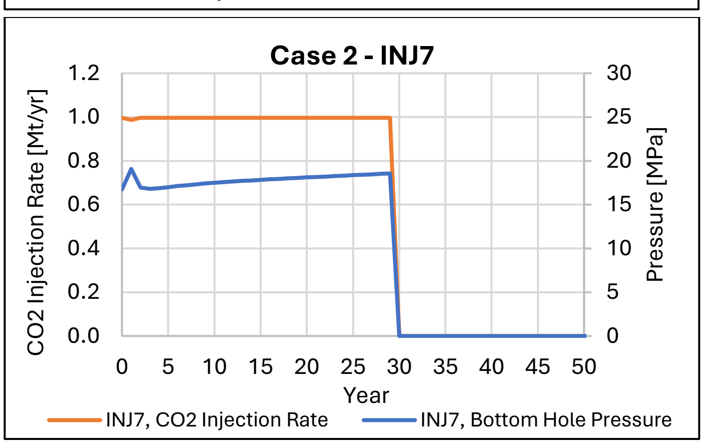
Case 2 - INJ7
CO2 Injection Rate [Mt/yr]
Pressure [MPa]
Year
INJ7, CO2 Injection Rate
INJ7, Bottom Hole Pressure

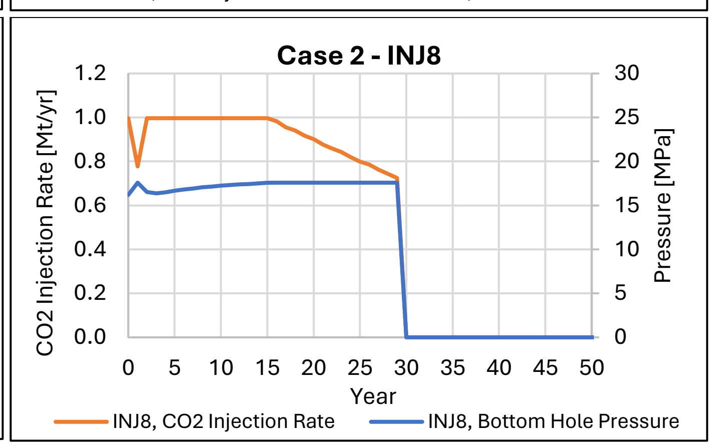
Case 2 - INJ8
CO2 Injection Rate [Mt/yr]
Pressure [MPa]
Year
INJ8, CO2 Injection Rate
INJ8, Bottom Hole Pressure

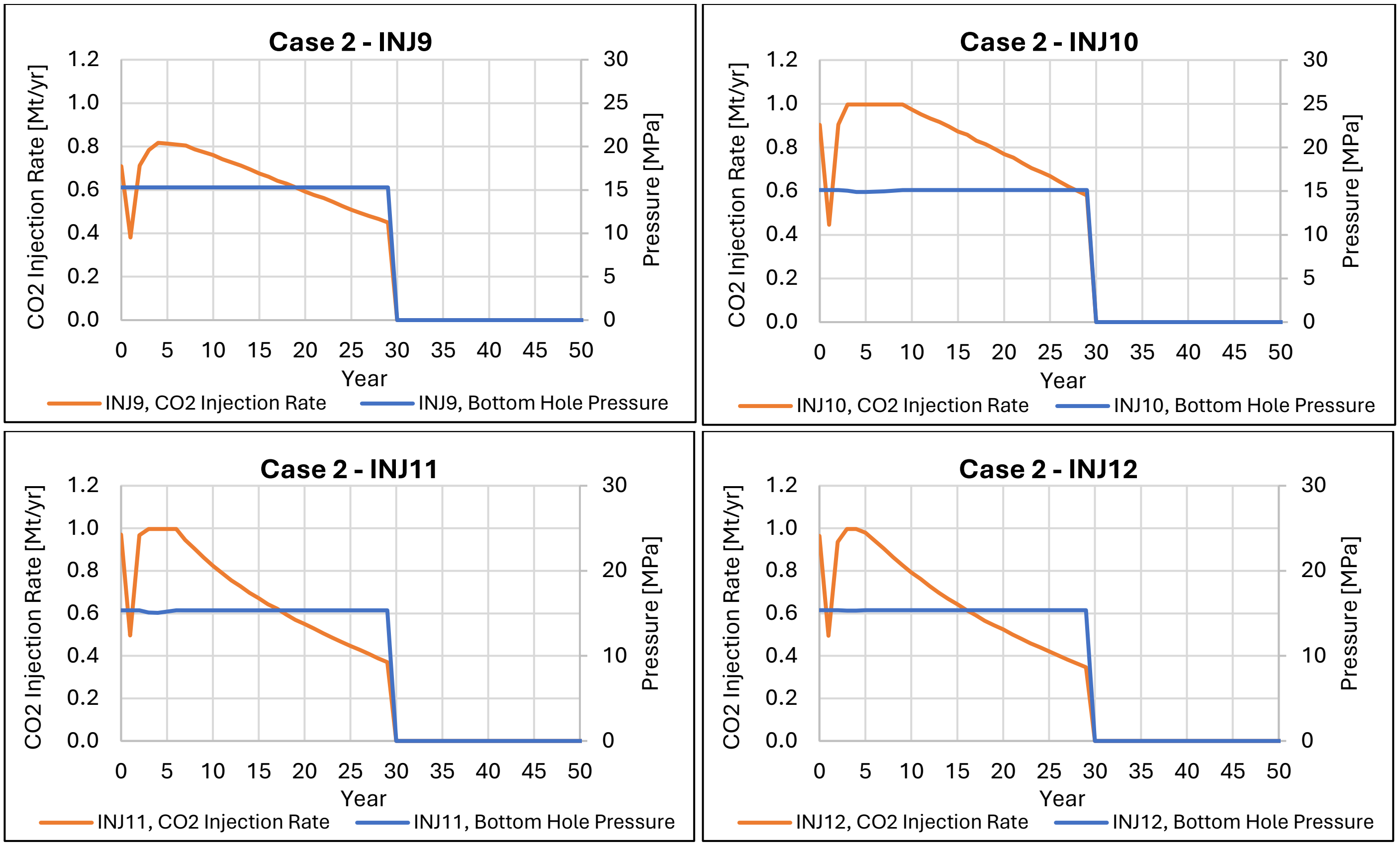

Figure 48: Case 2, Well injection rates and bottomhole pressures

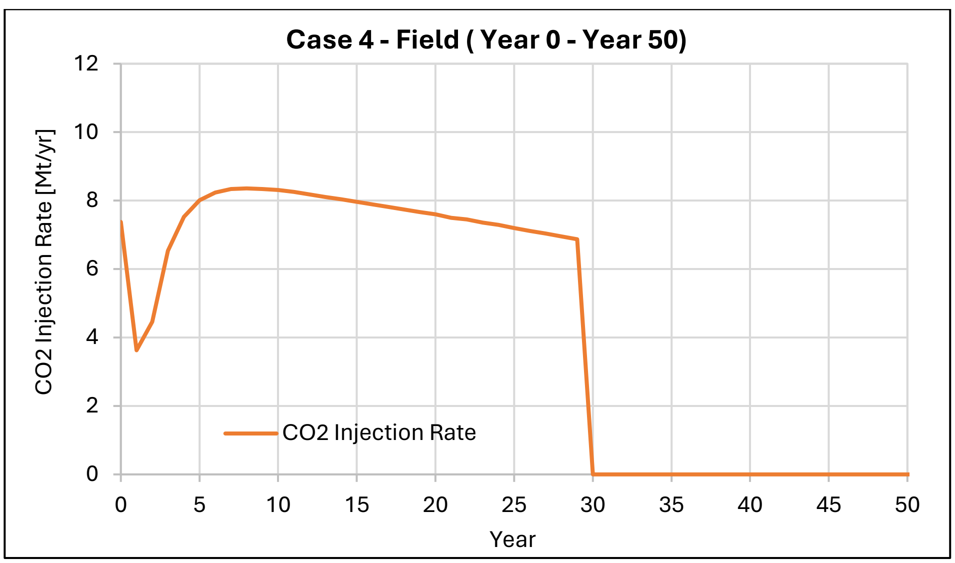

Figure 49. Case 4, Field injection rate

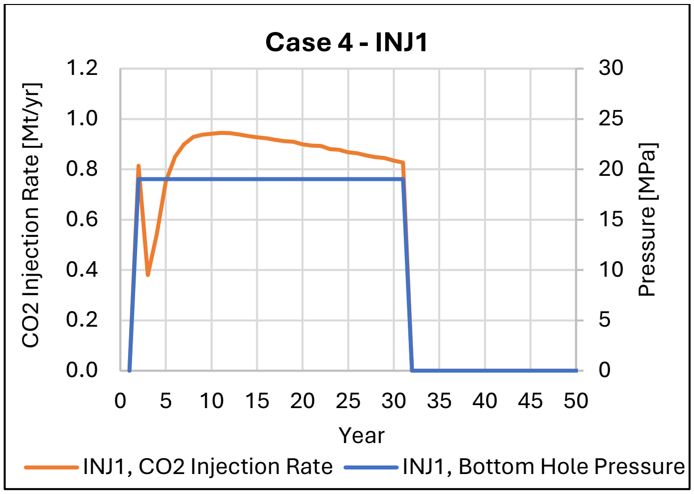
Case 4 - INJ1
CO2 Injection Rate [Mt/yr]
Pressure [MPa]
Year
INJ1, CO2 Injection Rate
INJ1, Bottom Hole Pressure

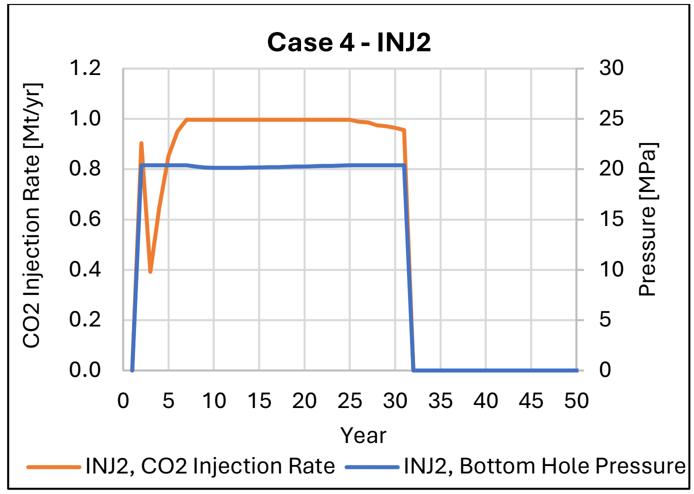
Case 4 - INJ2
CO2 Injection Rate [Mt/yr]
Pressure [MPa]
Year
INJ2, CO2 Injection Rate
INJ2, Bottom Hole Pressure

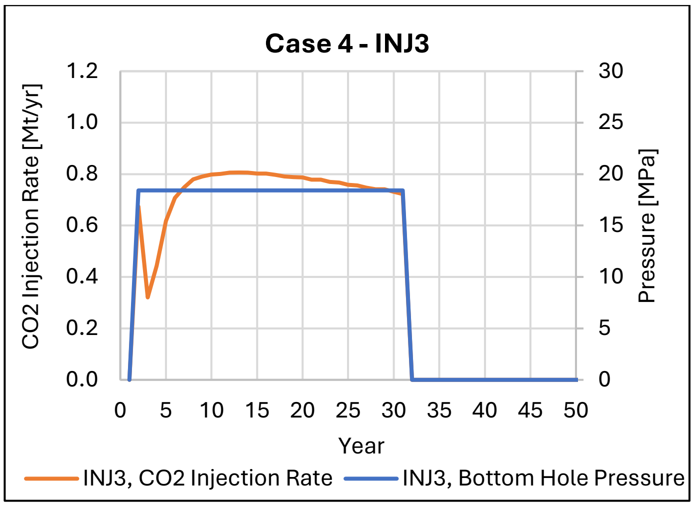
Case 4 - INJ3
CO2 Injection Rate [Mt/yr]
Pressure [MPa]
Year
INJ3, CO2 Injection Rate
INJ3, Bottom Hole Pressure

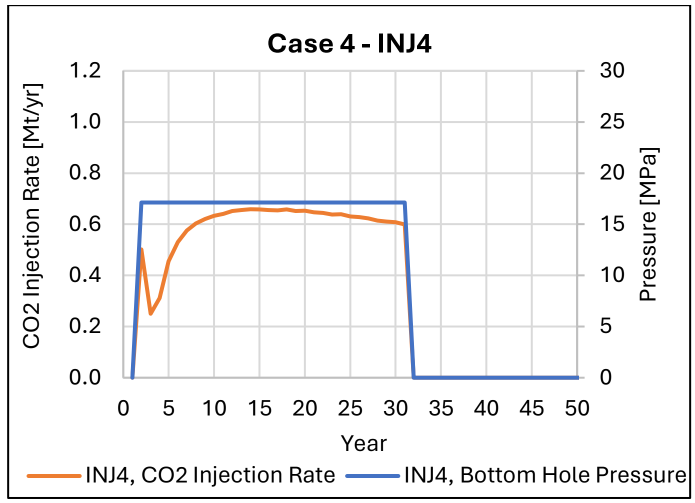
Case 4 - INJ4
CO2 Injection Rate [Mt/yr]
Pressure [MPa]
Year
INJ4, CO2 Injection Rate
INJ4, Bottom Hole Pressure

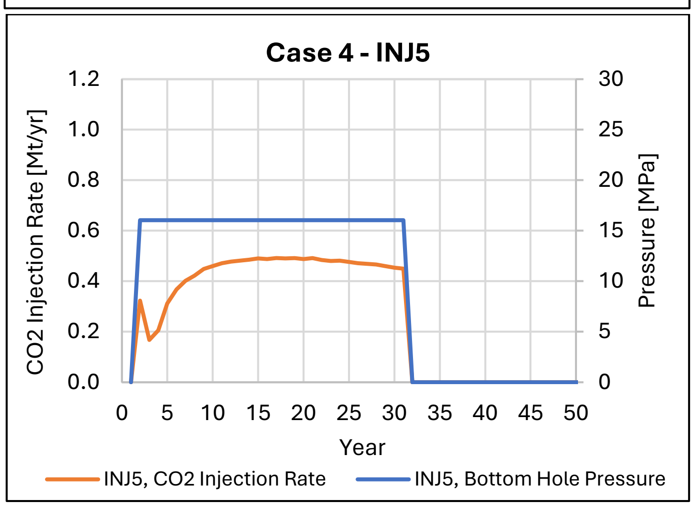
Case 4 - INJ5
CO2 Injection Rate [Mt/yr]
Pressure [MPa]
Year
INJ5, CO2 Injection Rate
INJ5, Bottom Hole Pressure

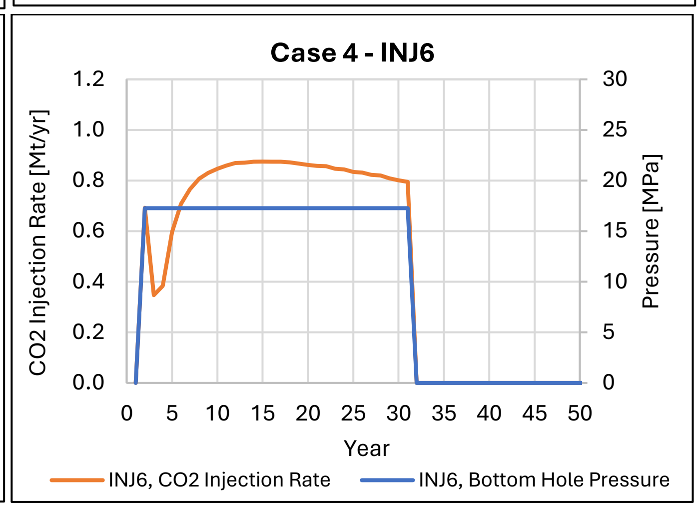
Case 4 - INJ6
CO2 Injection Rate [Mt/yr]
Pressure [MPa]
Year
INJ6, CO2 Injection Rate
INJ6, Bottom Hole Pressure

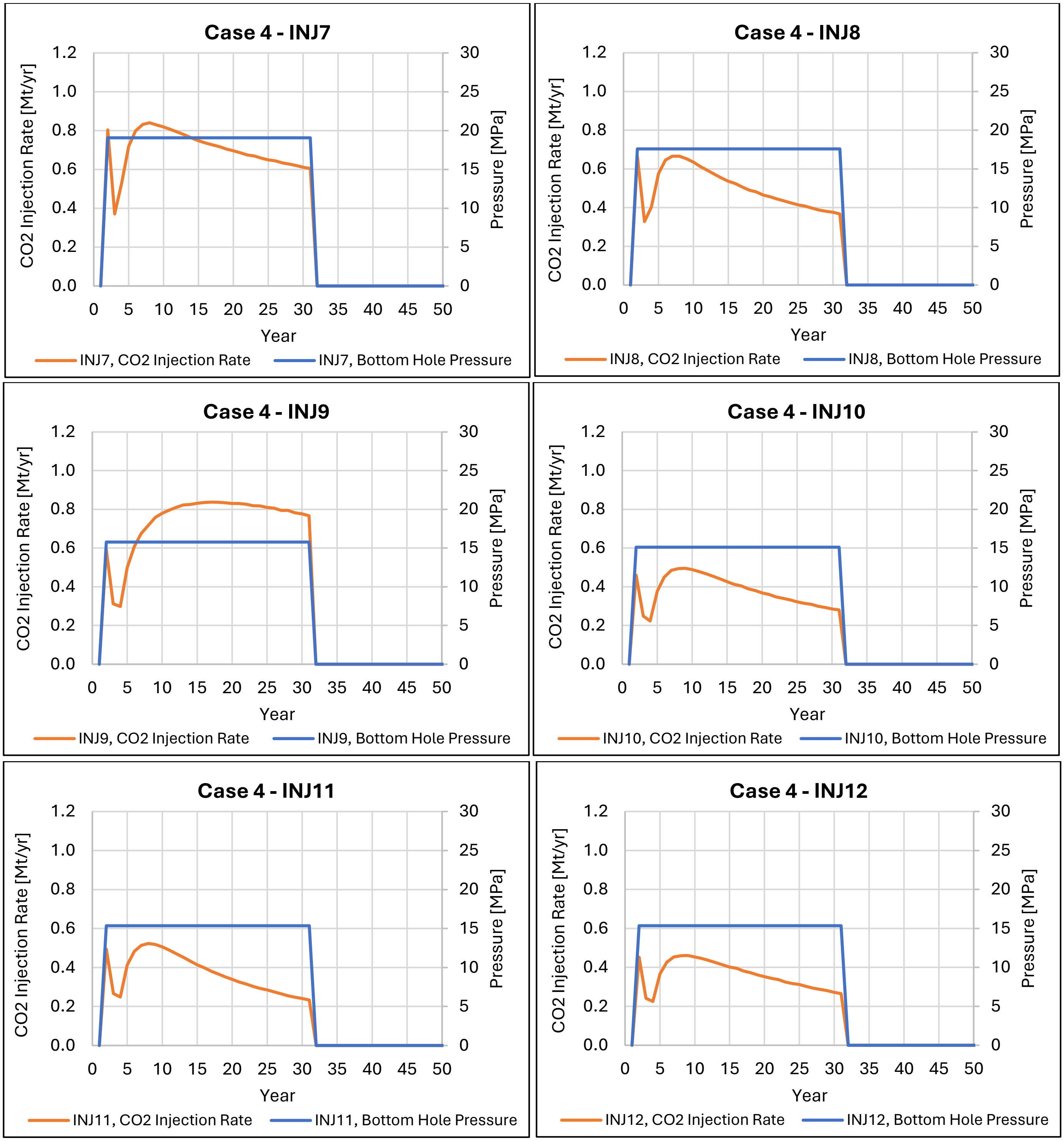

Figure 50: Case 4, Well injection rates and bottomhole pressures

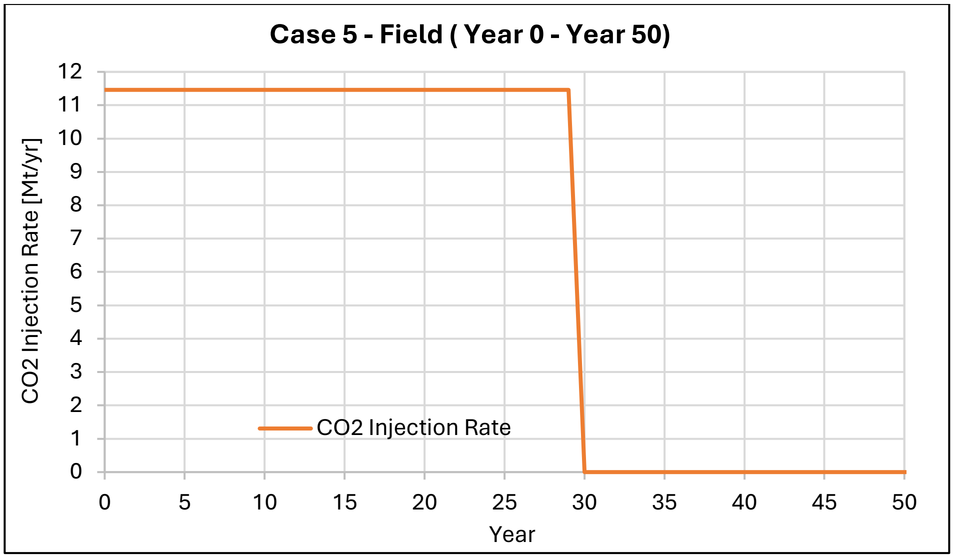

Figure 51: Case 5, Field injection rate

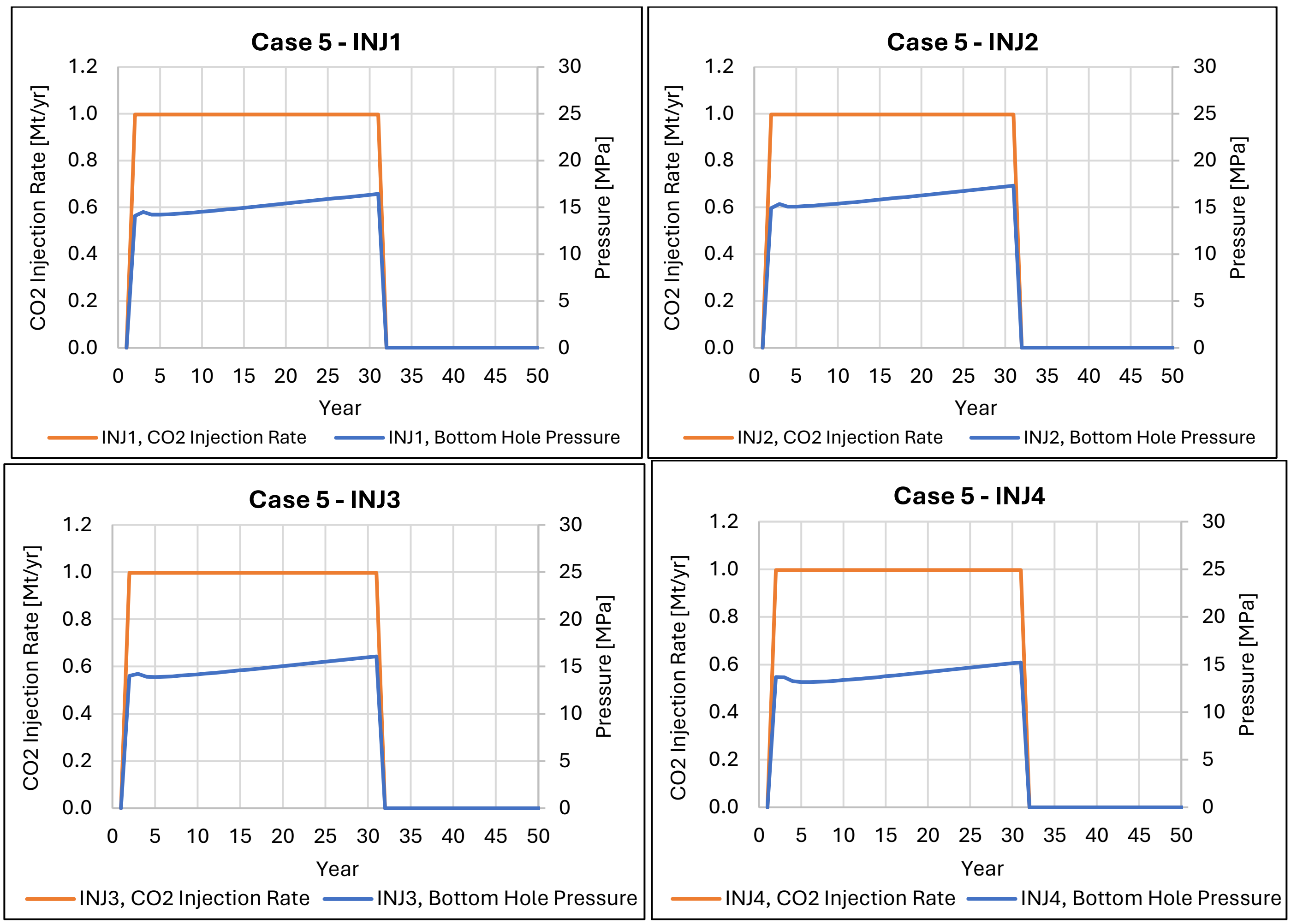

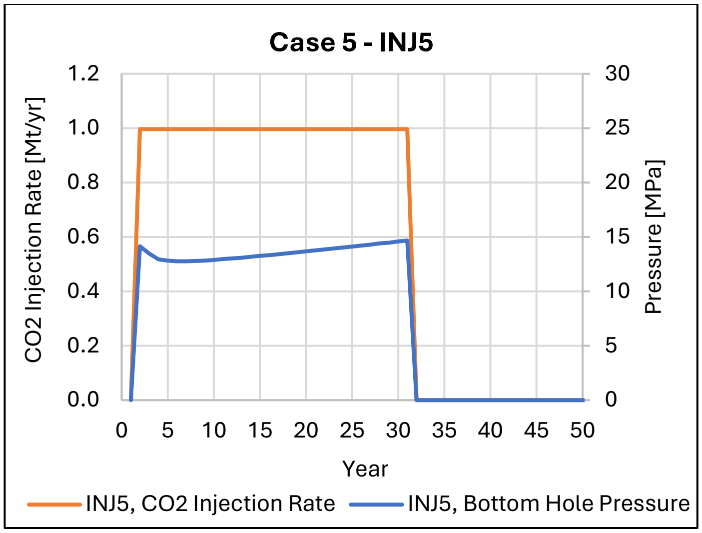
Case 5 - INJ5
CO2 Injection Rate [Mt/yr]
1.2
1.0
0.8
0.6
0.4
0.2
0.0
30
25
20
15
10
5
0
Pressure [MPa]
0 5 10 15 20 25 30 35 40 45 50
Year
INJ5, CO2 Injection Rate
INJ5, Bottom Hole Pressure

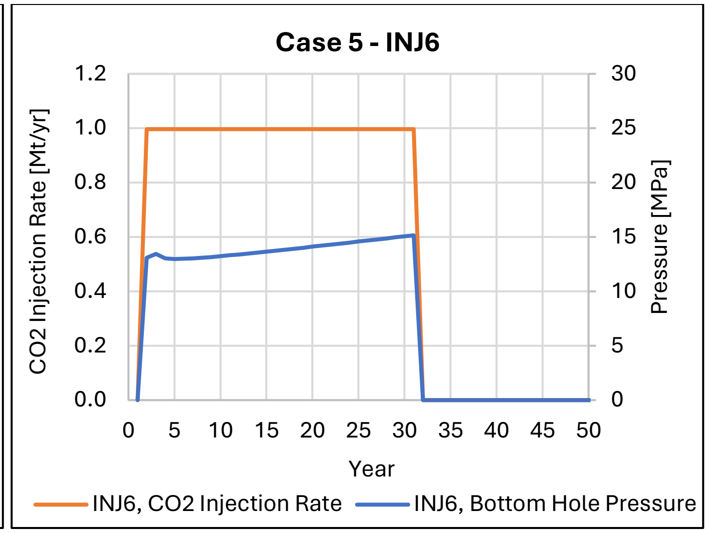
Case 5 - INJ6
CO2 Injection Rate [Mt/yr]
1.2
1.0
0.8
0.6
0.4
0.2
0.0
30
25
20
15
10
5
0
Pressure [MPa]
0 5 10 15 20 25 30 35 40 45 50
Year
INJ6, CO2 Injection Rate
INJ6, Bottom Hole Pressure

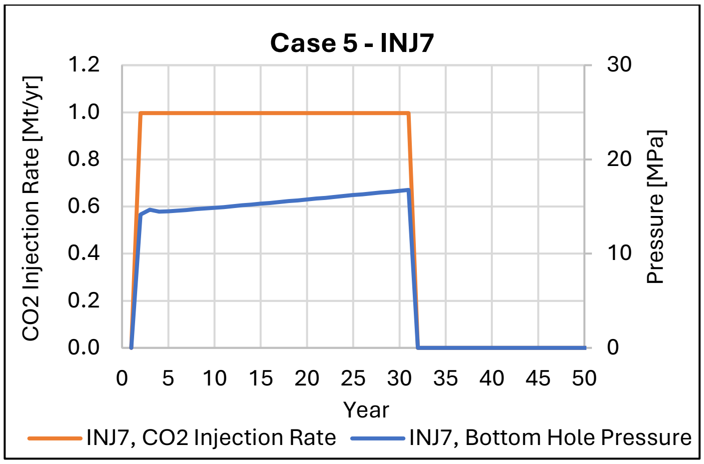
Case 5 - INJ7
CO2 Injection Rate [Mt/yr]
1.2
1.0
0.8
0.6
0.4
0.2
0.0
30
20
10
0
Pressure [MPa]
0 5 10 15 20 25 30 35 40 45 50
Year
INJ7, CO2 Injection Rate
INJ7, Bottom Hole Pressure

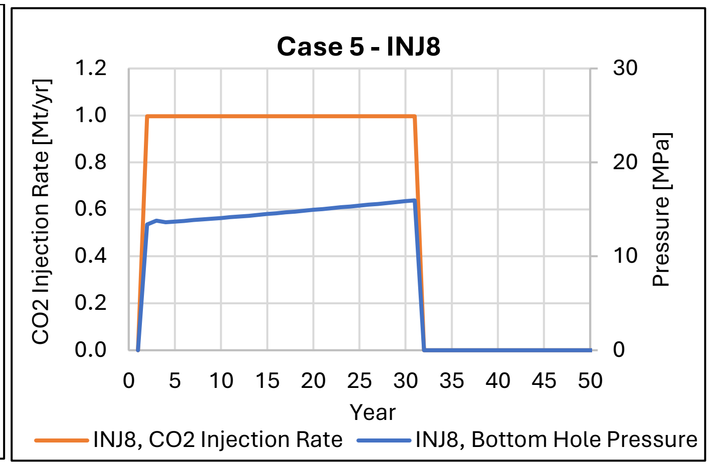
Case 5 - INJ8
CO2 Injection Rate [Mt/yr]
1.2
1.0
0.8
0.6
0.4
0.2
0.0
30
20
10
0
Pressure [MPa]
0 5 10 15 20 25 30 35 40 45 50
Year
INJ8, CO2 Injection Rate
INJ8, Bottom Hole Pressure

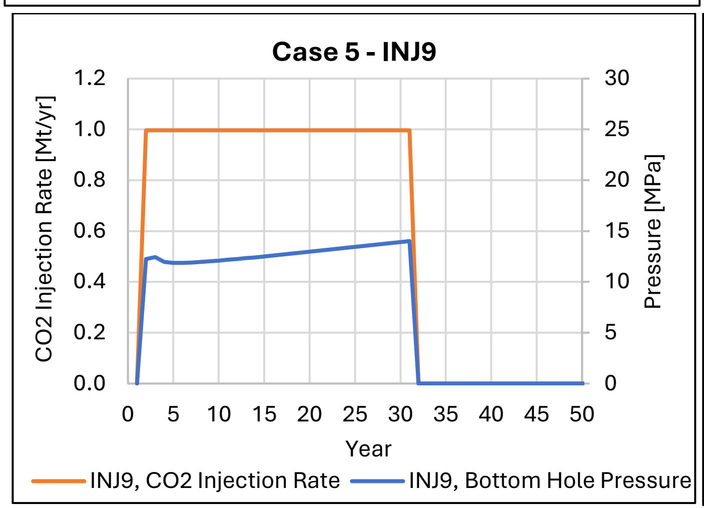
Case 5 - INJ9
CO2 Injection Rate [Mt/yr]
1.2
1.0
0.8
0.6
0.4
0.2
0.0
30
25
20
15
10
5
0
Pressure [MPa]
0 5 10 15 20 25 30 35 40 45 50
Year
INJ9, CO2 Injection Rate
INJ9, Bottom Hole Pressure

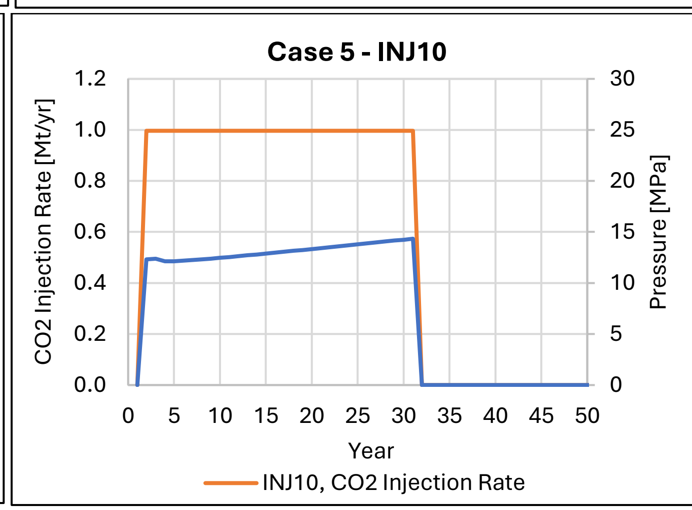
Case 5 - INJ10
CO2 Injection Rate [Mt/yr]
1.2
1.0
0.8
0.6
0.4
0.2
0.0
30
25
20
15
10
5
0
Pressure [MPa]
0 5 10 15 20 25 30 35 40 45 50
Year
INJ10, CO2 Injection Rate

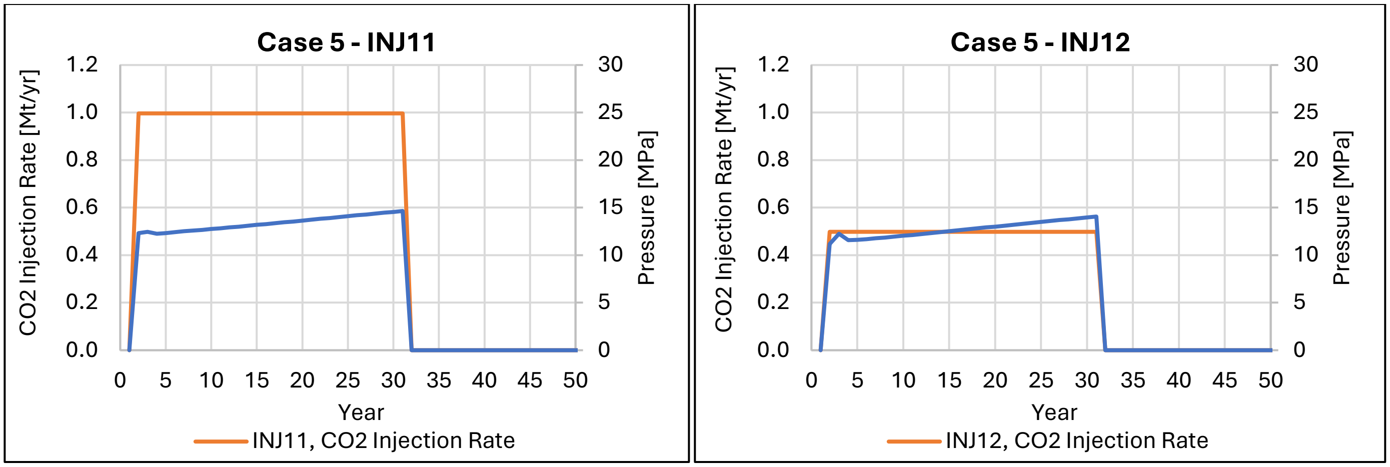

Figure 52: Case 5, Well injection rates and bottomhole pressures

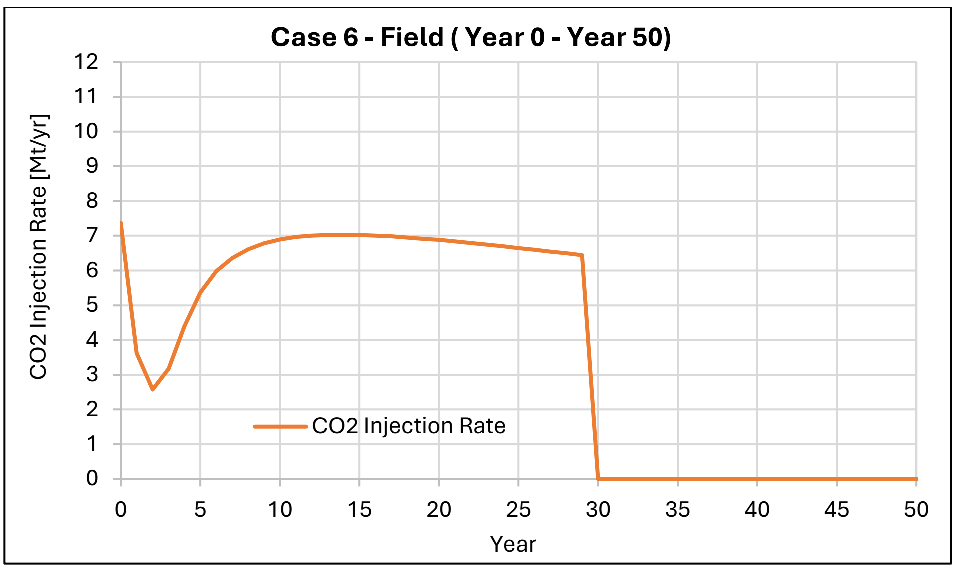

Figure 53: Case 6, Field injection rate

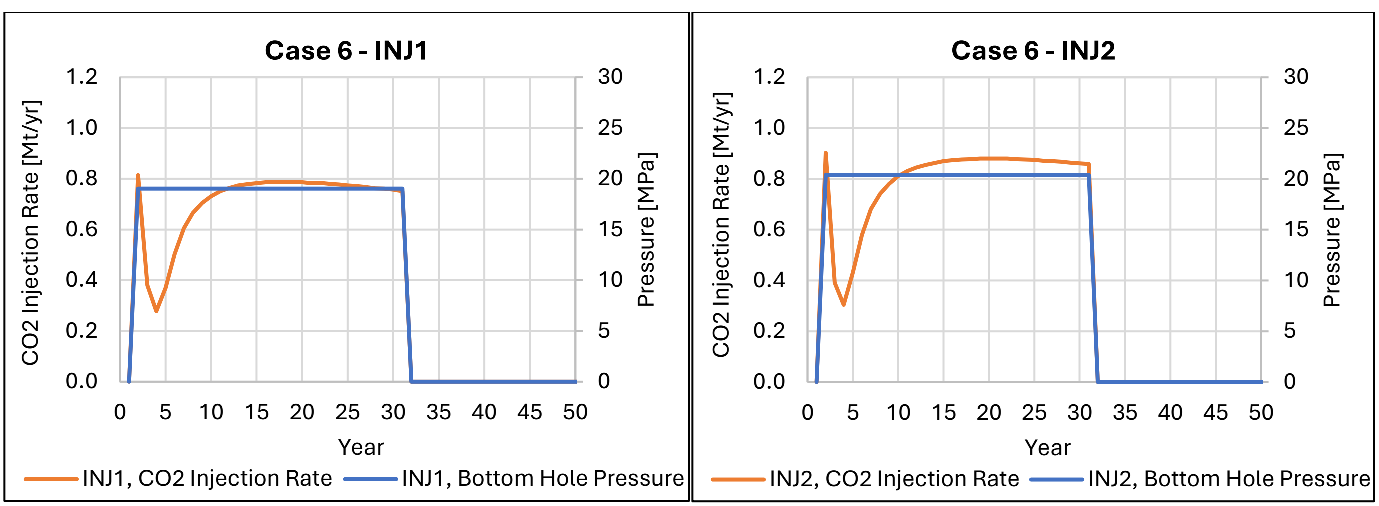

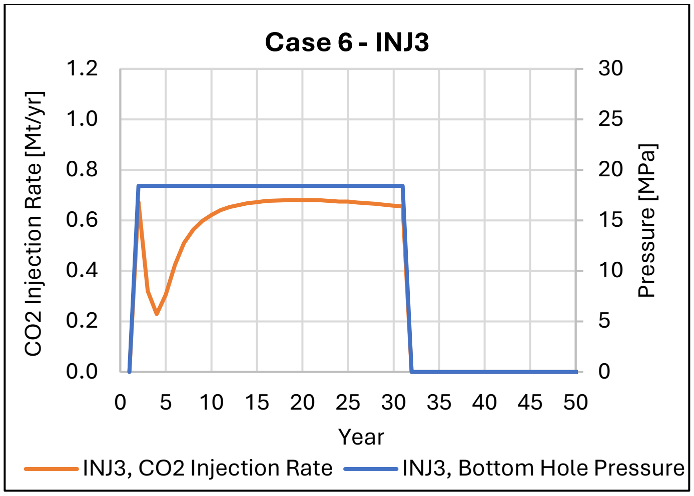
Case 6 - INJ3
CO2 Injection Rate [Mt/yr]
Pressure [MPa]
Year
INJ3, CO2 Injection Rate
INJ3, Bottom Hole Pressure

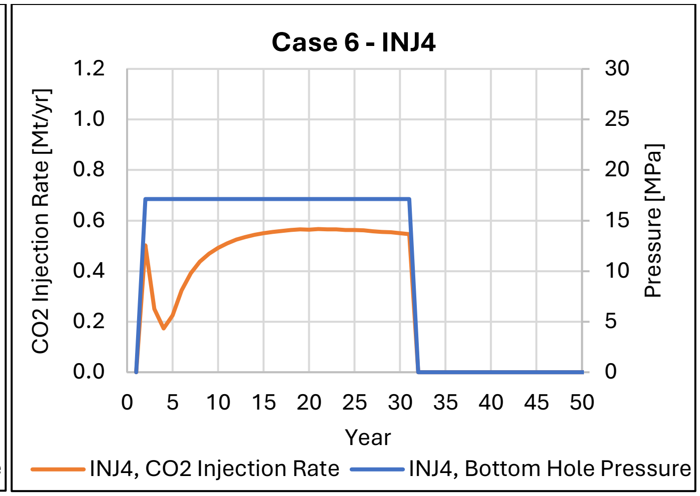
Case 6 - INJ4
CO2 Injection Rate [Mt/yr]
Pressure [MPa]
Year
INJ4, CO2 Injection Rate
INJ4, Bottom Hole Pressure

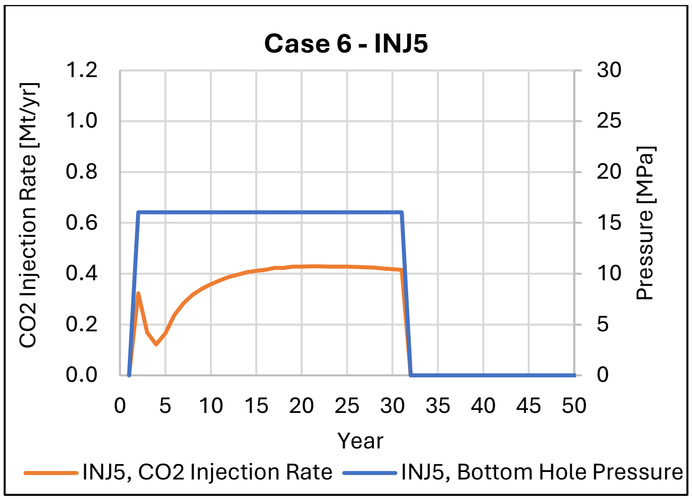
Case 6 - INJ5
CO2 Injection Rate [Mt/yr]
Pressure [MPa]
Year
INJ5, CO2 Injection Rate
INJ5, Bottom Hole Pressure

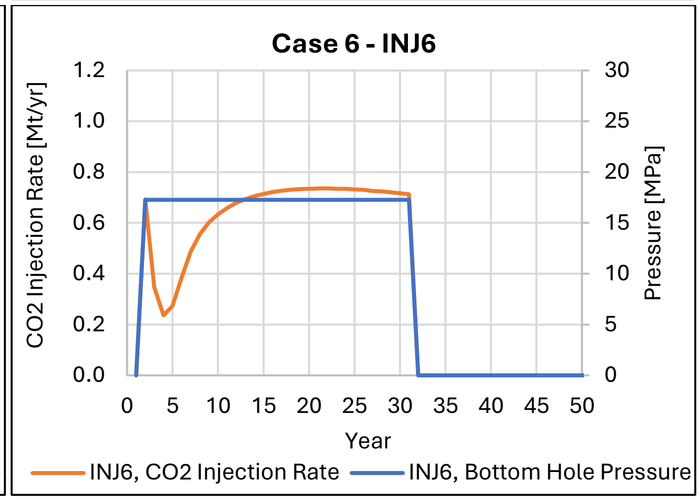
Case 6 - INJ6
CO2 Injection Rate [Mt/yr]
Pressure [MPa]
Year
INJ6, CO2 Injection Rate
INJ6, Bottom Hole Pressure

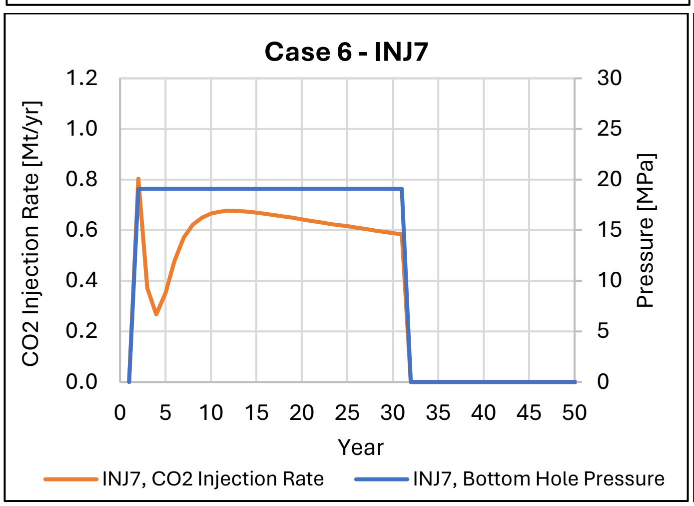
Case 6 - INJ7
CO2 Injection Rate [Mt/yr]
Pressure [MPa]
Year
INJ7, CO2 Injection Rate
INJ7, Bottom Hole Pressure

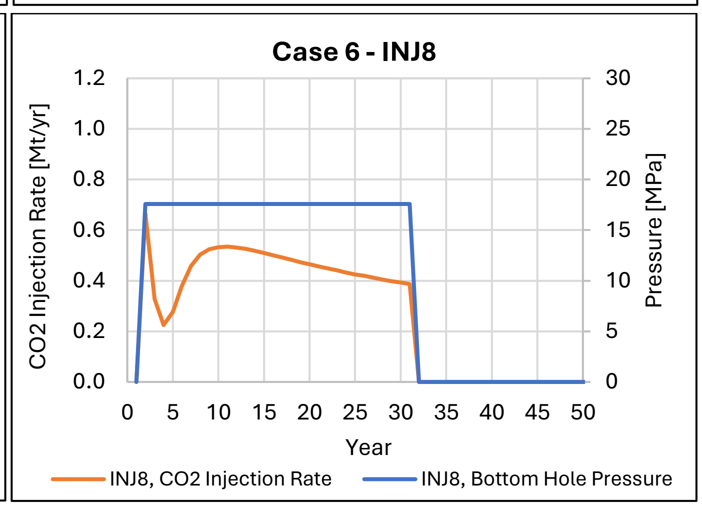
Case 6 - INJ8
CO2 Injection Rate [Mt/yr]
Pressure [MPa]
Year
INJ8, CO2 Injection Rate
INJ8, Bottom Hole Pressure

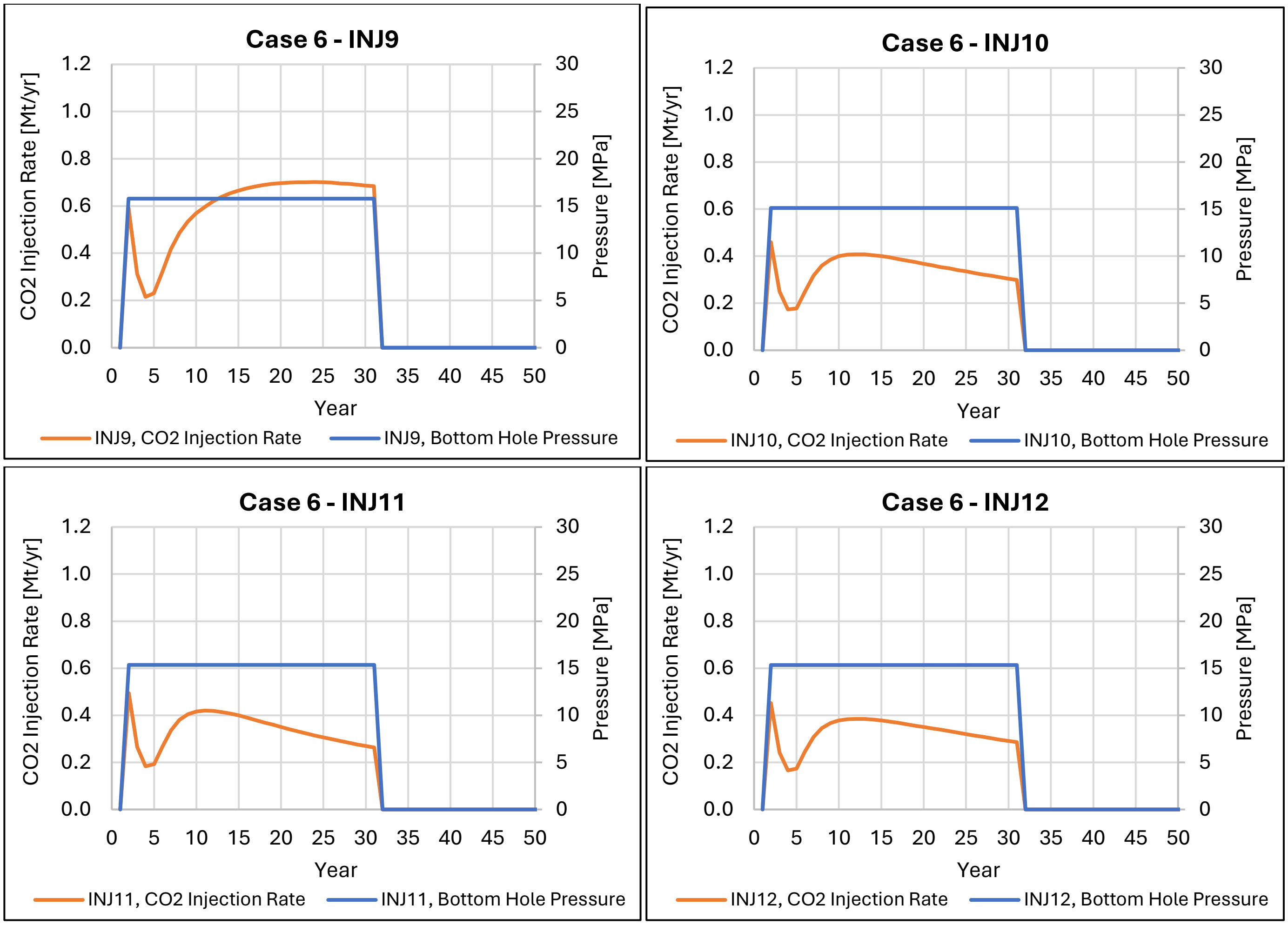

Figure 54: Case 6, Well injection rates and bottomhole pressures

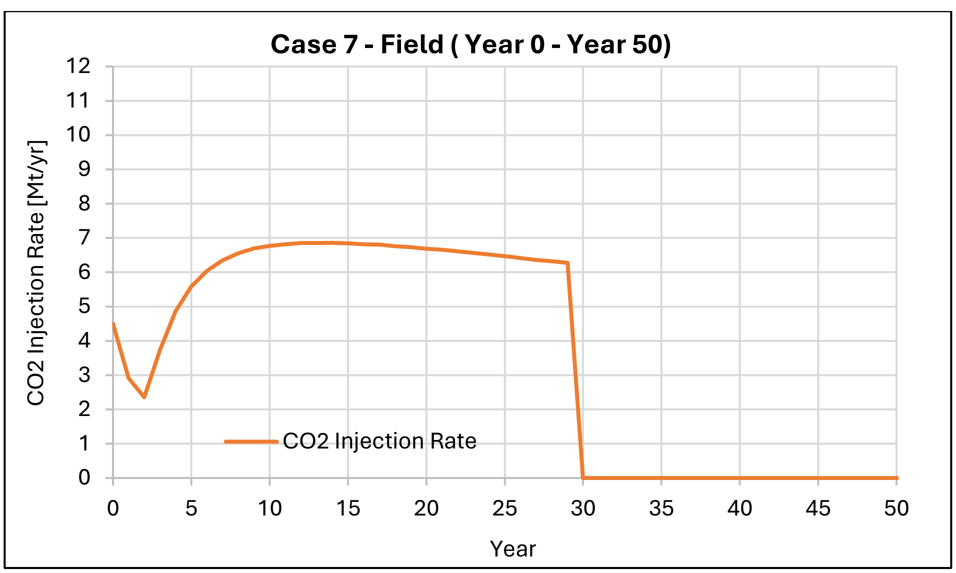

Figure 55. Case 7, Field injection rate

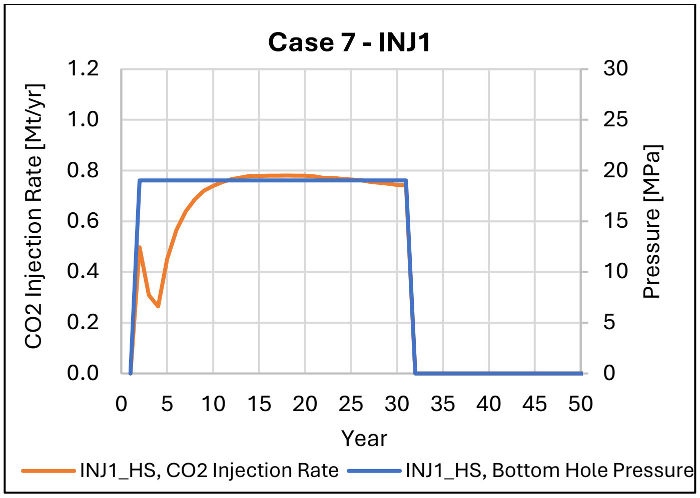
Case 7 - INJ1
CO2 Injection Rate [Mt/yr]
Pressure [MPa]
Year
INJ1_HS, CO2 Injection Rate
INJ1_HS, Bottom Hole Pressure

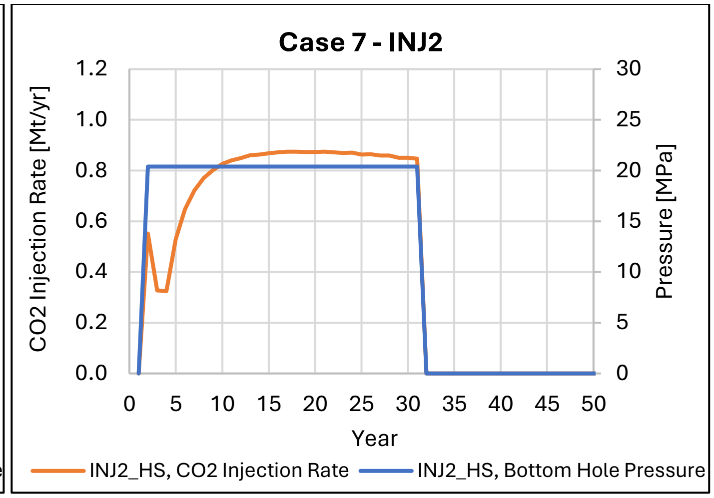
Case 7 - INJ2
CO2 Injection Rate [Mt/yr]
Pressure [MPa]
Year
INJ2_HS, CO2 Injection Rate
INJ2_HS, Bottom Hole Pressure

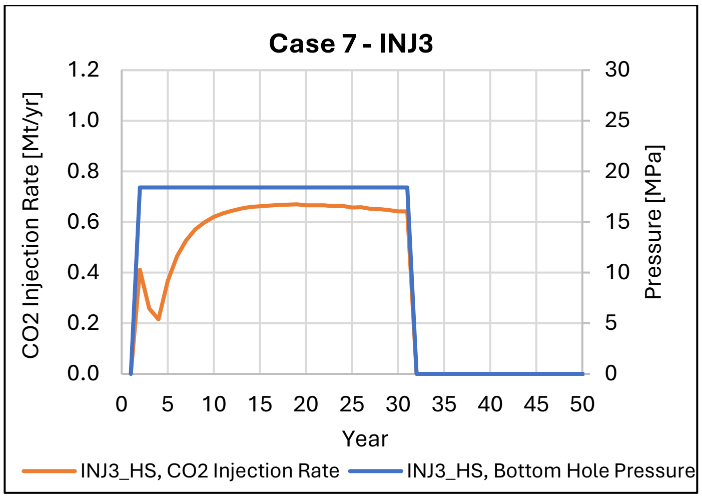
Case 7 - INJ3
CO2 Injection Rate [Mt/yr]
Pressure [MPa]
Year
INJ3_HS, CO2 Injection Rate
INJ3_HS, Bottom Hole Pressure

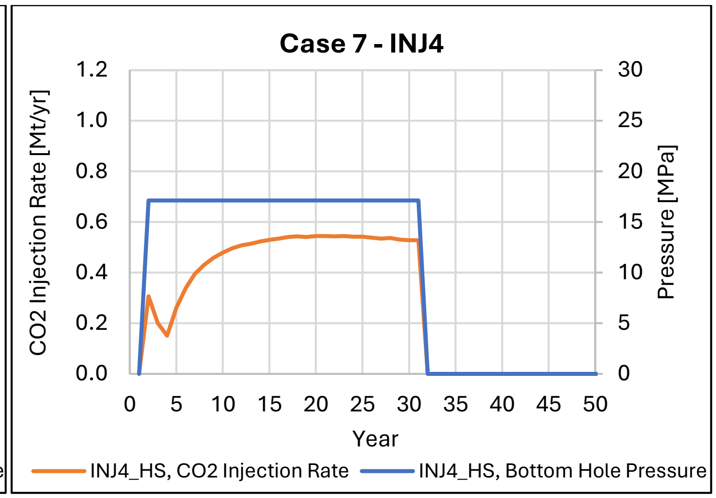
Case 7 - INJ4
CO2 Injection Rate [Mt/yr]
Pressure [MPa]
Year
INJ4_HS, CO2 Injection Rate
INJ4_HS, Bottom Hole Pressure

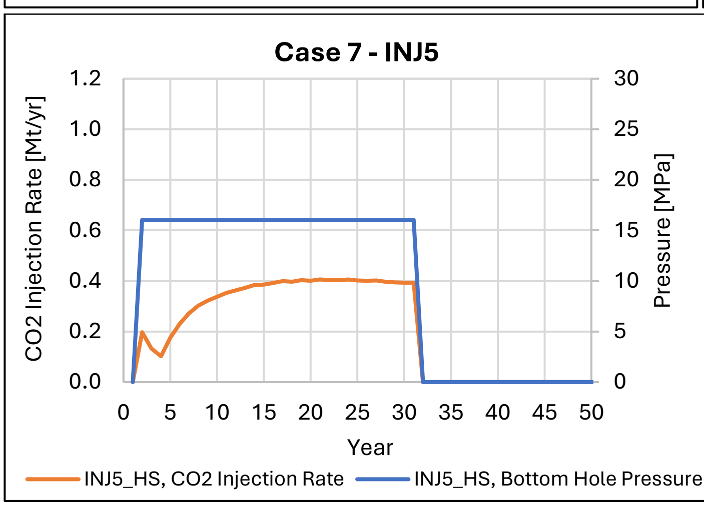
Case 7 - INJ5
CO2 Injection Rate [Mt/yr]
Pressure [MPa]
Year
INJ5_HS, CO2 Injection Rate
INJ5_HS, Bottom Hole Pressure

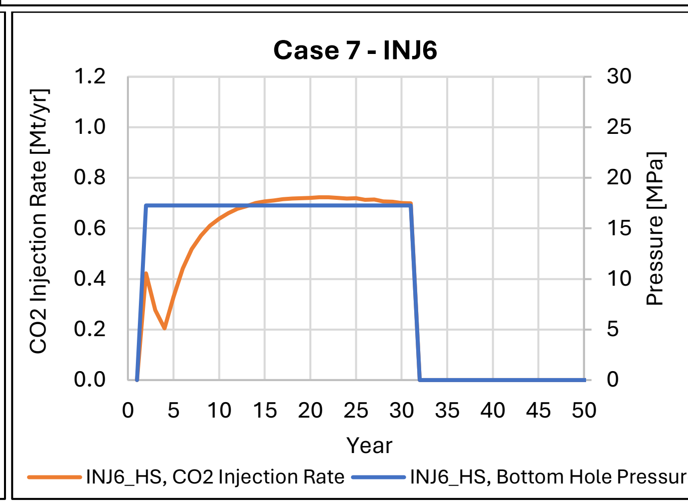
Case 7 - INJ6
CO2 Injection Rate [Mt/yr]
Pressure [MPa]
Year
INJ6_HS, CO2 Injection Rate
INJ6_HS, Bottom Hole Pressure

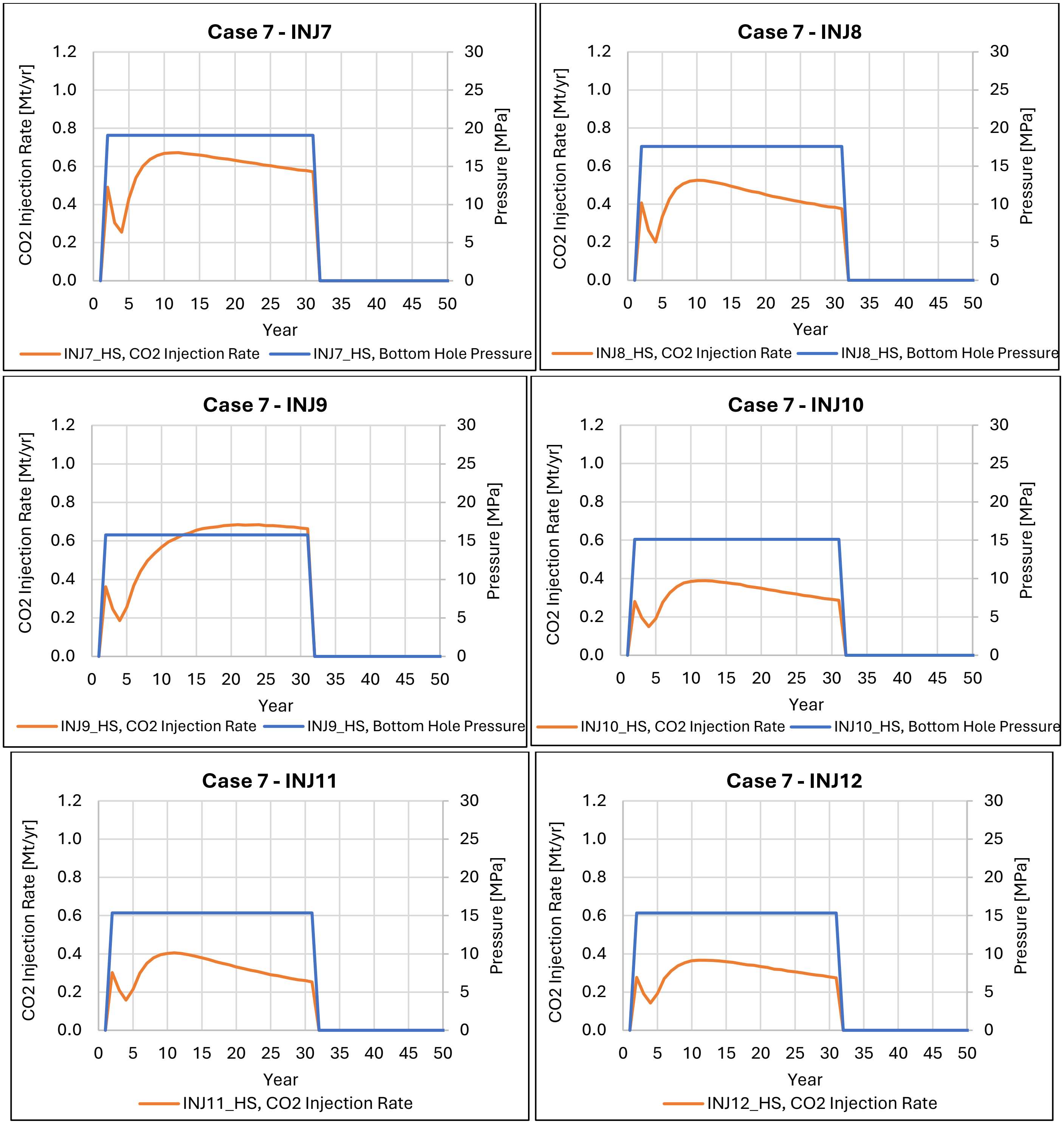

Figure 56: Case 7, Well injection rates and bottomhole pressures

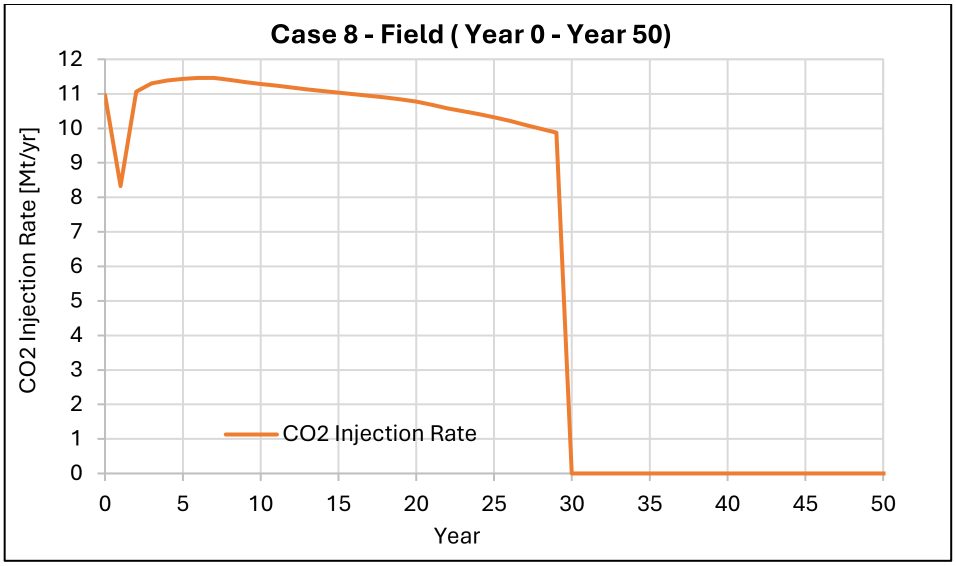

Figure 57: Case 8, Field injection rate

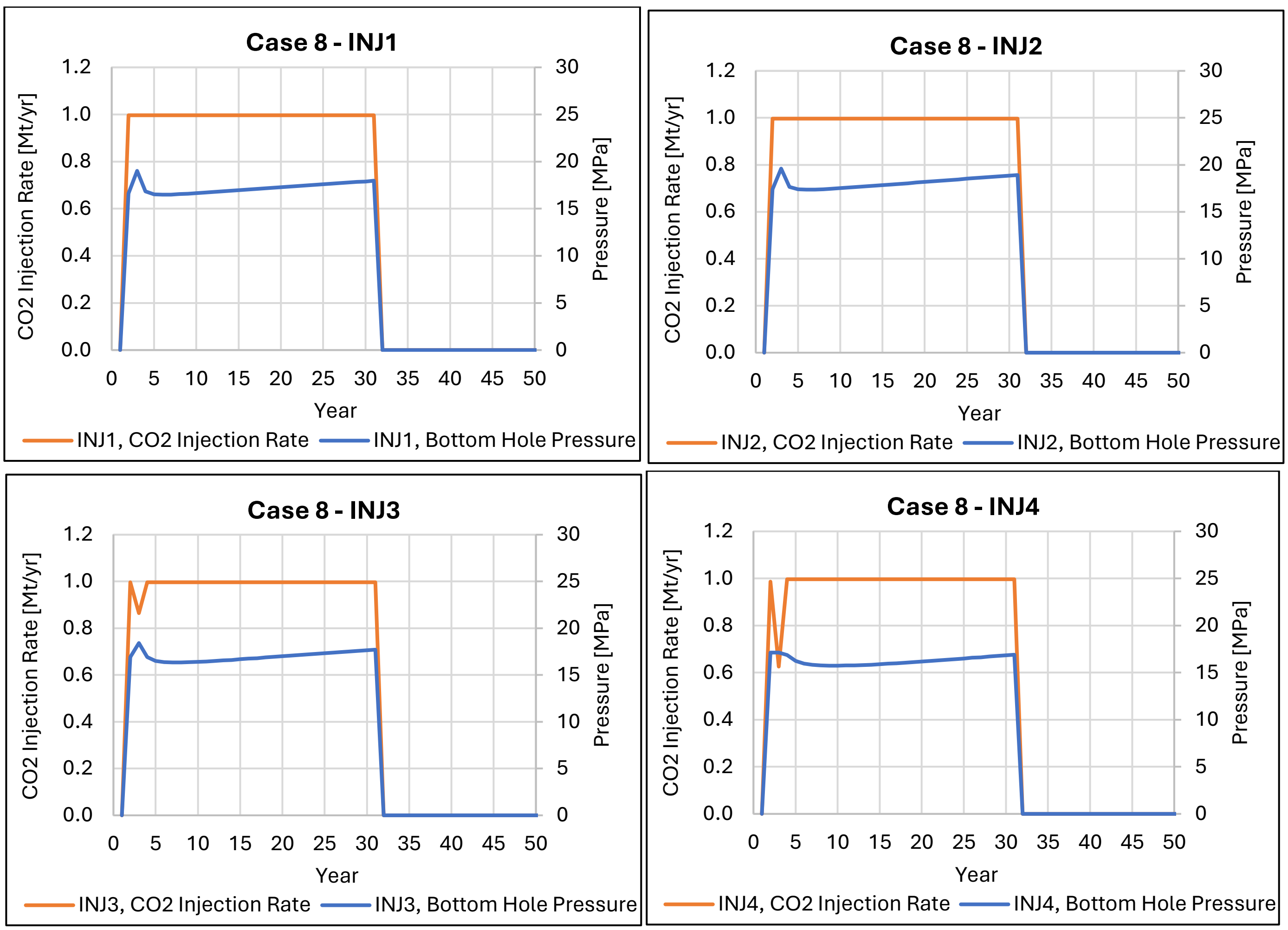

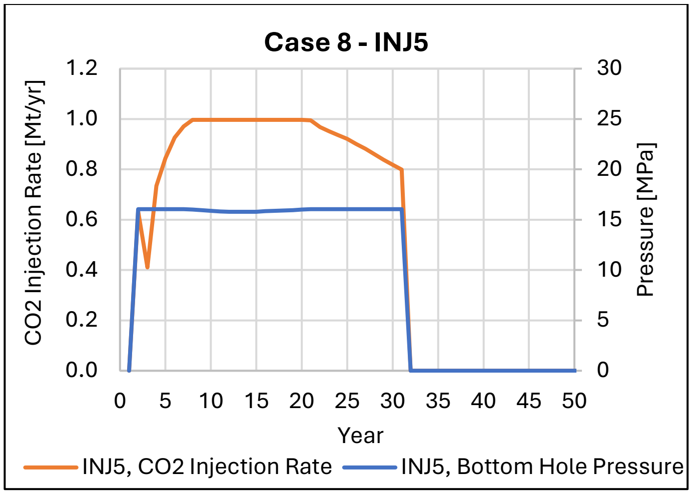
Case 8 - INJ5
CO2 Injection Rate [Mt/yr]
Pressure [MPa]
Year
INJ5, CO2 Injection Rate
INJ5, Bottom Hole Pressure

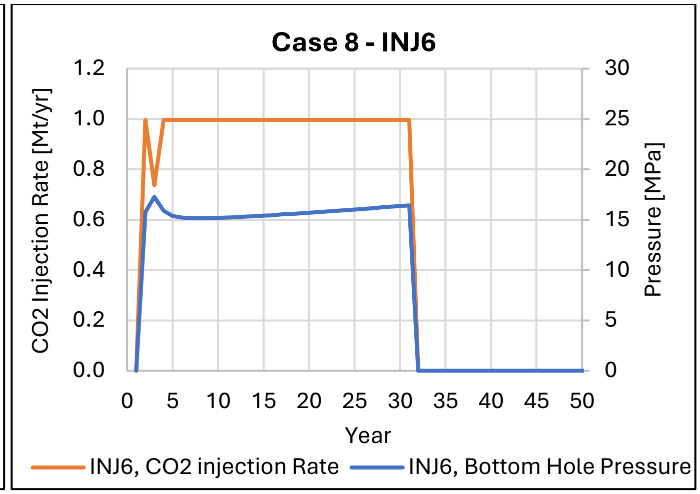
Case 8 - INJ6
CO2 Injection Rate [Mt/yr]
Pressure [MPa]
Year
INJ6, CO2 injection Rate
INJ6, Bottom Hole Pressure

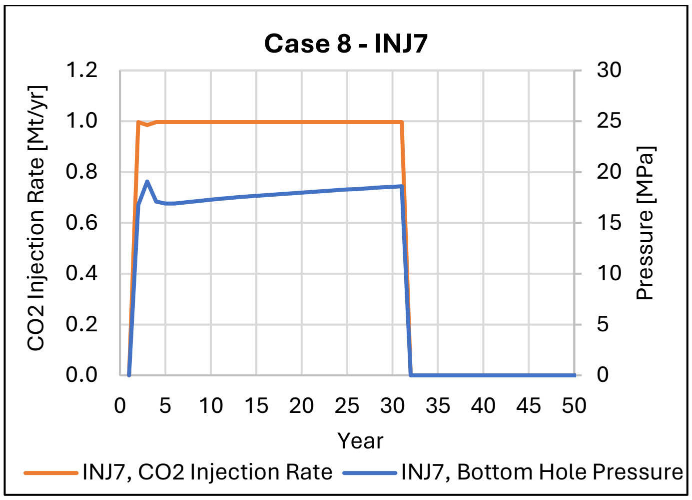
Case 8 - INJ7
CO2 Injection Rate [Mt/yr]
Pressure [MPa]
Year
INJ7, CO2 Injection Rate
INJ7, Bottom Hole Pressure

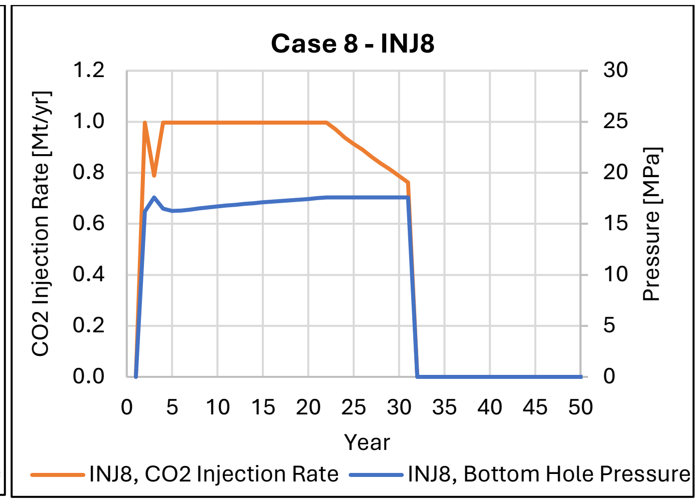
Case 8 - INJ8
CO2 Injection Rate [Mt/yr]
Pressure [MPa]
Year
INJ8, CO2 Injection Rate
INJ8, Bottom Hole Pressure

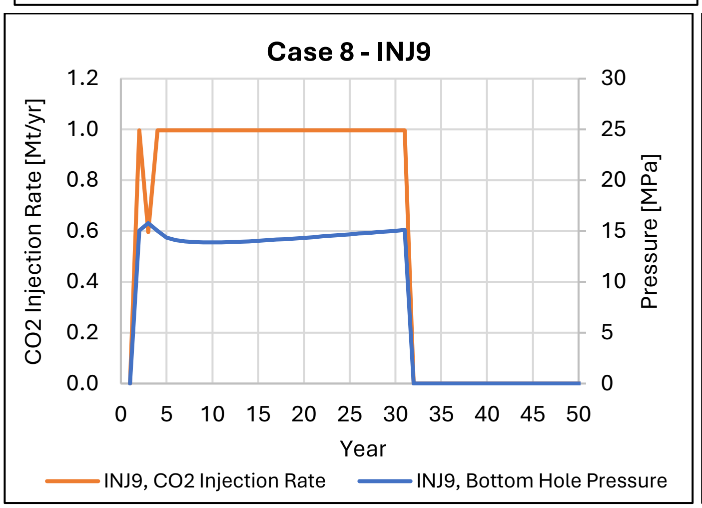
Case 8 - INJ9
CO2 Injection Rate [Mt/yr]
Pressure [MPa]
Year
INJ9, CO2 Injection Rate
INJ9, Bottom Hole Pressure

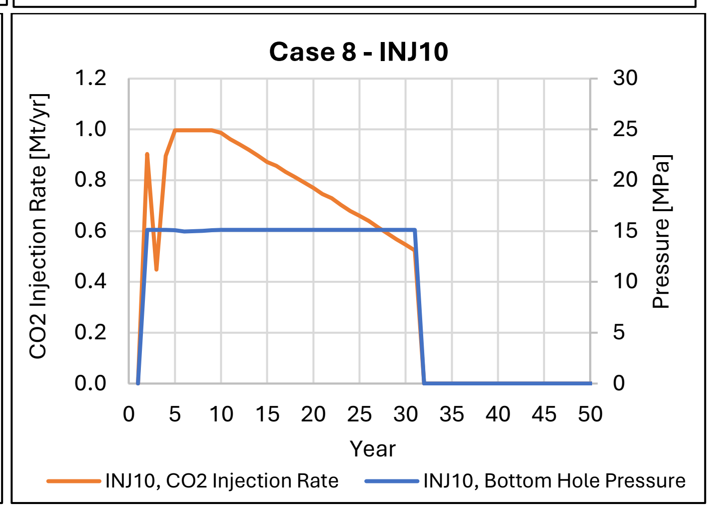
Case 8 - INJ10
CO2 Injection Rate [Mt/yr]
Pressure [MPa]
Year
INJ10, CO2 Injection Rate
INJ10, Bottom Hole Pressure

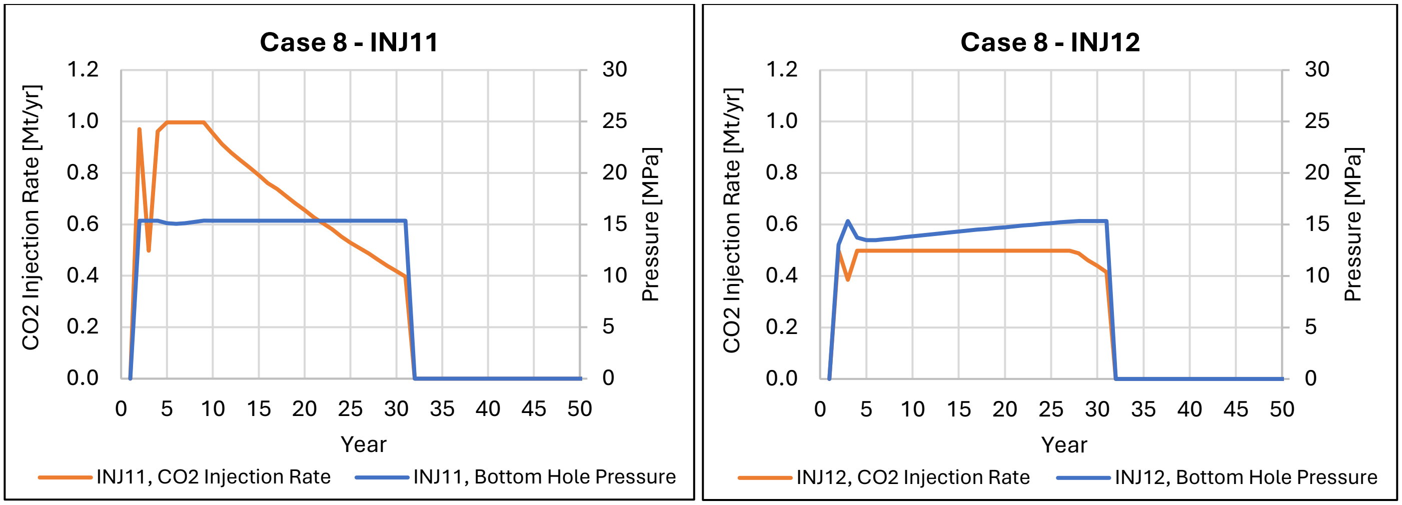

Figure 58: Case 8, Well injection rates and bottomhole pressures

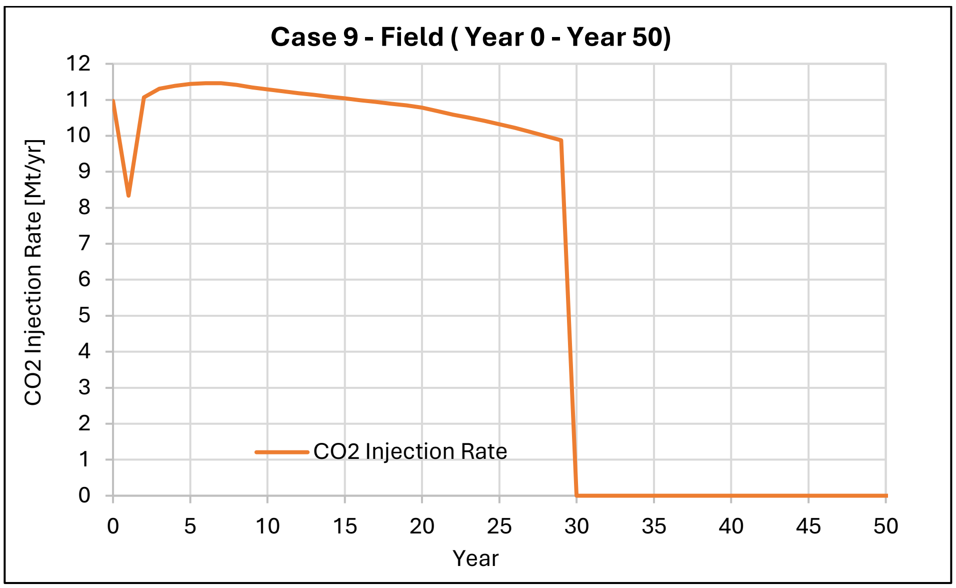

Figure 59: Case 9, Field injection rate

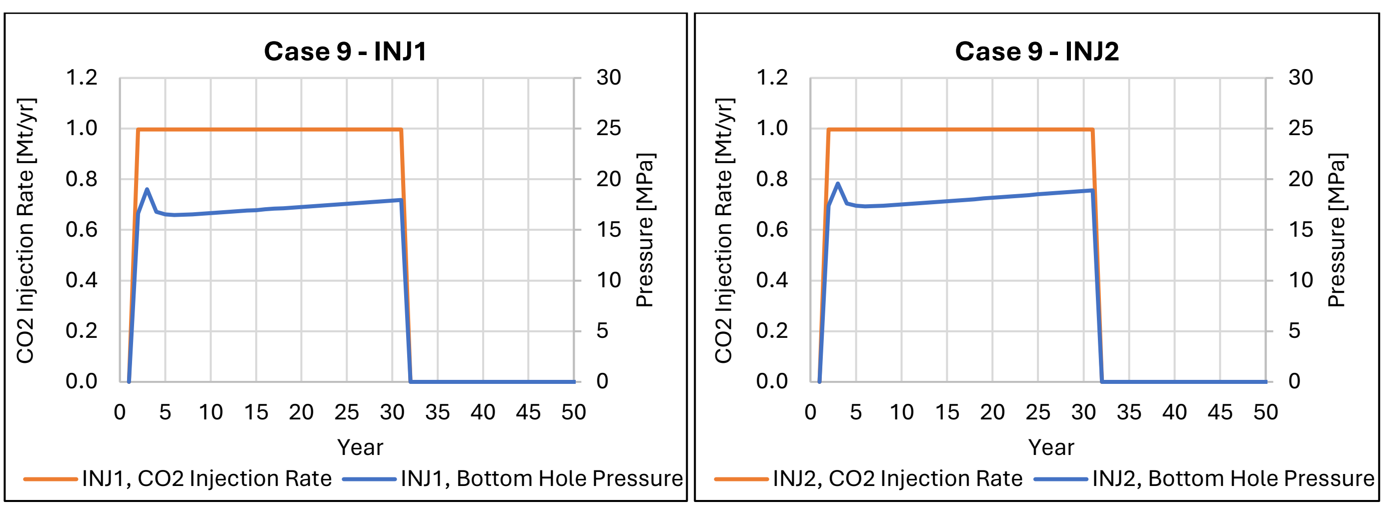

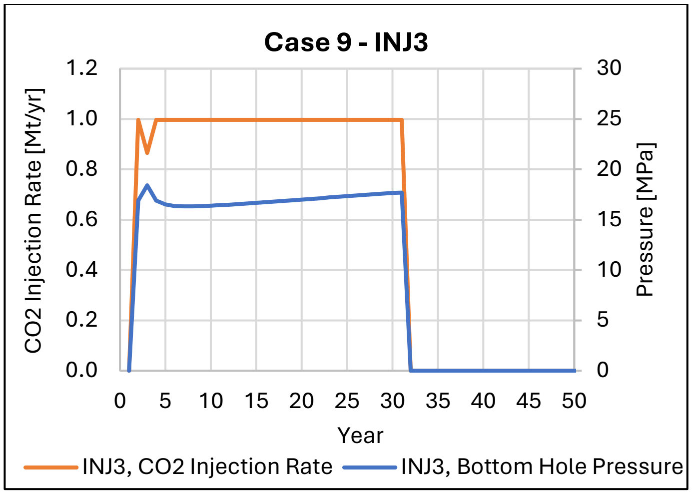
Case 9 - INJ3
CO2 Injection Rate [Mt/yr]
Pressure [MPa]
Year
INJ3, CO2 Injection Rate
INJ3, Bottom Hole Pressure

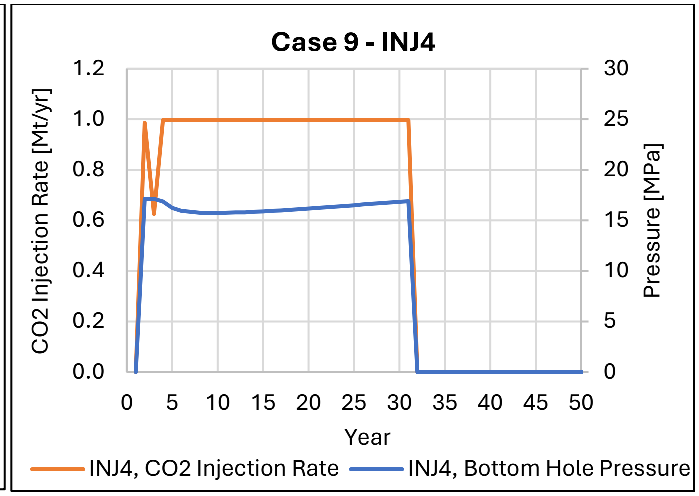
Case 9 - INJ4
CO2 Injection Rate [Mt/yr]
Pressure [MPa]
Year
INJ4, CO2 Injection Rate
INJ4, Bottom Hole Pressure

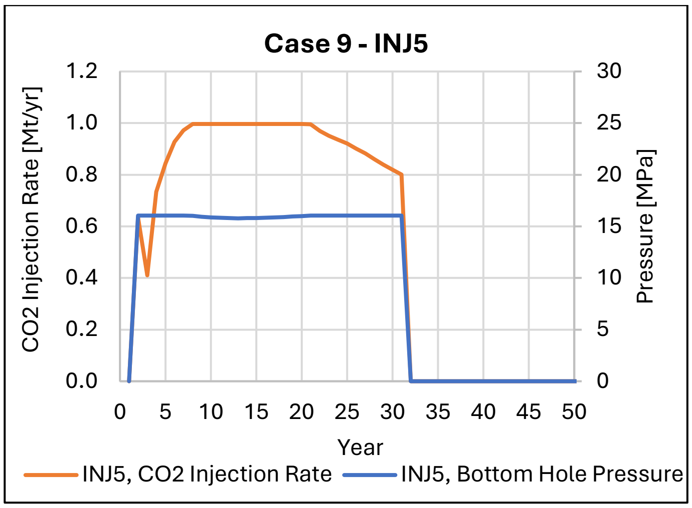
Case 9 - INJ5
CO2 Injection Rate [Mt/yr]
Pressure [MPa]
Year
INJ5, CO2 Injection Rate
INJ5, Bottom Hole Pressure

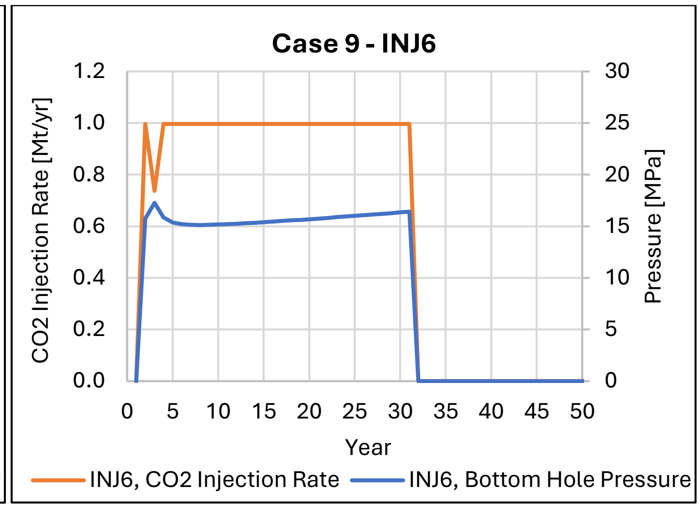
Case 9 - INJ6
CO2 Injection Rate [Mt/yr]
Pressure [MPa]
Year
INJ6, CO2 Injection Rate
INJ6, Bottom Hole Pressure

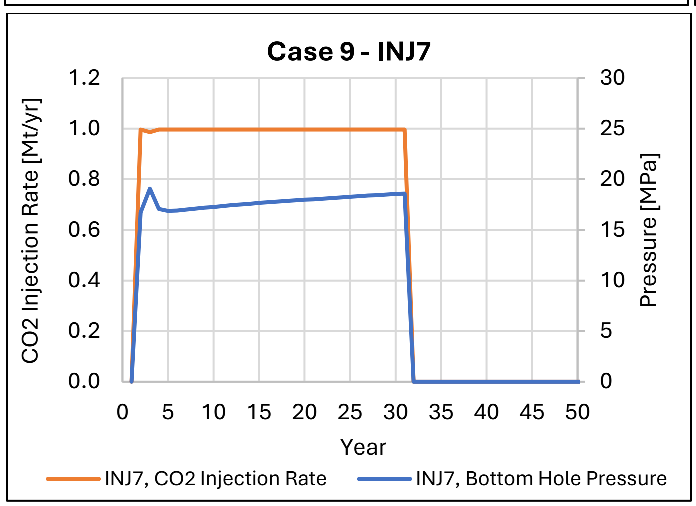
Case 9 - INJ7
CO2 Injection Rate [Mt/yr]
Pressure [MPa]
Year
INJ7, CO2 Injection Rate
INJ7, Bottom Hole Pressure

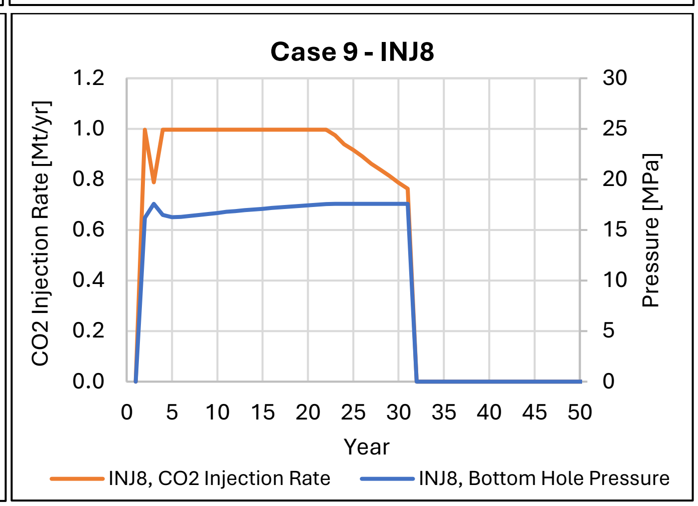
Case 9 - INJ8
CO2 Injection Rate [Mt/yr]
Pressure [MPa]
Year
INJ8, CO2 Injection Rate
INJ8, Bottom Hole Pressure

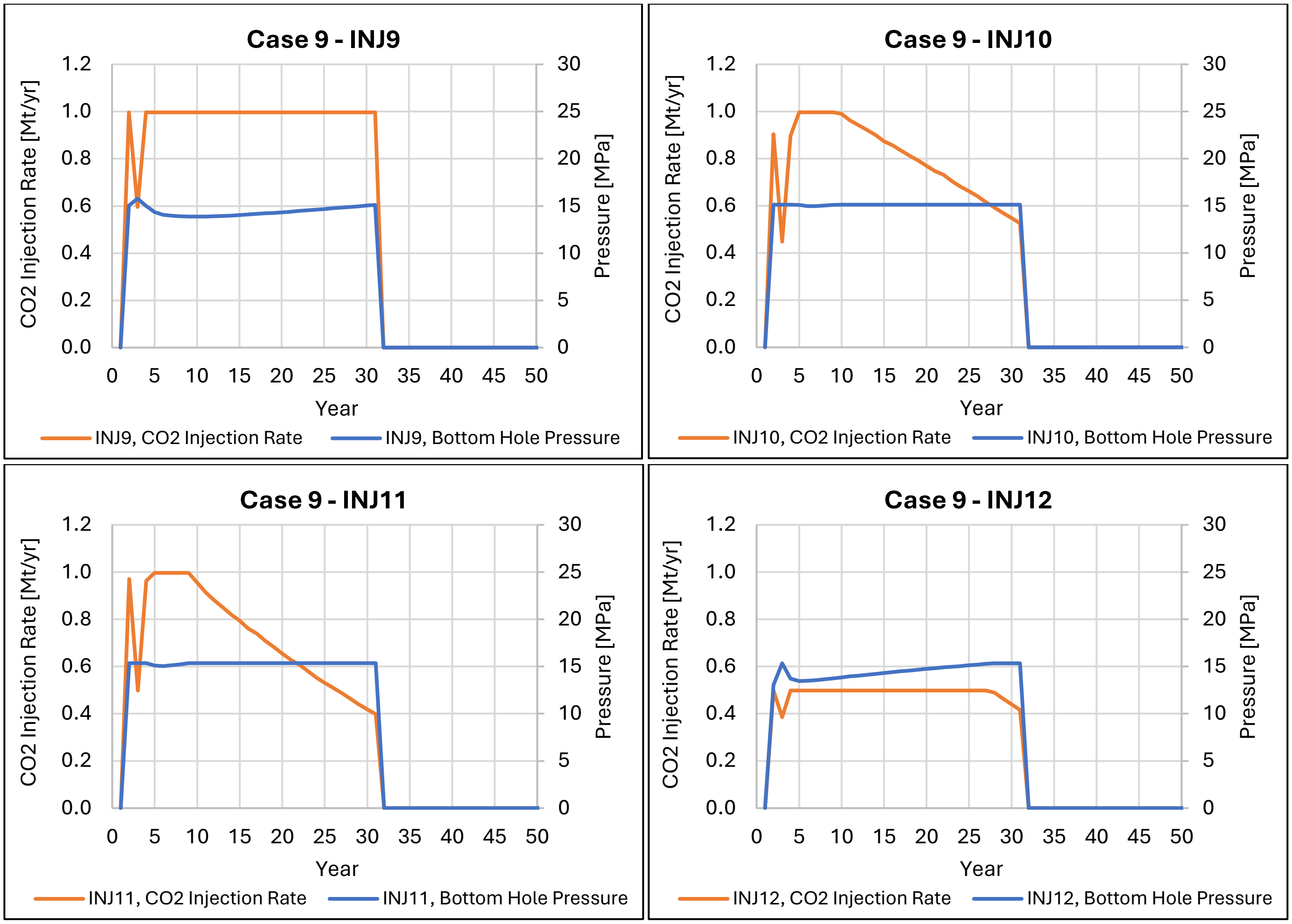

Figure 60: Case 9, Well injection rates and bottomhole pressures

Appendix 1.3: Baltic Sea Plume Top Views

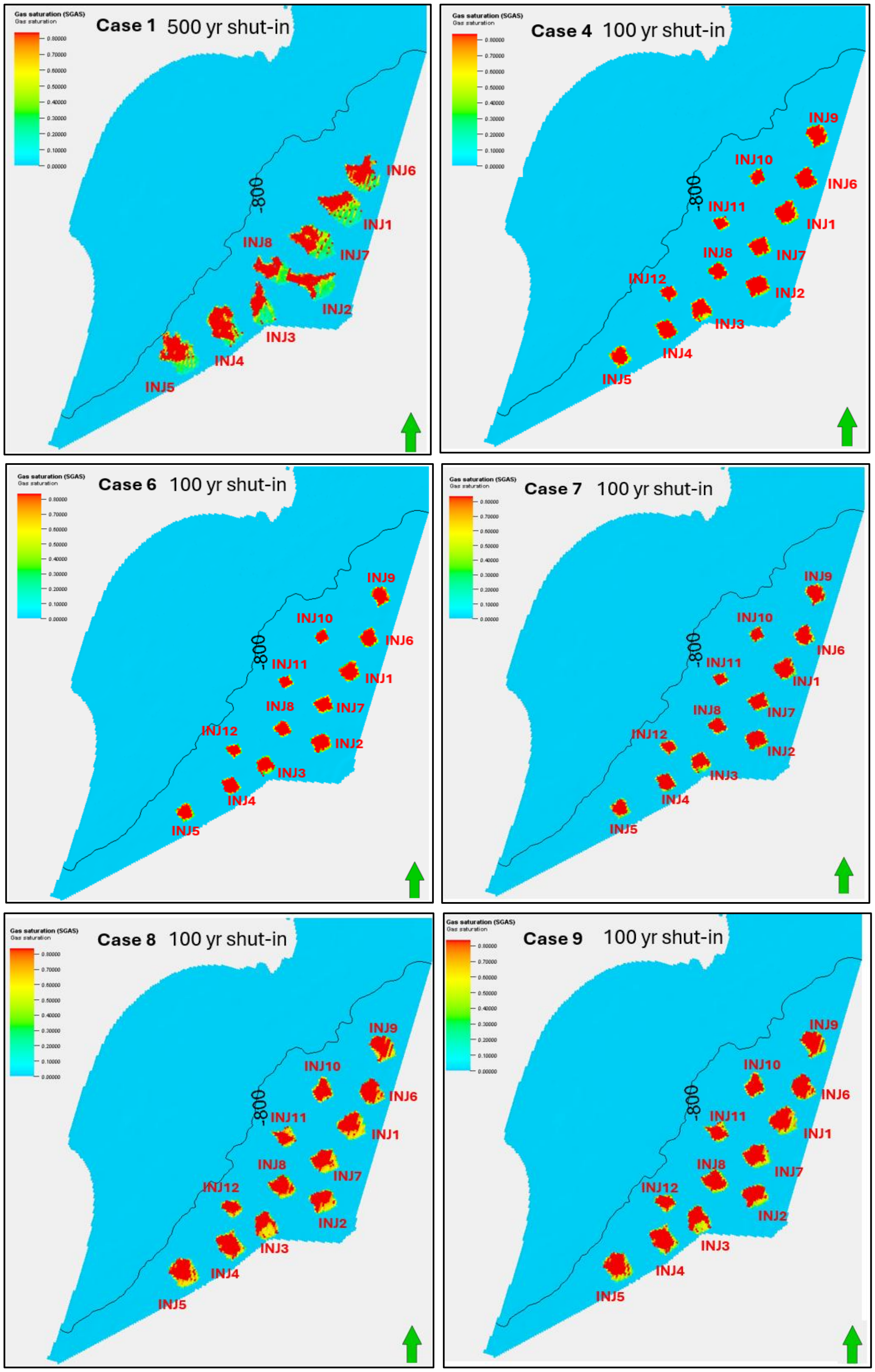

Figure 61: Top views of plumes

Appendix 2: Arnager Greensand (Skåne)

Additional plots related to the Skåne reservoir input parameters and detailed results of the simulation cases are summarized in the following sub-sections.

Appendix 2.1: Skåne Well Layout and Reservoir Property Variations

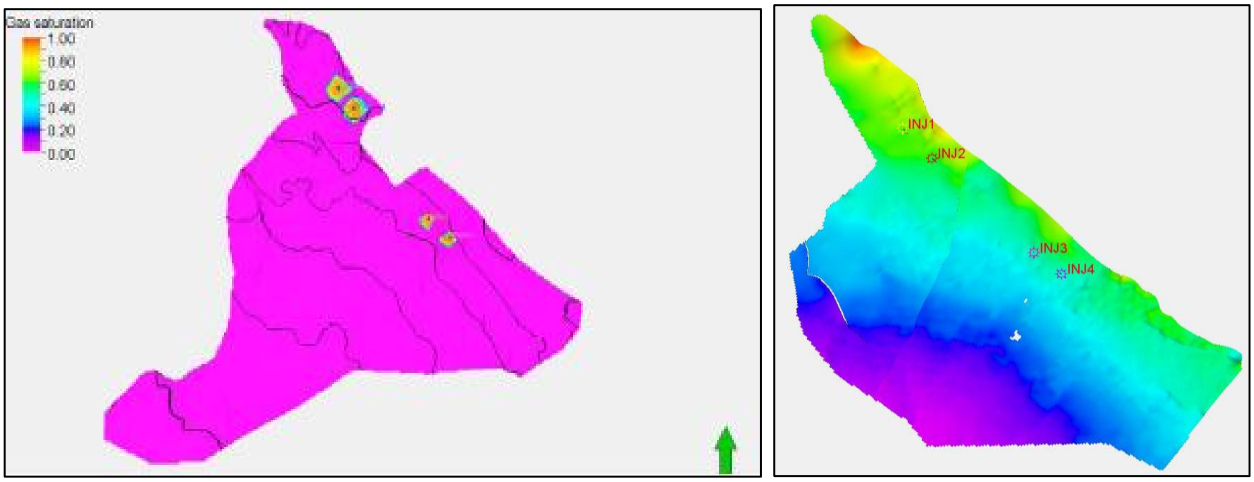

(a) Tested Previous Injection Sites (Lothe et al., 2015) (b) Well placement in the Test Runs

Figure 62: Tested injection sites in the deeper region

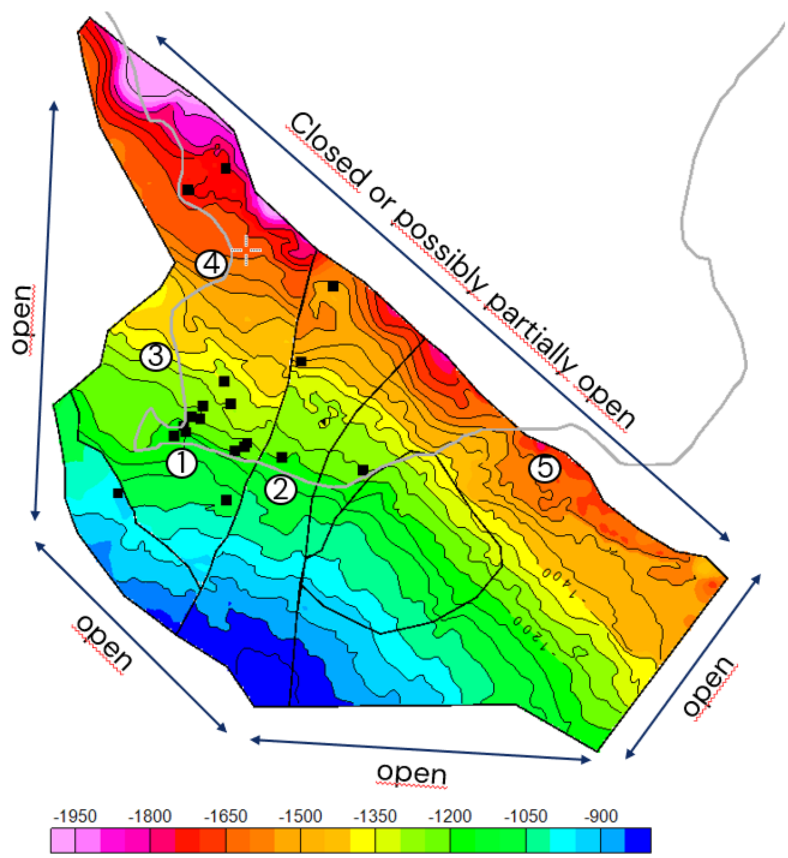

Figure 63: SGU suggested injection sites, costal line, and boundary conditions

Table 13: Summary of various properties for the Arnager Greensand

Parameter	Average All areas	HG-South (Höllviken Halfgraben) (H-1, H-2, Gr-1, Ma-1öllviken-1, Maglarp-1, Es-1, Ku-1, Hnäs-, Lju-1, Sm-1), Ha-1, Hå-1, Skåre-1)			HG-North (Höllviken Halfgraben) North, area (FCC-1, Ba-1, Nv-1)			Falsterbo High (F-1)			Skurup Platform, Area A (Tr-1, Sv-1, Mo-1)			Skurup Platform Area B			Skurup Platform Area C (L. Beddinge-1)		
		Low	Mean	High	Low	Mean	High	Low	Mean	High	Low	Mean	High	Low	Mean	High	Low	Mean	High
Gross thickness, m	41[2]	30[3]	45[3]	55[3]	15[1]	25[3]	35[3]	15[1]	20[3]	25[1]	15[1]	30[1]	45[3]	0[1]	5[1]	10[1]	10[1]	20[1]	30[1]
Net/gross ratio, cut off phie=10% or 100 mD	0.7[1]	0.7[3]	0.8[3]	0.9[3]	0.2[1]	0.4[1]	0.6[1]	0.7[1]	0.8[1]	0.9[1]	0.3[1]	0.5[1]	0.7[1]	-	0.3[1]	0.5[1]	0.3[1]	0.5[1]	0.7[1]
Total porosity, %	22.5[2]	17[2]	22[2]	32[2]	15	20	23	17	22	32	22[2]	24[2]	31[2]	0[1]	15[1]	20[1]	15[1]	20[1]	25[1]
Gas perm. mD	308[2]	100[1]	350[1]	2000[1]	50[1]	100[1]	200[1]	100[1]	350[1]	2000[1]	50[1]	100[1]	1000[1]	0[1]	50[1]	100[1]	50[1]	100[1]	200[1]
Kh/Kv	0.5?	-	-	-	-	-	-	-	-	-	-	0.5 [5]	-	-	-	-	-	-	-
Temp., °C	40-55°C																		
Therm. Cond. W/mK	1.5	-	-	-	-	-	-	-	-	-	-	-	-	-	-	-	0.8[4]	1.5[4]	2.4[4]
Salinity, g/l		Höllviken-2 1200 m 124 g/l Svedala-1 1495 m 160 g/l Höllviken-1 1247 m 123 g/l Trelleborg-1 1193 m 158 g/l Granvik-1 1251 m 130 g/l																	
TDS, g/l		Skåre-1, 1213 m, 148 g/l FFC-1, 1610 m, 174 g/l															L. Beddinge-1, 1275 m, 141 g/l [6]		
Comments		The Arnager Greensand consists in the south of largely unconsolidated, medium-grained sand with high porosity and permeability. Towards the north and the FFC-1 and Barsebäck-1 wells the sandstone becomes gradually finer grained and less permeable which also coincides with the gradual decrease in gross thickness as well as the gross to net sand ratio. The results from the core analyses represent scattered intervals in few wells and of relatively consolidated parts of the sandstone.						Very little is known about the sandstone properties in this area. The assessments are based on well information from Falsterborev-1 and evaluation of seismic data. No core data exists. Judged to have similar properties as in the south part of the Höllviken Halfgraben			The properties of the Arnager Greensand in the western part of the platform, (Area A) is in the south judged to be like the properties in the Höllviken Halfgraben, as indicated by core data from the upper part of the Arnager Greensand in Trelleborg-1. In comparison, core analyses from Svedala-1, located north of Trelleborg-1 show slightly lower permeability. Although, the porosity is still relatively high. To the east, towards Area B there is a gradual decrease in permeability and net sand. Again, this seems to coincide with a decreasing thickness of the sandstone. The characteristic of the sandstone in Area C is poorly known. Likewise, we anticipate a sandstone that decreases gradually in thickness towards Area B where it likely onlaps this central high area. Similarly, we judge the net sand to decrease in the same direction.								

1) Judged 2) Based on evaluation of core analyses 3) Based on well logs 4) Lilla Beddinge-1 5) one data point in Svedala-1 6) TDS (mg/L) = 1.656 · Cl (mg/L) – 3528 (mg/L) (Schovsbo et al 2025)

Appendix 2.2: Skåne Injection Rates and Pressures

Table 14: Per well basis cumulative injected CO_2 amount in the Skåne model

Injector No.	Case 1 [Mt]	Case 2 [Mt]	Case 3 [Mt]	Case 4 [Mt]	Case 5 [Mt]	Case 6 [Mt]	Case 7 [Mt]	Case 8 [Mt]	Case 9 [Mt]
INJ1	29.9	29.7	16.7	29.9	14.0	29.6	29.7	29.7	29.1
INJ2	6.9	6.7	3.9	14.8	3.1	5.6	6.6	6.7	6.2
INJ3	29.9	29.9	22.3	29.9	17.7	29.8	29.9	29.9	29.9
INJ4	13.3	12.2	5.7	14.9	4.6	9.5	12.1	12.1	15.0
INJ5	6.2	5.0	2.8	8.4	2.4	4.3	5.0	5.0	7.0
INJ6	-	11.3	5.7	14.9	4.7	9.2	11.3	11.3	15.0
INJ7	-	6.4	3.7	10.9	3.2	5.8	6.4	6.4	8.6

Note: INJ4, INJ5, INJ6, INJ7 are vertical wells in Cases 1-8, while are horizontal wells in Case 9.

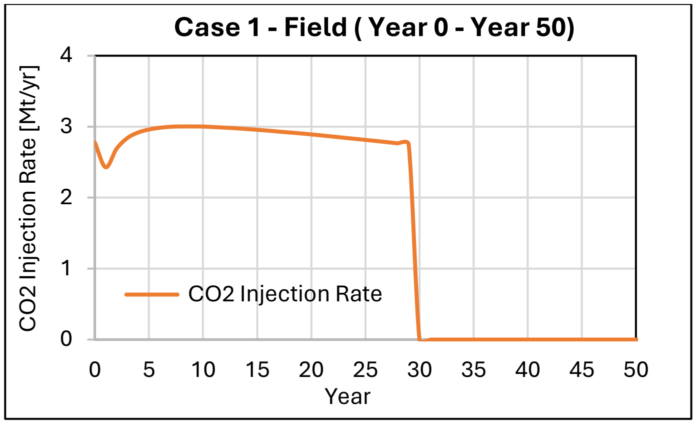

Figure 64: Case 1, Field injection rate

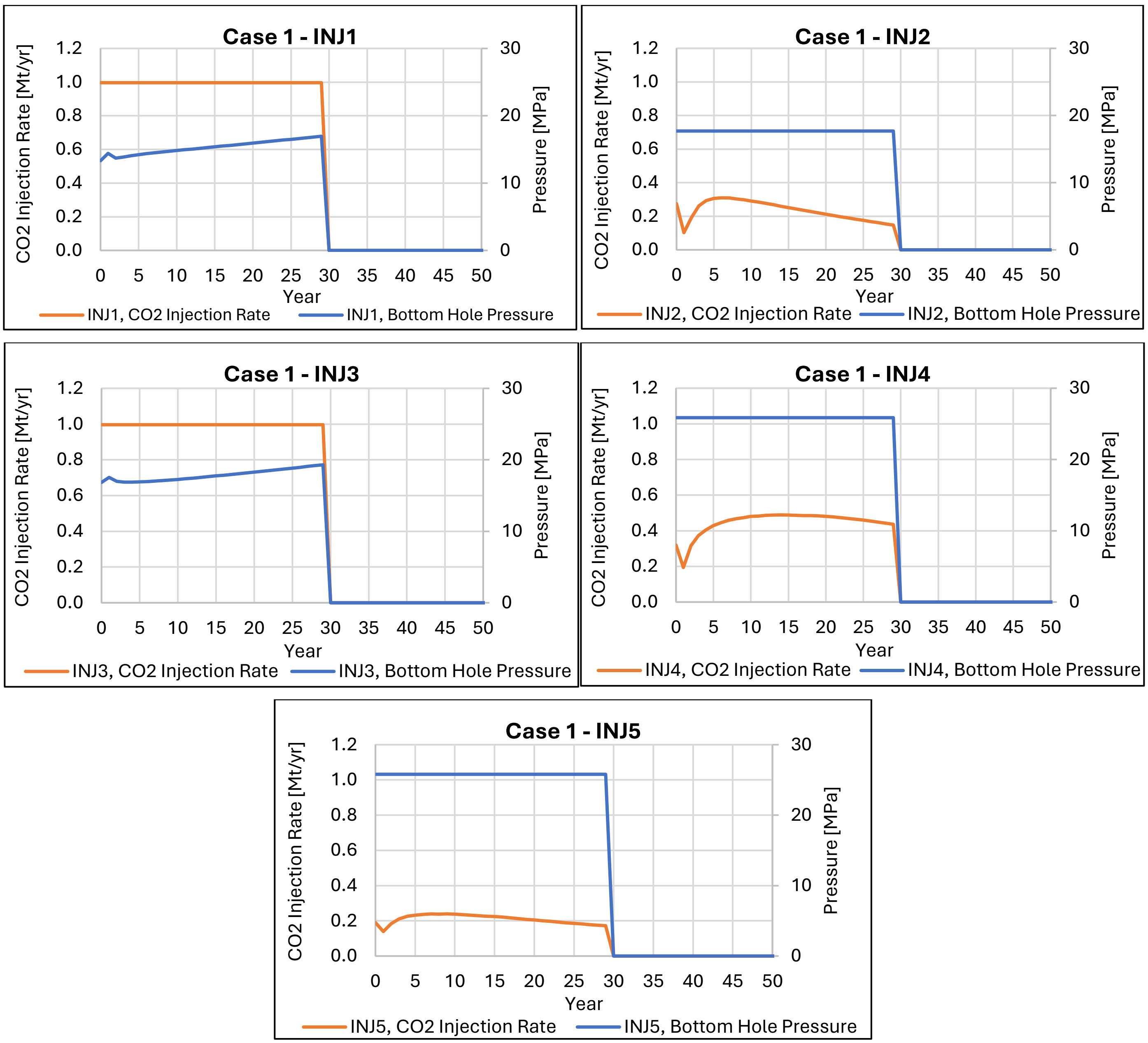

Figure 65: Case 1, Well injection rates and bottomhole pressures

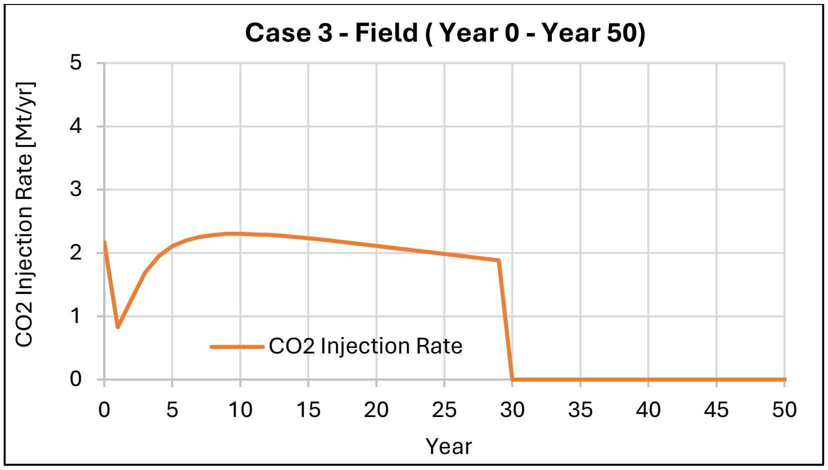

Figure 66: Case 3, Field injection rate

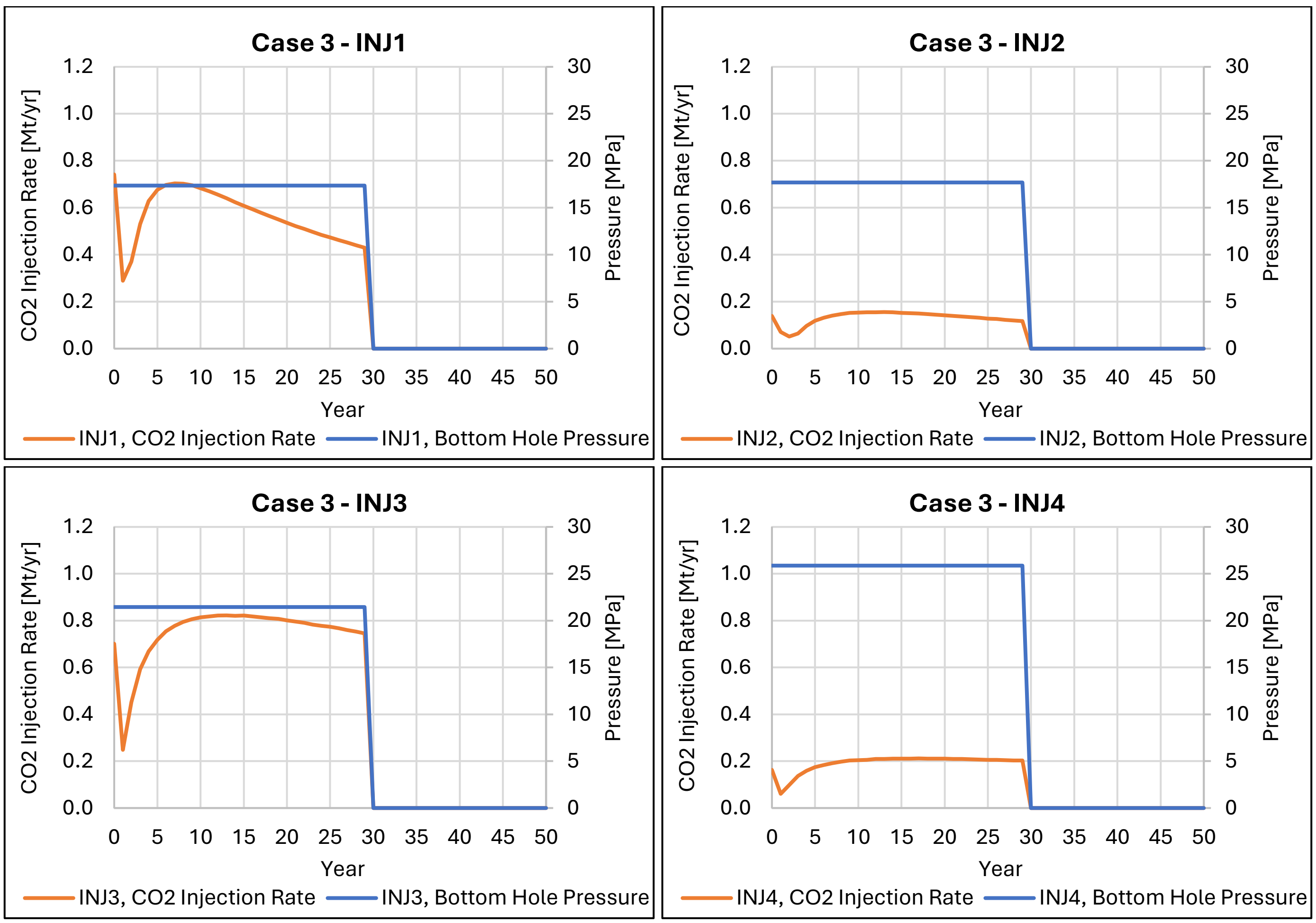

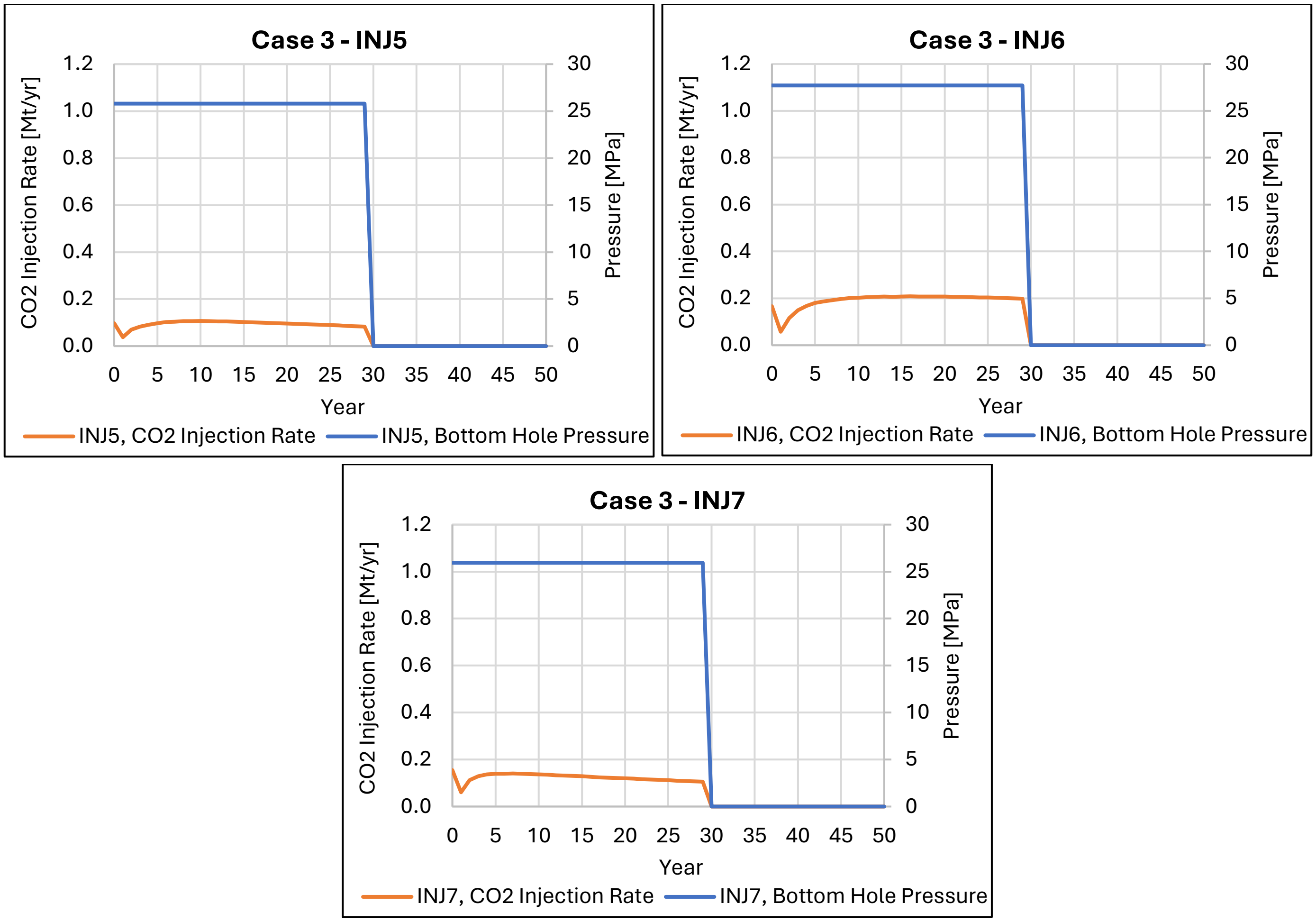

Figure 67: Case 3, Well injection rates and bottomhole pressures

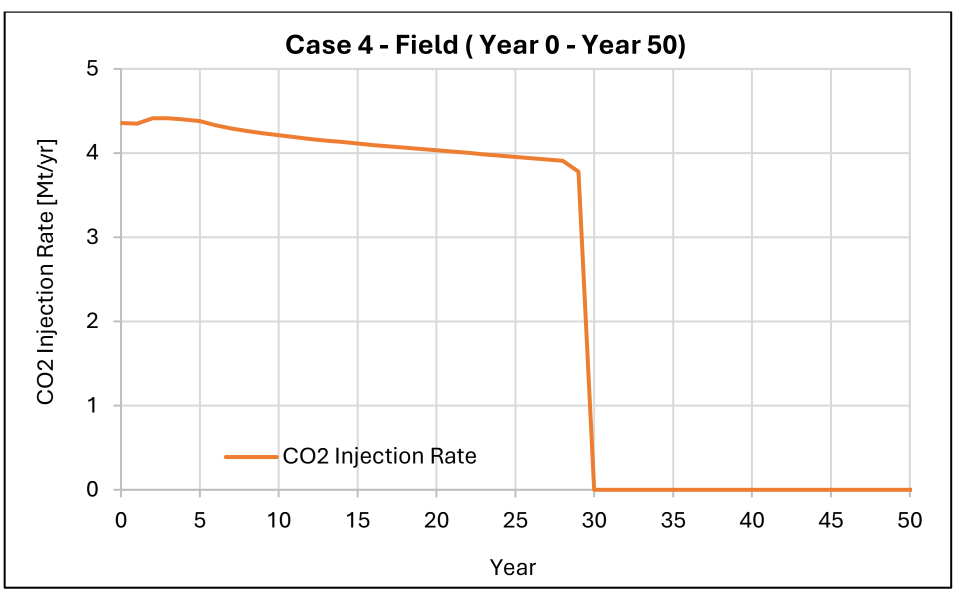

Figure 68: Case 4, Field injection rate

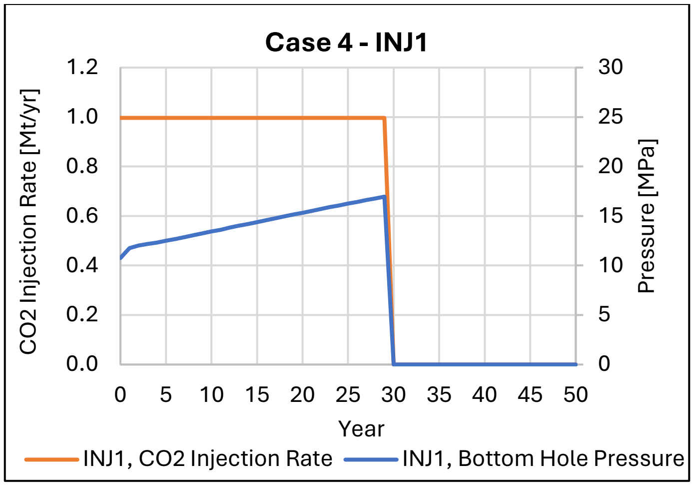

Case 4 - INJ1
CO2 Injection Rate [Mt/yr]
Pressure [MPa]
Year
INJ1, CO2 Injection Rate
INJ1, Bottom Hole Pressure

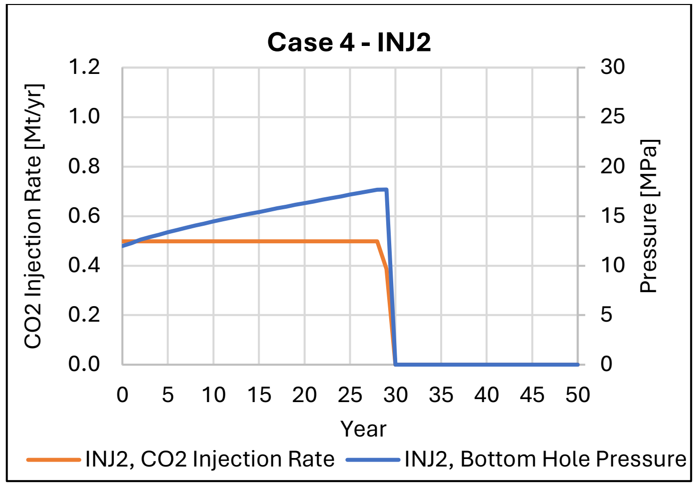

Case 4 - INJ2
CO2 Injection Rate [Mt/yr]
Pressure [MPa]
Year
INJ2, CO2 Injection Rate
INJ2, Bottom Hole Pressure

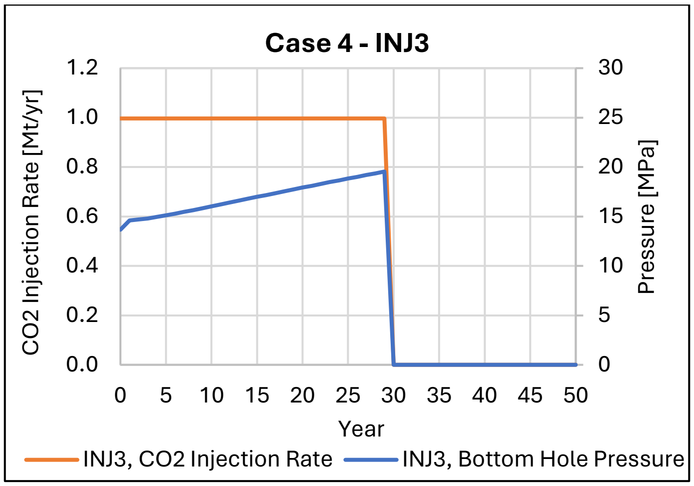

Case 4 - INJ3
CO2 Injection Rate [Mt/yr]
Pressure [MPa]
Year
INJ3, CO2 Injection Rate
INJ3, Bottom Hole Pressure

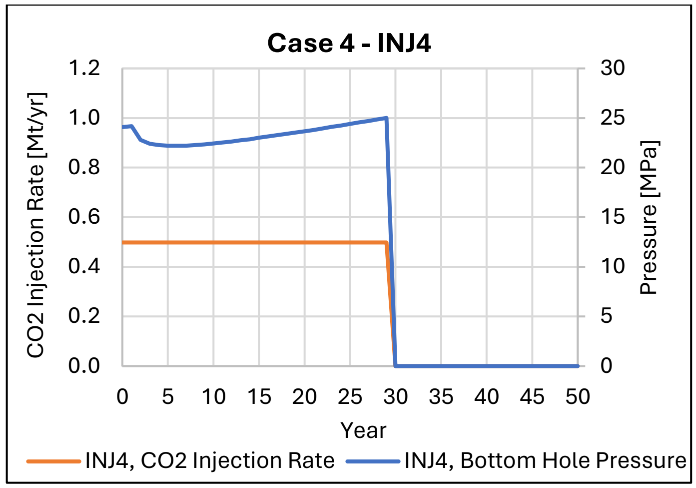

Case 4 - INJ4
CO2 Injection Rate [Mt/yr]
Pressure [MPa]
Year
INJ4, CO2 Injection Rate
INJ4, Bottom Hole Pressure

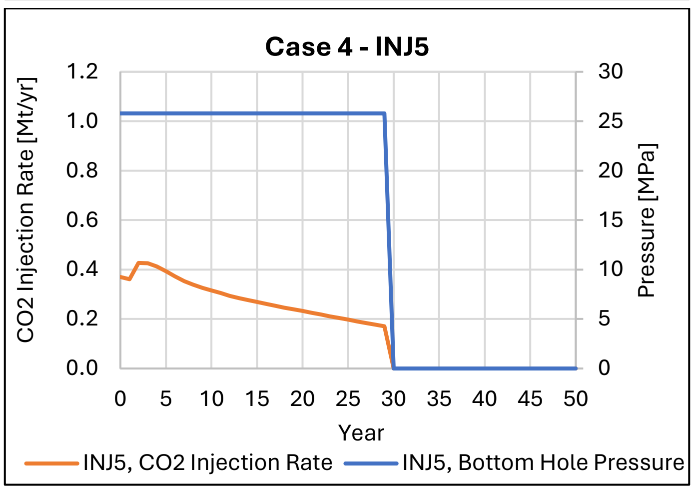

Case 4 - INJ5
CO2 Injection Rate [Mt/yr]
Pressure [MPa]
Year
INJ5, CO2 Injection Rate
INJ5, Bottom Hole Pressure

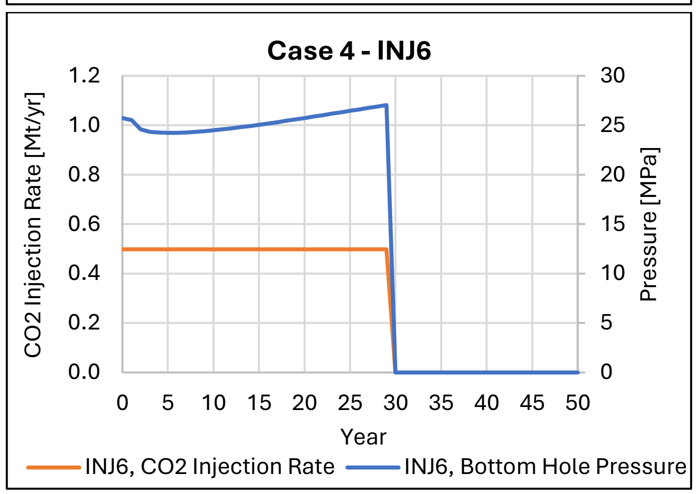

Case 4 - INJ6
CO2 Injection Rate [Mt/yr]
Pressure [MPa]
Year
INJ6, CO2 Injection Rate
INJ6, Bottom Hole Pressure

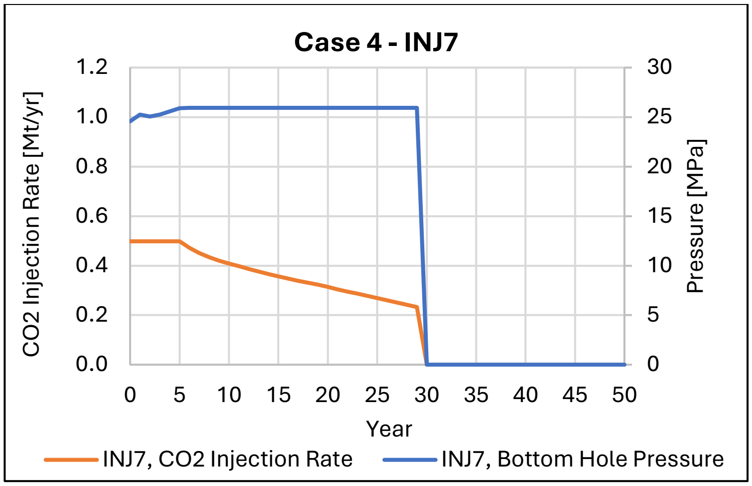

Figure 69: Case 4, Well injection rates and bottomhole pressures

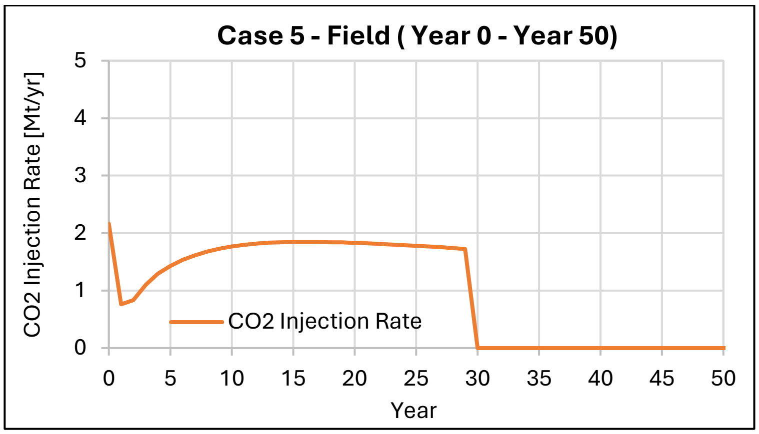

Figure 70: Case 5, Field injection rate

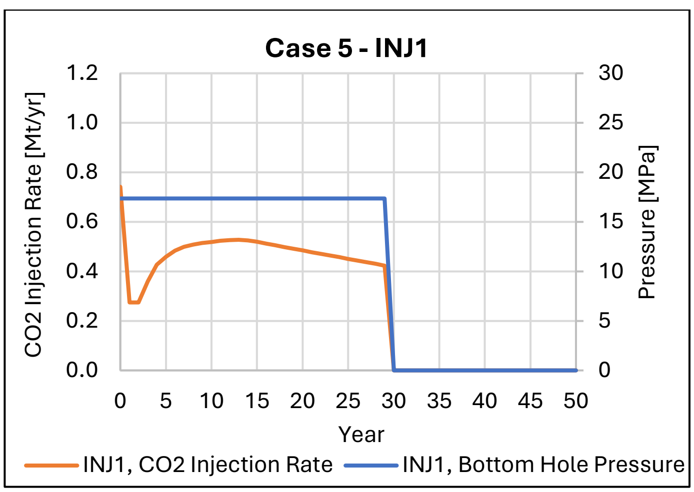

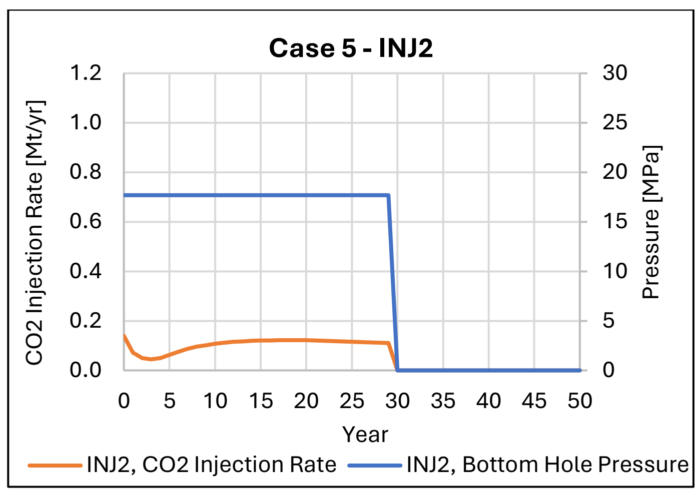

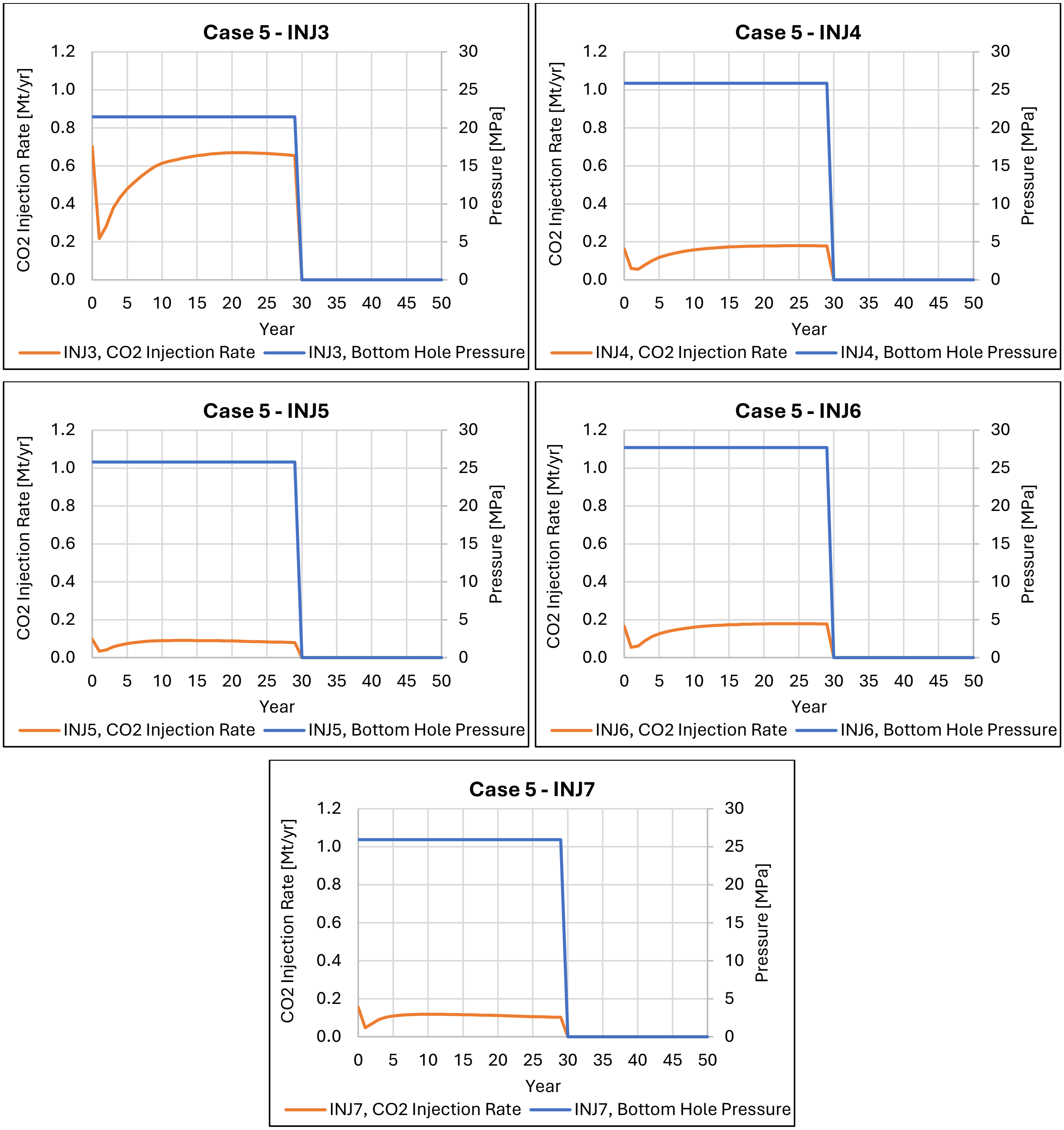

Figure 71: Case 5, Well injection rates and bottomhole pressures

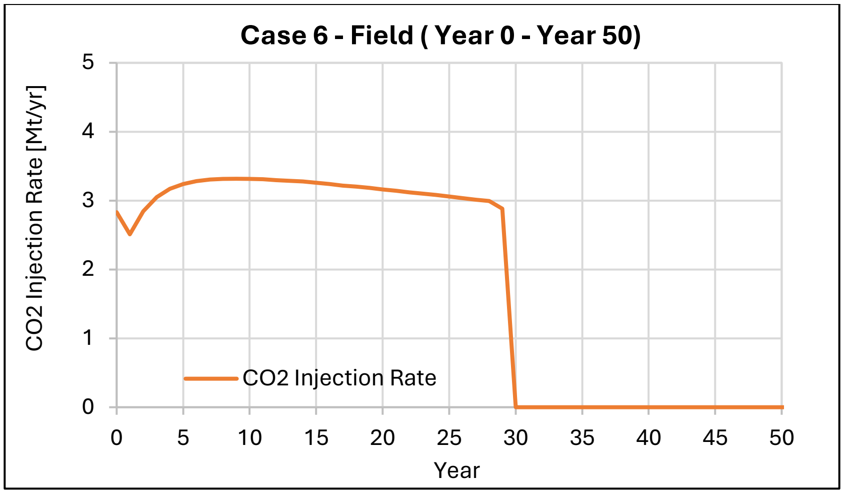

Figure 72: Case 6, Field injection rate

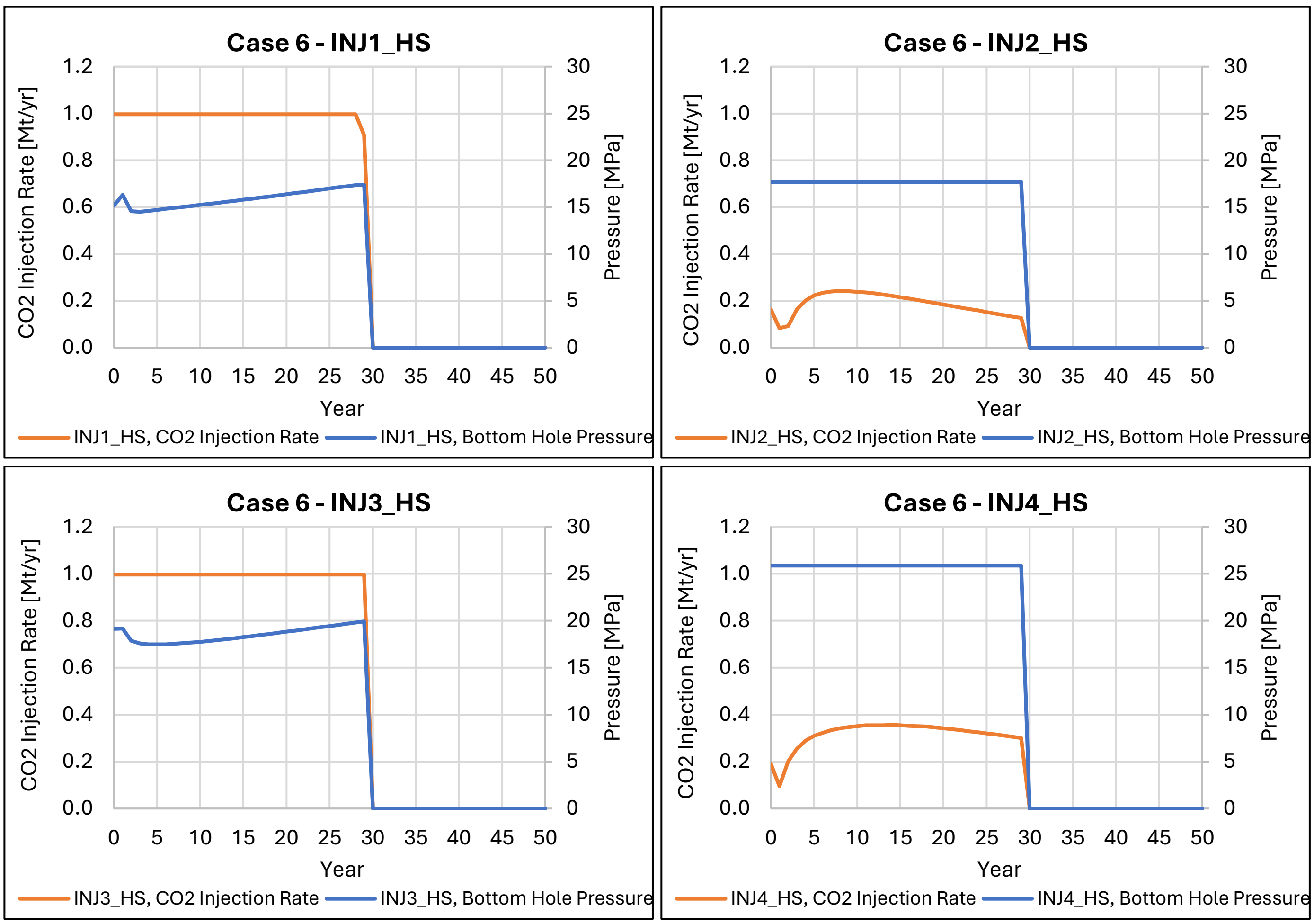

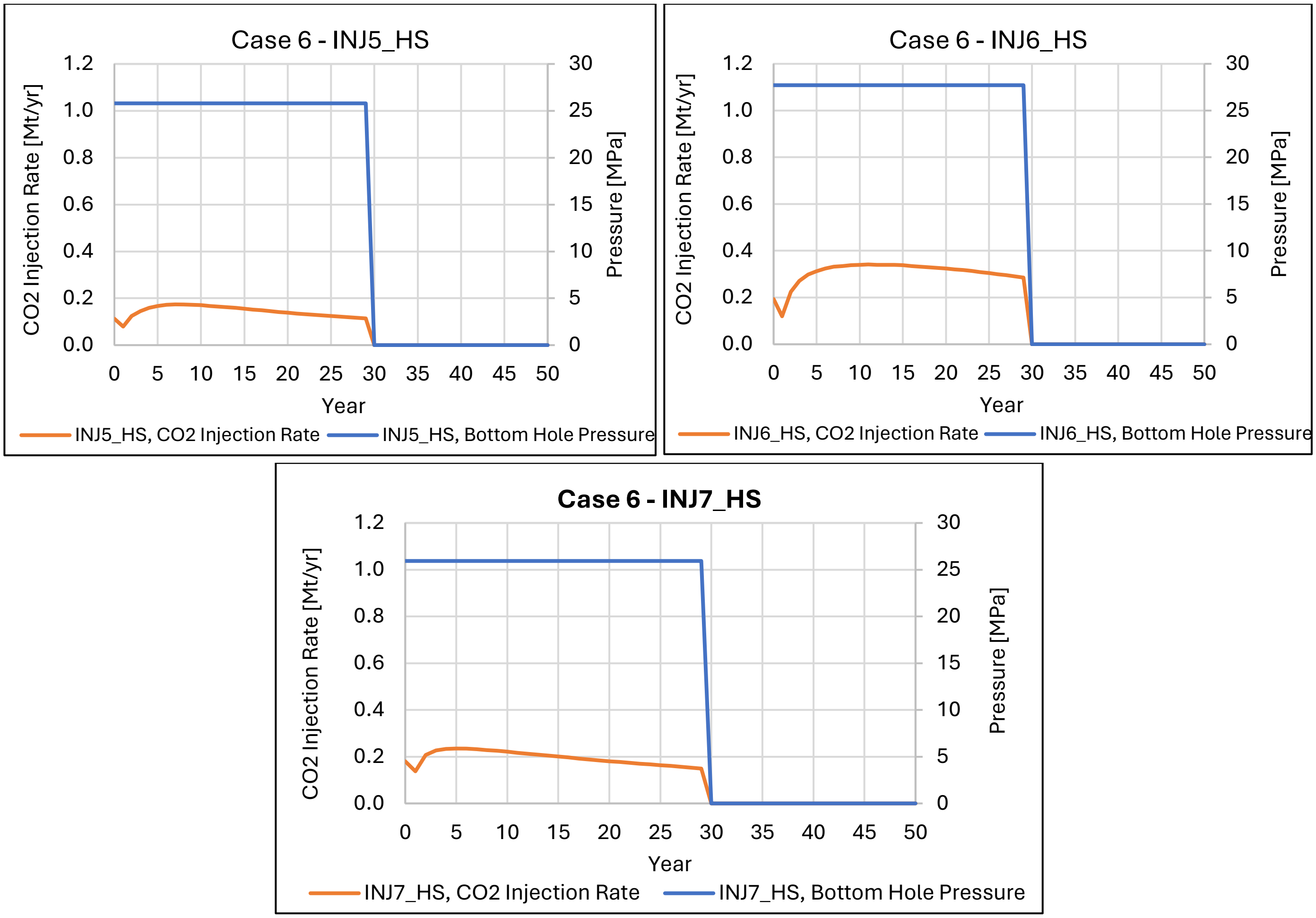

Figure 73: Case 6, Well injection rates and bottomhole pressures

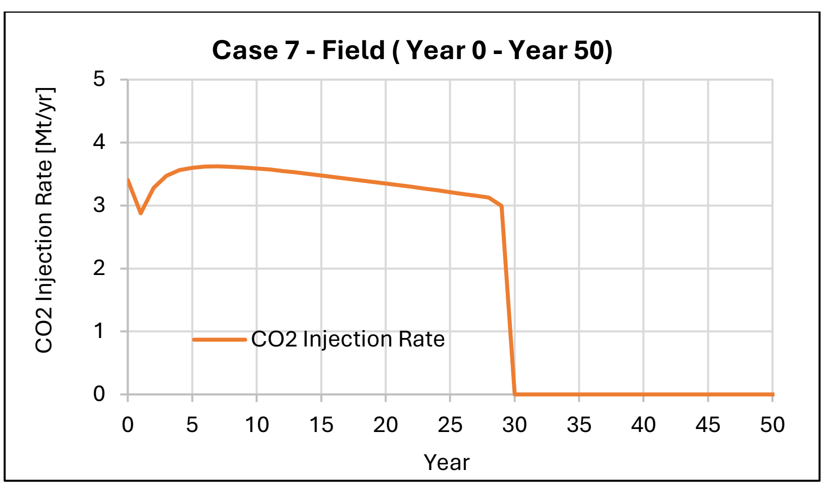

Figure 74: Case 7, Field injection rate

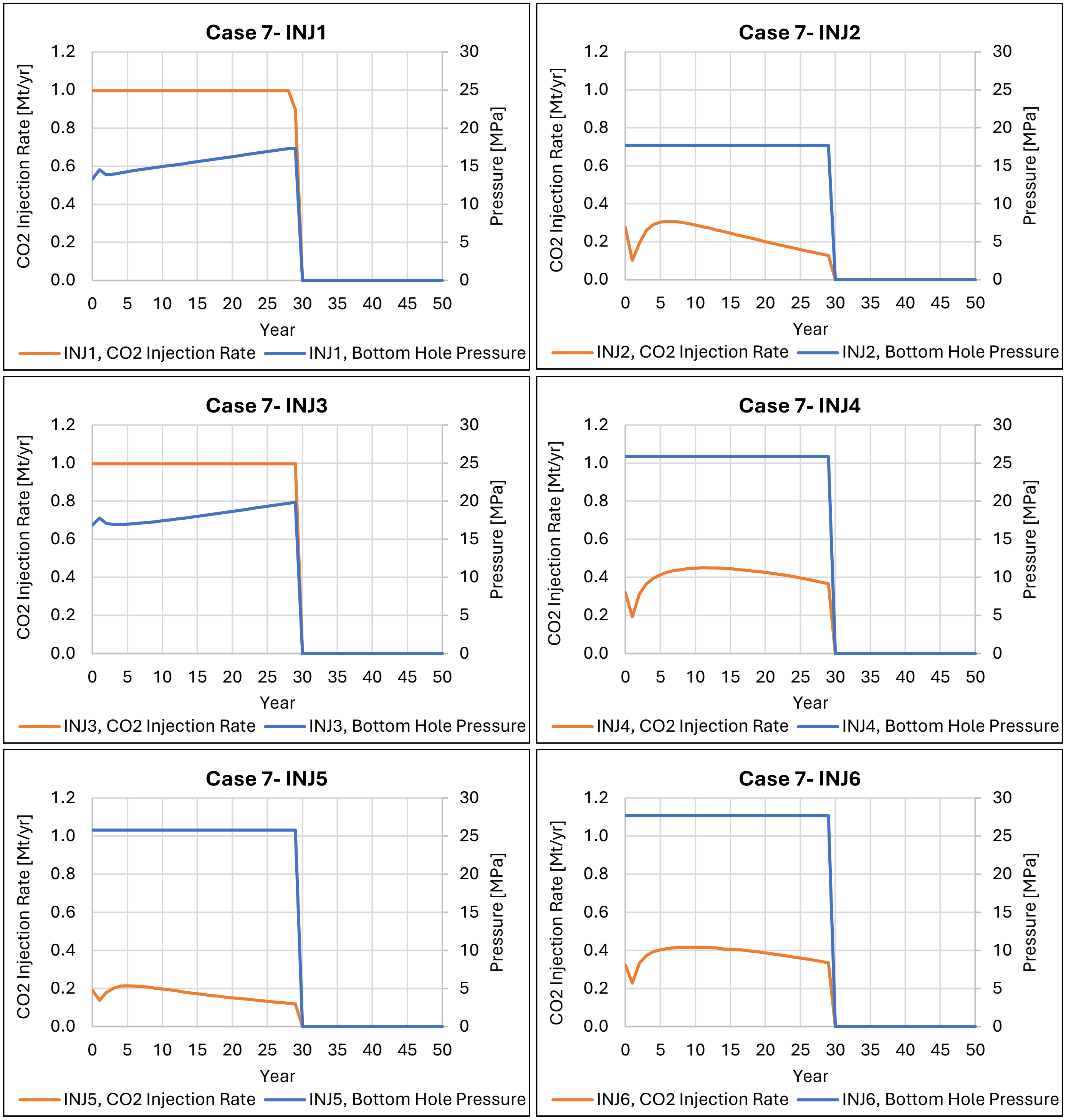
Case 7- INJ1
Case 7- INJ2
Case 7- INJ3
Case 7- INJ4
Case 7- INJ5
Case 7- INJ6
CO2 Injection Rate [Mt/yr]
Pressure [MPa]
Year
1.2
1.0
0.8
0.6
0.4
0.2
0.0
30
25
20
15
10
5
0
0 5 10 15 20 25 30 35 40 45 50
INJ1, CO2 Injection Rate
INJ1, Bottom Hole Pressure
INJ2, CO2 Injection Rate
INJ2, Bottom Hole Pressure
INJ3, CO2 Injection Rate
INJ3, Bottom Hole Pressure
INJ4, CO2 Injection Rate
INJ4, Bottom Hole Pressure
INJ5, CO2 Injection Rate
INJ5, Bottom Hole Pressure
INJ6, CO2 Injection Rate
INJ6, Bottom Hole Pressure

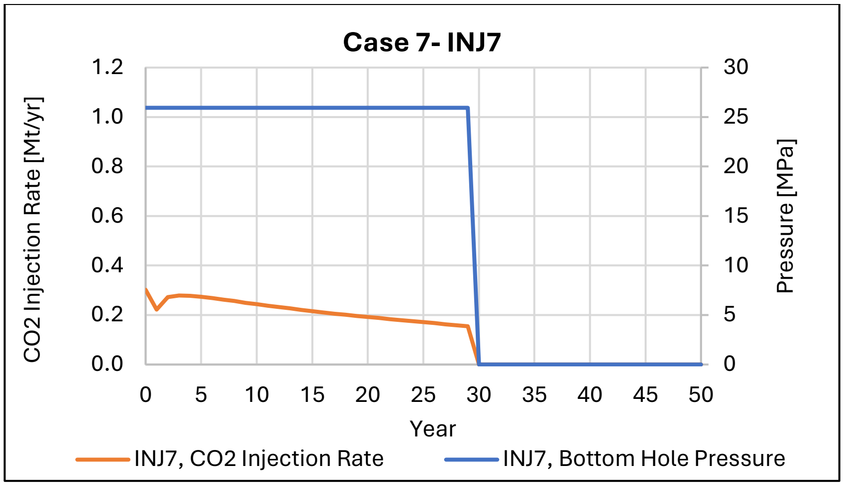

Figure 75: Case 7, Well injection rates and bottomhole pressures

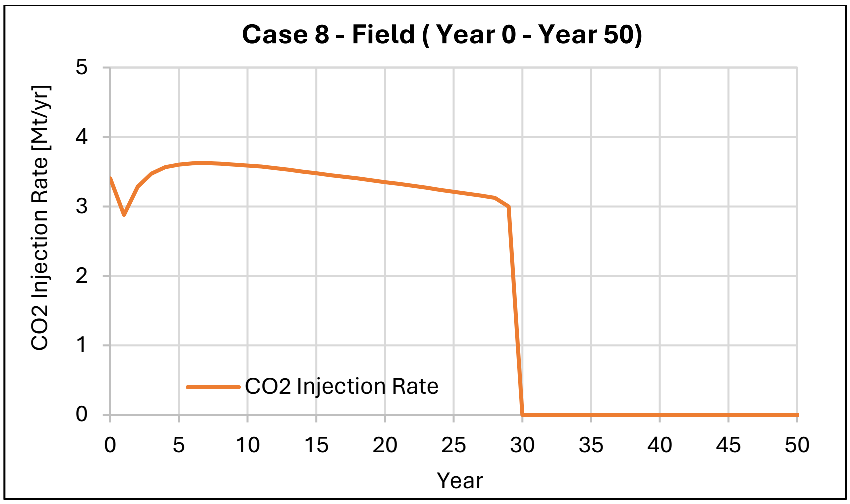

Figure 76: Case 8, Field injection rate

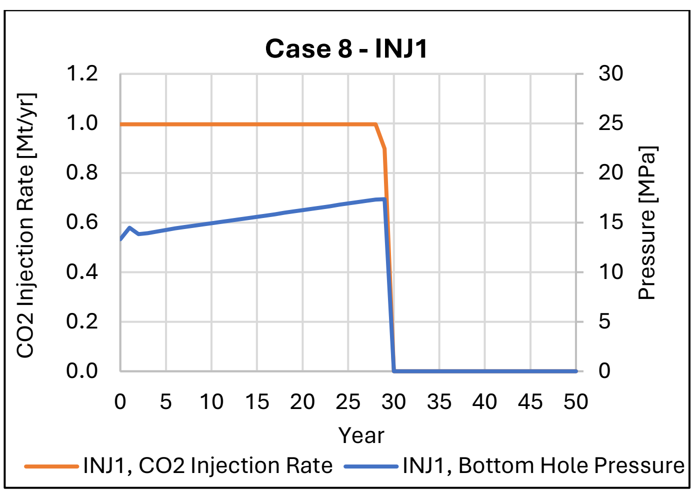

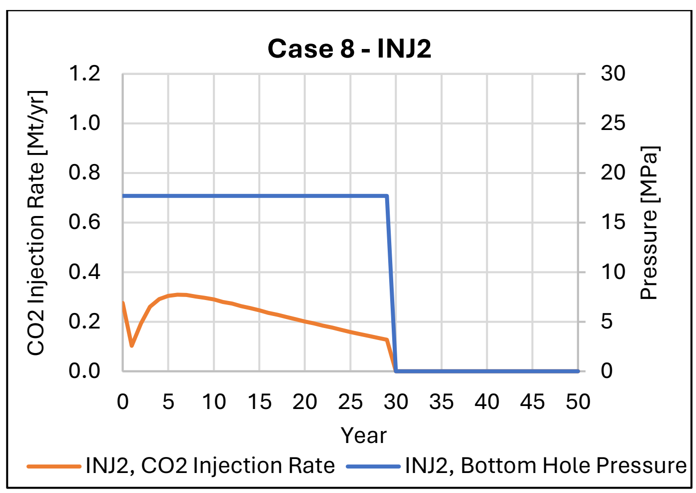

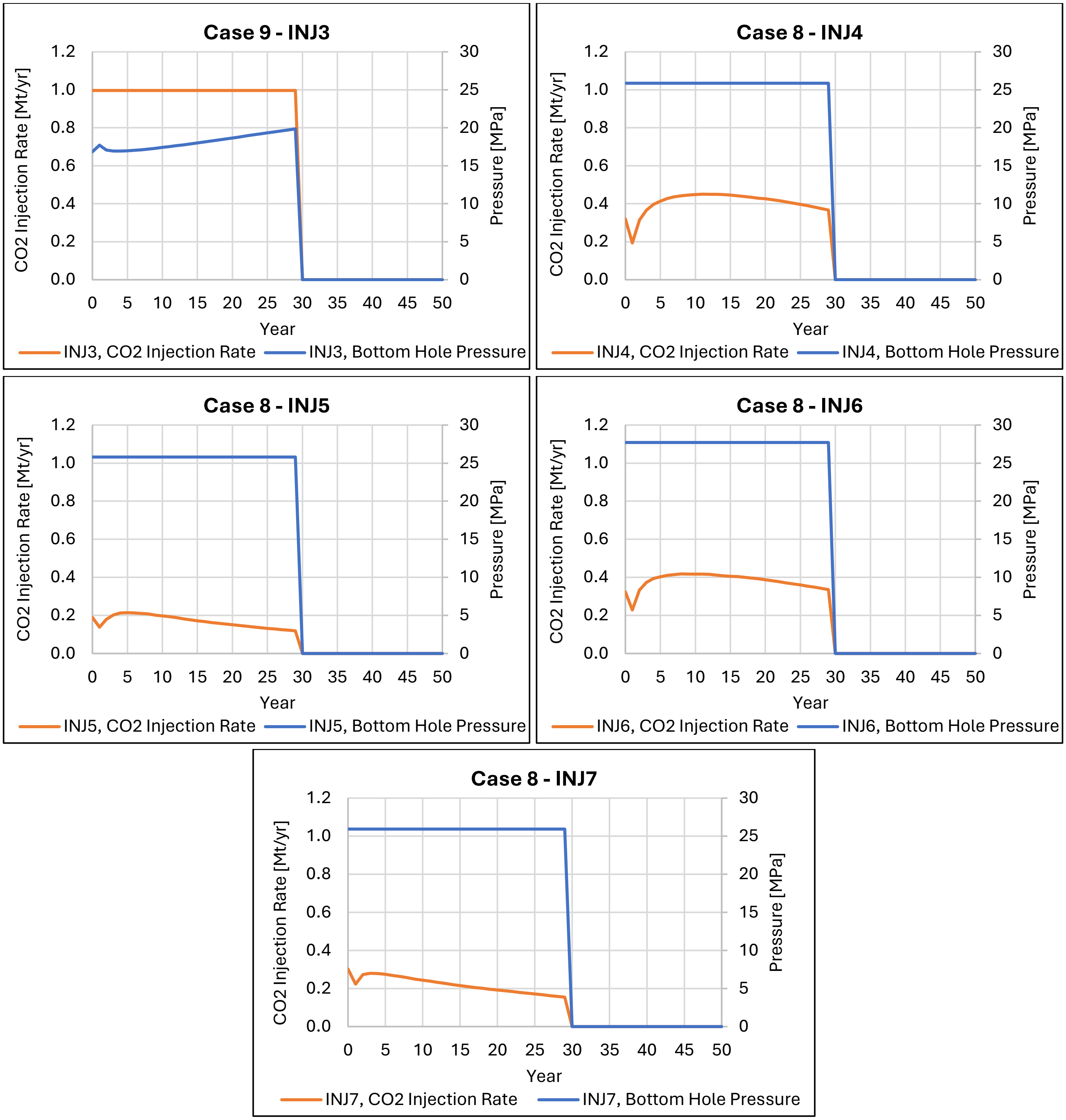

Figure 77: Case 8, Well injection rates and bottomhole pressures

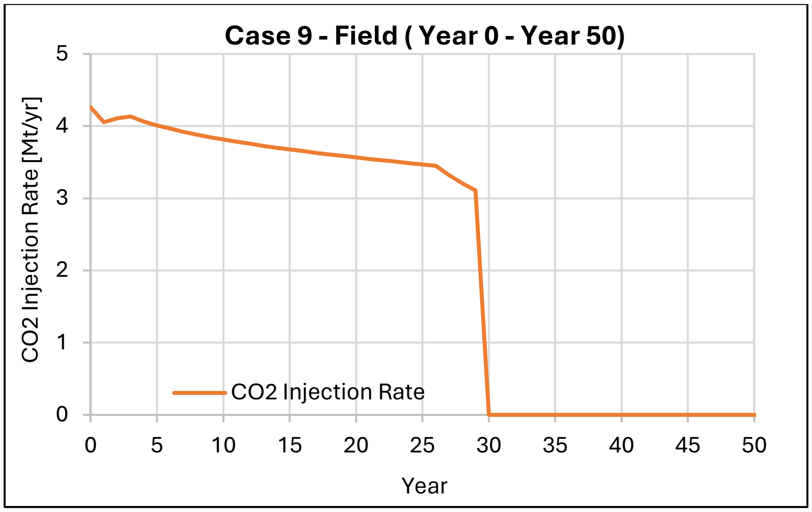

Figure 78: Case 9, Field injection rate

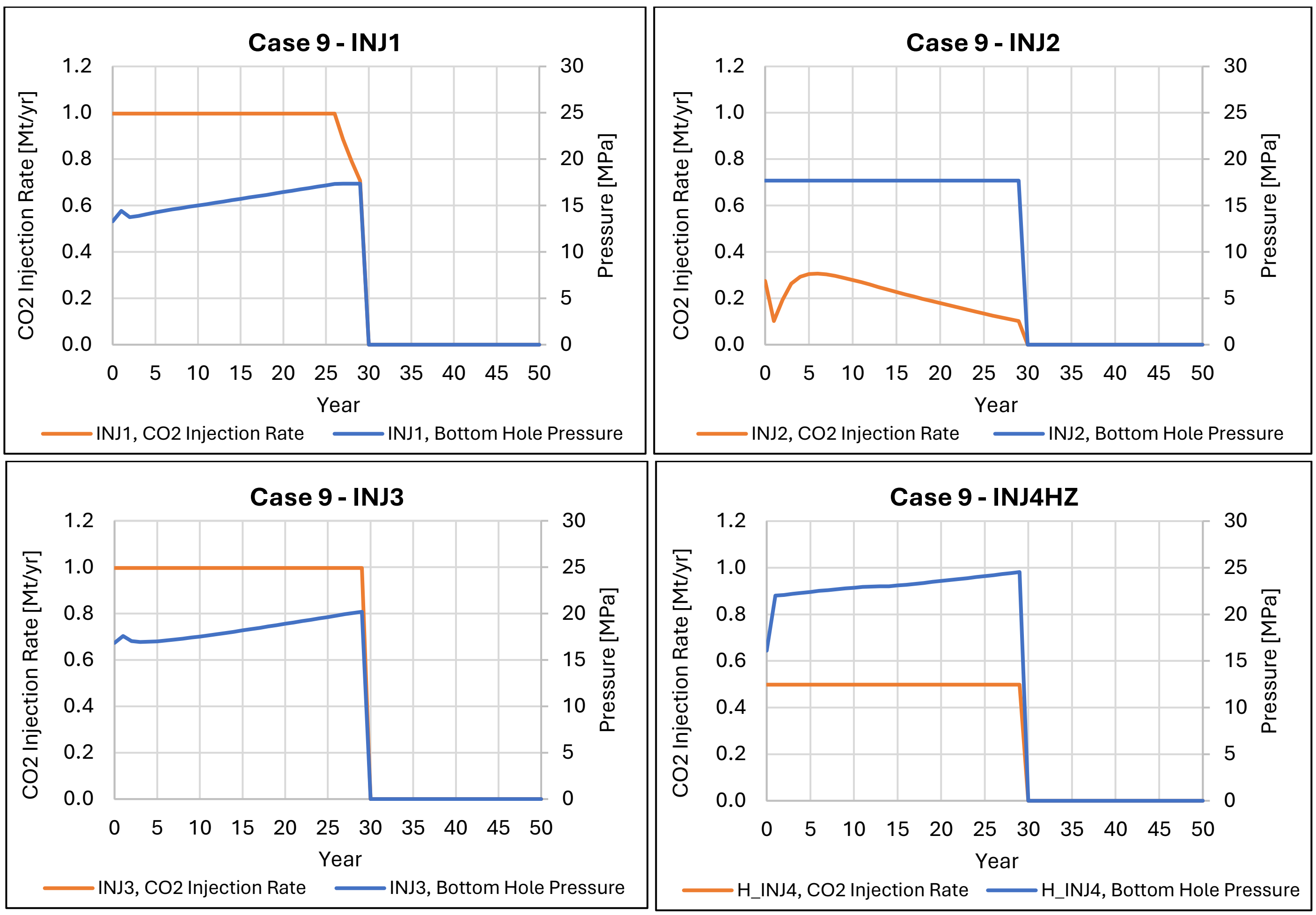

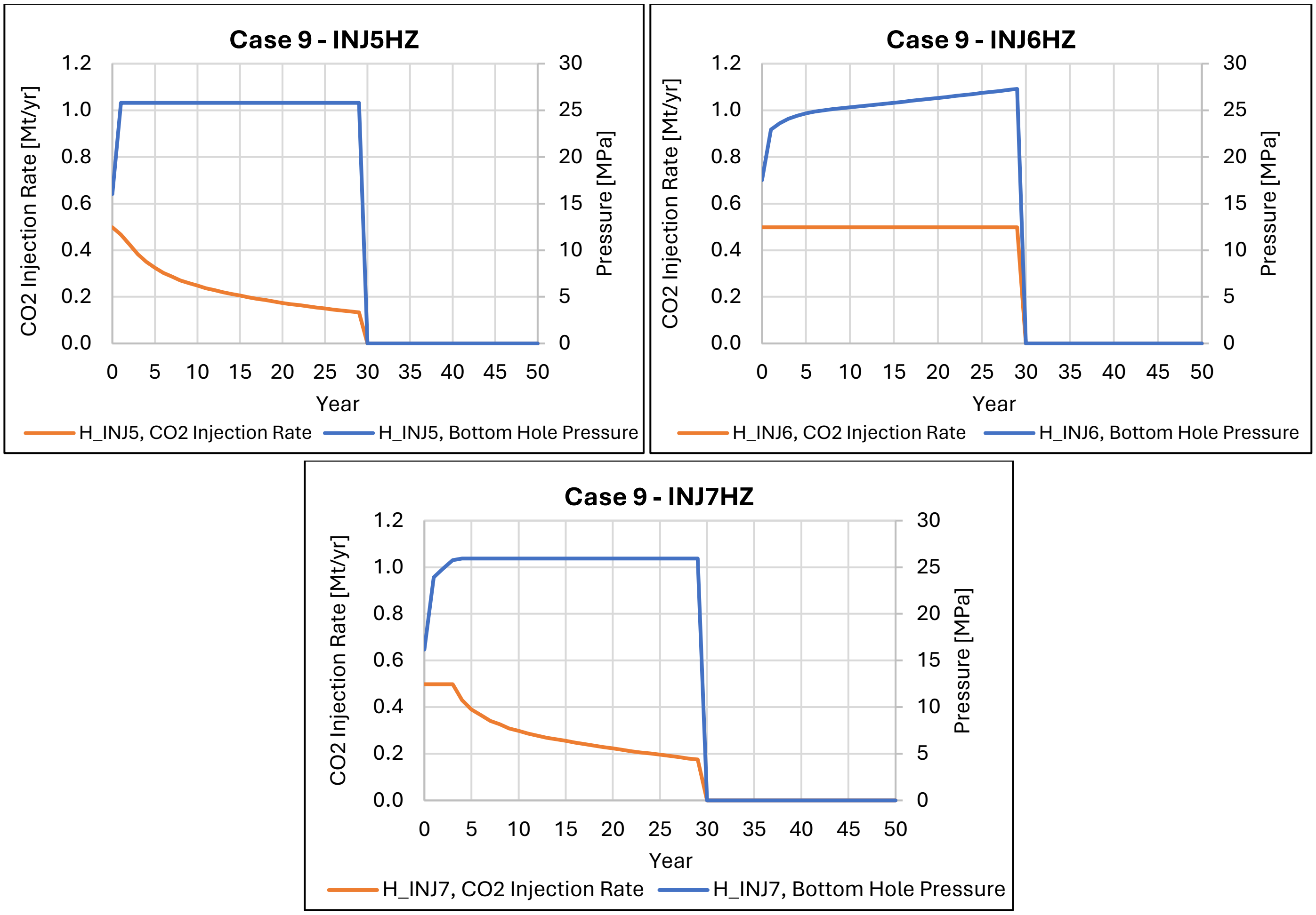

Figure 79: Case 9, Well injection rates and bottomhole pressures

Appendix 2.3: Skåne Plume Overviews

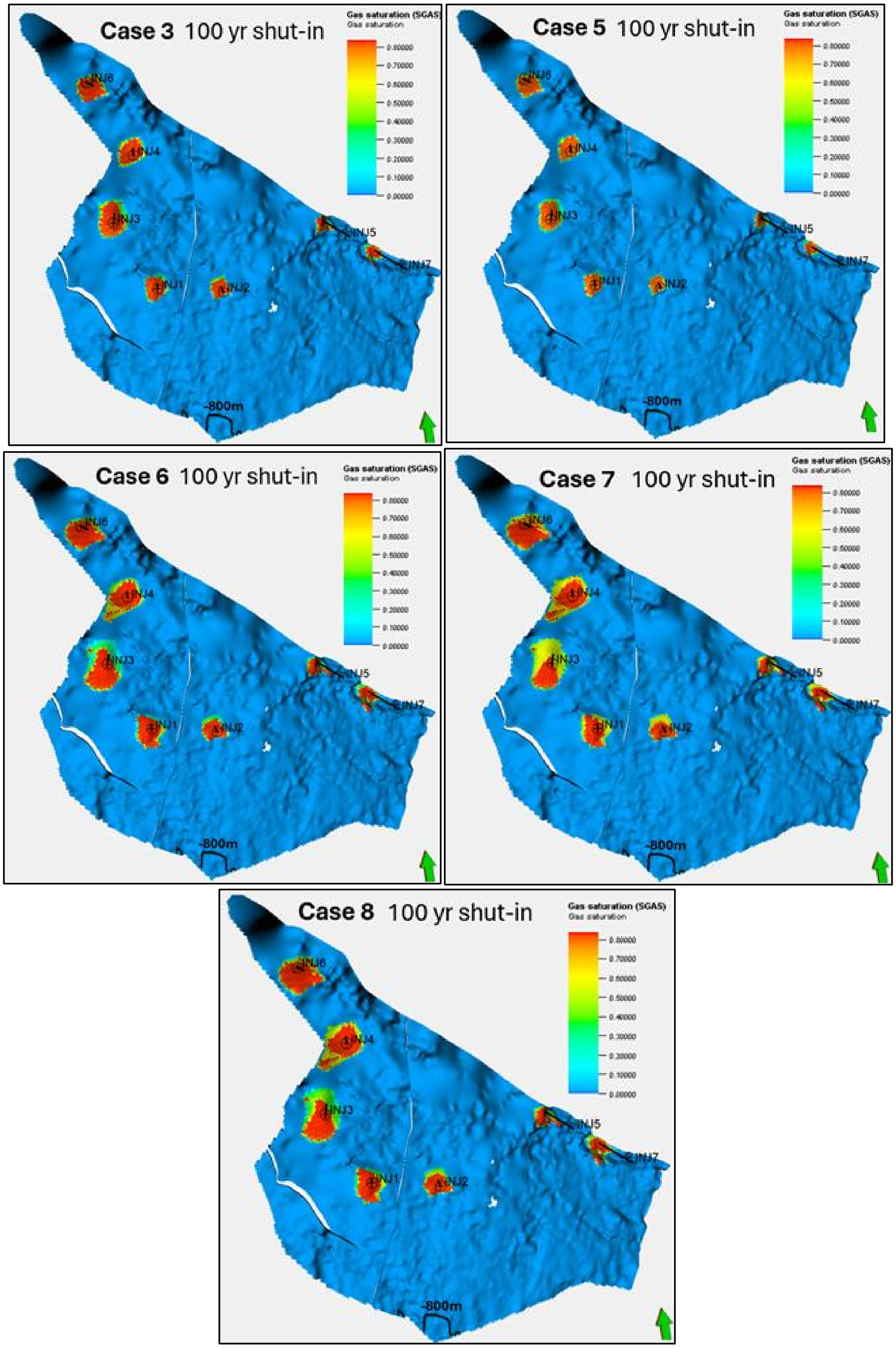

Figure 80: 3D view of CO_2 plumes at shut-in

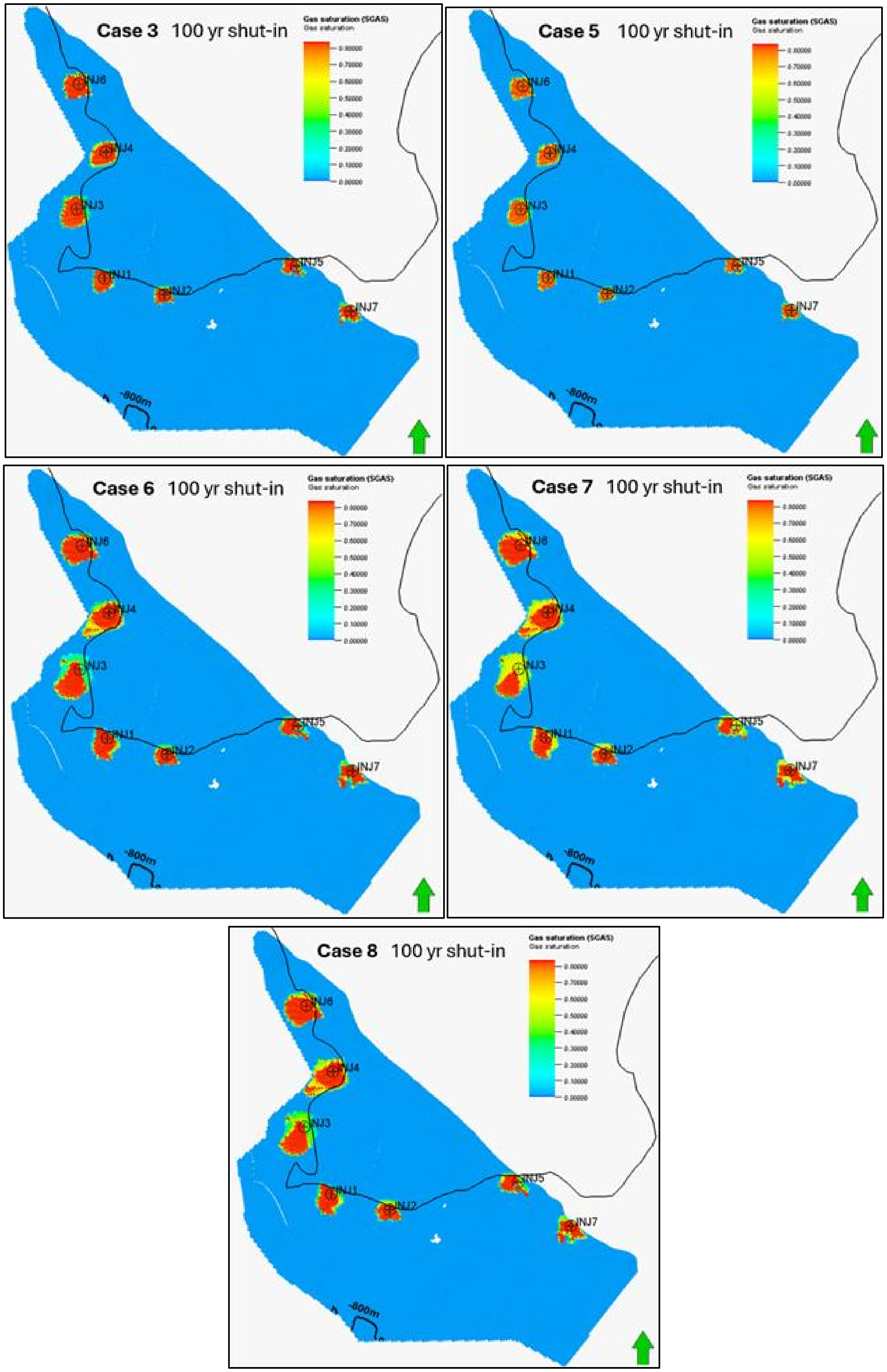

Figure 81: 2D views of plumes with coastline

Appendix 2.4: Technical Risk Register

				Inherent Risk		
Storage Parameter	**Target Injection zone**	**Key uncertainty (short description)**	**Risk (short description)**	**Likelihood (L/M/H)**	**Consequence (L/M/H)**	**Mitigation**
Injectivity	**Arnager**	According to SGU dataset, Arnager Greensand NTG ranges from 0.4 – 0.8, which possibly implies the presence of significant heterogeneities in the sand	Due to the use of constant property values (porosity, NTG, perm) in the geomodel, there is a risk that reservoir heterogeneities are under-stated leading to inaccurate injectivity estimates	M	M	▪ Likelihood M because given the know heterogeneity of the reservoir and limitations in understanding injectivity estimates with different reservoir properties. ▪ Consequence M because the well data support the average reservoir properties used and show potential for injectivity. actual injectivity could be lower. The following technical mitigations focus on reducing uncertainty associated with injectivity: **1. Improve Subsurface Characterization** · High-resolution 3D seismic surveys (and 4D baseline acquisition) to better define structure and faults · Appraisal wells and coring programs to directly measure porosity, permeability, capillary entry pressure, and residual trapping characteristics. · Constrain the poro-perm relationship with log data (when more data becomes available) · Integrate any future well results that confirm injectivity (this would include but not be limited to injectivity tests results on new drills) and/or any geomechanical results that may impact injectivity. · Comprehensive well logging (e.g., density, neutron, NMR, image logs) to refine storage capacity estimates. · Laboratory testing on core samples to determine CO_2–brine–rock interactions and geomechanical properties. · Pressure transient testing and injectivity testing to validate dynamic reservoir behavior. **2. Advanced Modeling & Uncertainty Management** · Create a new geomodel or update the current geomodel. **GLJ conducted a thorough review of the current Leapfrog model which is focused on structure modeling; however, no reservoir properties are available. GLJ recommends that the geological heterogeneity and uncertainties be captured.** **GLJ conducted a sensitivity analysis on a range of permeability values and results indicated that the size of the CO_2 plume is impacted by permeability changes, with higher permeability leading to greater lateral plume migration and lower permeability restricting plume spread.** · Static and dynamic reservoir modeling with multiple geological realizations. · Probabilistic capacity assessments (Monte Carlo simulations) to quantify uncertainty ranges (P10/P50/P90). · Coupled geomechanical modeling to assess pressure limits and fracture risk. · History matching of analogue fields to benchmark assumptions.
Capacity	**Both**	Capacity is primarily impacted by: · **Geologic uncertainty** · **Migration pathways uncertainty** and to a lesser extent: · Regulatory framework uncertainty (sensitive areas, protected areas, ...) * International boundaries	Due to **geological uncertainty**, there is a risk that the subsurface capacity to store CO_2 underground is under- or overestimated, leading to inadequate storage planning, potential over-pressurization or underutilization of the reservoir, increased monitoring and mitigation costs, and possible failure to meet long-term carbon storage targets	H	H	▪ Likelihood H because of the simplicity of the current model in the area limits understanding of migration pathways and container volume. ▪ Consequence H because if CO2 migrates out of zone including international boundaries (in the southwestern Baltic Sea and Skåne area) and impact sensitive areas The following technical mitigations focus on reducing uncertainty before injection and managing uncertainty during operations: **1. Improve Subsurface Characterization (Pre-Injection)** · High-resolution 3D seismic surveys (and 4D baseline acquisition) to better define structure and faults · Appraisal wells and coring programs to directly measure porosity, permeability, capillary entry pressure, and residual trapping characteristics. · Comprehensive well logging (e.g., density, neutron, NMR, image logs) to refine storage capacity estimates. · Laboratory testing on core samples to determine CO_2-brine-rock interactions and geomechanical properties. · Pressure transient testing and injectivity testing to validate dynamic reservoir behavior. **2. Advanced Modeling & Uncertainty Management** **GLJ conducted a Sensitivity Analysis on boundary conditions which showed a significant impact on storage capacity.** · Static and dynamic reservoir modeling with multiple geological realizations. · Probabilistic capacity assessments (Monte Carlo simulations) to quantify uncertainty ranges (P10/P50/P90). · Coupled geomechanical modeling to assess pressure limits and fracture risk. · History matching of analogue fields to benchmark assumptions. **3. Phased / Adaptive Development Strategy** · Pilot injection phase to validate injectivity and plume behavior before full-scale deployment. · Step-rate injection testing to determine fracture gradients and safe pressure limits. · Modular facility design to allow scaling up or down depending on verified capacity. **4. Monitoring, Measurement & Verification (MMV)** · Time-lapse (4D) seismic monitoring to track plume migration. · Downhole pressure and temperature monitoring to detect unexpected reservoir response. · Deformation monitoring (seabed monitoring systems) to track geomechanical effects. · Reservoir simulation updates (model recalibration) using real injection data. **5. Pressure & Capacity Management**

						· Brine production (pressure management wells) to increase effective storage capacity and reduce overpressure risk. · Use of multiple injection wells or zones to distribute pressure more evenly.
Capacity	**Both**	Capacity is primarily impacted by: · **Geologic uncertainty** · **Migration pathways uncertainty** and to a lesser extent: · Regulatory framework uncertainty (sensitive areas, protected areas, …) · International boundaries	Due to uncertainty in **CO_2 migration pathways**, there is a risk that effective storage capacity is reduced or overestimated, as injected CO_2 may preferentially migrate into unanticipated areas or outside the intended storage complex, leading to inefficient plume distribution, early pressure constraints, potential loss of containment, and reduced overall injectivity and storage performance.	H	H	▪ Likelihood H because of the simplicity of the current model in the area limits understanding of migration pathways and container volume. ▪ Consequence H because if CO2 migrates out of zone including international boundaries and impact sensitive areas · In addition to the mitigations identified above related to capacity, conduct an offset wellbore risk assessment to identify the risk associated with vintage wells and **map CO_2 injection avoidance areas**
Containment	**Both**	Abandonment of vintage offset wellbore (abandonment status and integrity of cement)	Due to the presence of vintage wellbores within or near the storage complex, there is a risk that degraded well integrity could create preferential pathways for CO_2 migration, leading to leakage from the storage reservoir, reduced containment security, regulatory non-compliance, and increased monitoring or remediation costs over the long term.	M	M	▪Likelihood M because limited number of vintage wellbores and large avoidance area ▪Consequence M because until a full wellbore risk assessment is complete. The following technical mitigations focus on reducing uncertainty associated with well integrity of vintage wellbores to minimize CO_2 leakage risk:**1. Well Assessment & Inspection:** · Conduct detailed records review, logging, and inspection of legacy wells to assess current integrity. · Use downhole tools (e.g., cement bond logs, ultrasonic imaging) to detect casing or cement degradation.**2. Risk-Based Prioritization:** · Classify wells based on proximity to the CO_2 plume, integrity status, and potential impact on containment. · Prioritize high-risk wells for remediation or monitoring.**3. Remediation & Reinforcement:** · Perform targeted well interventions such as cement squeeze, casing repairs, or abandonment and plugging where necessary. · Apply CO_2-resistant materials for remediation to ensure long-term sealing performance.**4. Monitoring & Verification:** · Install pressure and temperature sensors in high-risk wells for continuous integrity monitoring. · Integrate monitoring data into the MMV program to detect early signs of leakage.**5. Operational Controls:** · Maintain safe injection pressures to reduce stress on legacy wells. · Include contingency plans for rapid response in case of detected leakage.

Monitorability	**Both**	Site-specific MMV (Monitoring, Measurement and Verification) plans have not yet been developed	Due to the absence of a comprehensive Monitoring, Measurement and Verification (MMV) plan in a geologically challenging area, there is a risk that CO_2 plume migration, pressure build-up, or potential leakage pathways are not detected in a timely manner, leading to undetected loss of containment, regulatory non-compliance, reduced stakeholder confidence, and increased remediation costs.	M	M	▪ Likelihood M because due to absence of MMV plan which will be developed in future project stages ▪ Consequence M because due to absence of MMV plan which will be developed in future project stages The following technical mitigations focus on the development and implement a comprehensive, site-specific Monitoring, Measurement, and Verification (MMV) plan that addresses the unique challenges of offshore operations and long-distance tie-backs to shore. The MMV plan should include: **1. Baseline Characterization:** · Conduct high-resolution 3D seismic and geophysical surveys across the storage complex and along the tie-back corridor to identify faults, fractures, and stratigraphic heterogeneities. · Establish baseline geochemical, pressure, and temperature data in both the reservoir and overlying formations. · Assess legacy well infrastructure and subsea features along the tie-back route for potential leakage pathways. **2. Downhole and Subsea Monitoring:** · Install downhole pressure, temperature, and fluid composition sensors in injection and observation wells (monitoring both the shallow and deep geosphere within the injection zone and above it) to track plume behavior and pressure evolution in real-time. · Deploy subsea chemical and acoustic sensors along the tie-back pipeline and near the seabed to detect early signs of leakage or seepage. **3. Time-Lapse (4D) Seismic Monitoring:** · Implement periodic 4D seismic surveys to map CO_2 plume migration and ensure conformance within the intended storage complex. · Integrate seismic data with reservoir simulation for more accurate plume prediction. **4. Adaptive and Remote Monitoring Systems:** · Integrate data from subsea and downhole sensors into a centralized monitoring system onshore for continuous evaluation. · Establish threshold-based triggers for automated operational responses, including injection rate adjustments or well shut-ins. · Where feasible, use remote monitoring technologies to minimize offshore intervention needs and improve safety. **5. Dynamic Reservoir Modeling and Risk Updating:** · Regularly update reservoir and plume models based on monitoring data to refine storage capacity estimates, migration predictions, and pressure management strategies. · Incorporate probabilistic modeling to account for geological uncertainty and operational variability. **6. Regulatory and Stakeholder Alignment:** · Ensure the MMV plan meets regulatory requirements for offshore CO_2 storage and demonstrates proactive risk management. · Provide transparent reporting to stakeholders, highlighting plume behavior, injection volumes, and any anomalies detected.
Induced Seismicity	**Arnager**	Changes in pore pressure as a result of CO_2 injection	Due to CO_2 injection, there is a risk that changes in reservoir pore pressure could exceed safe limits, leading to reservoir fracturing, fault reactivation, induced seismicity, reduced injectivity, potential leakage pathways, and compromised containment integrity of the storage complex.	M	L	▪ Likelihood M because of uncertainty in basement fault and orientation relative to the storage area ▪ Consequence L because likely limited seismic magnitude, offshore context and limited impacted populations The following risk treatment will reduce the likelihood and impact of excessive pore pressure, ensuring safe CO_2 injection while preserving reservoir integrity and storage containment: **1. Reservoir and Geomechanical Characterization:** Map and understand basement faults Update the current geomodel and explicitly model all the relevant faults Conduct detailed reservoir modeling and geomechanical analysis to predict pore pressure response and define safe operating limits. Use multiple geological realizations to capture uncertainty in reservoir connectivity and fault behavior. **2. Controlled Injection Operations:** Implement step-rate or ramped injection strategies to gradually increase pressure while monitoring reservoir response. Distribute injection across multiple wells or zones to avoid localized overpressure. Adjust injection rates and pressures dynamically based on monitoring data. **3. Pressure Management Measures:** Install brine production or pressure-relief wells to manage excess pressure in sensitive zones. Define operational thresholds and automated triggers for reducing injection rates or shutting in wells if pressures approach critical limits. **4. Monitoring, Measurement & Verification (MMV):** Deploy downhole pressure and temperature sensors in injection and observation wells. Integrate monitoring data into reservoir models for continuous calibration and early warning of abnormal pressure trends. Use seismic monitoring to detect microseismic events indicative of fault reactivation or fracturing. **5. Adaptive Operational Planning:** Maintain contingency procedures to respond to unexpected pressure excursions, including operational adjustments offshore. Update injection strategy and pressure management plan iteratively based on observed reservoir behavior.

Injectivity	**Both**	Brine salinity and Salt precipitation	Due to continuous CO_2 injection, there is a risk that brine and CO_2 interactions lead to salt (e.g., halite) precipitation within the reservoir pore space, causing reduced injectivity, localized clogging of wells or reservoir pathways, increased injection pressures, and potentially limiting overall storage efficiency and capacity.	M	L	▪ Likelihood M because of lack of modelling and testing in this area, yet low salinity ▪ Consequence L because of observed impact in higher salinity areas (Aquistore project in Saskatchewan, https://ptrc.ca/aquistore) The following mitigations support the implementation an integrated strategy to prevent and manage salt precipitation in the offshore CO_2 storage complex, including: **1. Reservoir and Brine Characterization:** · Conduct detailed geochemical analysis of formation brines and reservoir rock to identify saturation levels and precipitation risks. · Model CO_2-brine interactions under reservoir pressure and temperature conditions to predict salt formation zones. · Note that brine salinity in the Arnager Greensand or the Faludden sandstone (~130,000 mg/L and ~ 60,000 mg/L respectively) at target depth is much lower than that of other projects in Alberta (commonly 150,000–350,000 mg/L TDS). **In order to model salt precipitation, and its effect on injectivity, GLJ conducted a Sensitivity Analysis using skin factor as proxy for salt precipitation effect.** **2. Injection Strategy Optimization:** · Use controlled injection rates and pressures to minimize rapid CO_2-brine mixing that can trigger salt precipitation. · Consider alternating CO_2 injection with brine or water slugs in sensitive zones to reduce localized supersaturation. · Sequence injection across multiple wells to distribute pressure and minimize localized clogging risk. **3. Well Design and Completion Adaptations:** · Select corrosion- and scale-resistant materials for subsea well tubing and completions. · Install downhole monitoring and sampling systems to detect early signs of salt deposition. · Design wells with access for chemical treatment or mechanical intervention if clogging occurs. **4. Monitoring, Measurement & Verification (MMV):** · Incorporate pressure, temperature, and flow sensors to detect increasing injection pressures indicative of blockage. · If feasible, use periodic sampling of produced fluids or wellbore monitoring to track salt accumulation. · Integrate data into reservoir models to forecast potential precipitation zones and adapt injection plans in real time. **5. Remediation & Contingency Planning:** · Prepare chemical or mechanical well-cleaning procedures for subsea intervention. · Include flexible offshore operational protocols to adjust injection rates and/ or swap or redistribute injection across wells if precipitation is detected.
Containment	**Both**	CO_2 plume size	Due to the large size of the CO_2 plume in the storage reservoir, there is a risk that the plume could migrate **beyond the intended storage zone or containment boundaries, potentially encountering faults, fractures, or legacy wells,** leading to leakage, regulatory non-compliance, reduced storage efficiency, and increased monitoring or remediation requirements.	M	M	▪ Likelihood M because limited modeling of possible migration pathways ▪ Consequence M because of the number of controls available to monitor size of plume The following mitigations form part of a strategy to manage long-term plume containment: **1. Reservoir Modeling & Plume Prediction** · Conduct more detailed fault analysis and modelling (refer to optional scope: Option 1 – Dynamic simulation within additional reservoirs). · Build a geomodel with all overlying formations to ensure that the overburden is explicitly modelled and pressure dissipation and transport mechanisms are fully understood. · Develop high-resolution static and dynamic reservoir models to simulate plume migration under different injection scenarios. **GLJ completed a sensitivity analysis on various plume size control mechanisms including capillary vs hysteresis trapping.** · Identify zones with favorable geochemistry for mineral trapping. · Perform multiple geological realizations and sensitivity analyses to assess worst-case plume extents. **2. Enhanced Containment via Mineralization** · Target injection in reservoir formations with high reactive mineral content to accelerate CO_2 mineralization. · Use geochemical modeling to estimate rates of mineral trapping and predict the fraction of CO_2 immobilized over time. · Integrate mineralization potential into plume migration forecasts to reduce the risk of lateral or vertical encroachment. **3. Controlled Injection Strategy** · Implement step-rate or ramped injection to manage plume growth while allowing sufficient residence time for mineralization reactions. · Distribute injection across multiple wells or zones to maximize contact between CO_2 and reactive minerals, enhancing immobilization. · Adjust injection rates based on real-time monitoring and mineralization model updates. · Evaluate potential for horizontal wells to control plume size. **4. Pressure & Plume Management** · Install brine production or pressure-relief wells to control reservoir pressure and limit lateral plume expansion. · Apply zonal isolation or selective completions to confine CO_2 within target intervals and optimize mineral trapping opportunities. **5. Monitoring, Measurement & Verification (MMV)** · Conduct time-lapse (4D) seismic surveys to track lateral and vertical plume migration. · Deploy downhole pressure, temperature, and geochemical sensors to monitor mineralization progress and plume containment. · Use tracer studies to confirm CO_2 immobilization and detect any potential off-zone migration. · Continuously update reservoir and geochemical models with monitoring data to refine plume and trapping forecasts. **6. Contingency Planning & Adaptive Management** · Establish threshold-based operational triggers for injection adjustment or well shut-in if plume approaches containment boundaries. · Prepare remedial strategies such as targeted pressure relief, injection redirection, or reactive mineral stimulation to enhance mineralization where necessary.